ESA STR-212
May 1984

The corrosion properties of Spacelab structural alloy aluminium 2219 - T851

B D Dunn
European Space Research and Technology Centre
Noordwijk, The Netherlands

european space agency / agence spatiale européenne
8-10, rue Mario-Nikis, 75738 PARIS CEDEX 15, France

Approved for publication: 28th February 1984
Edited by: W.R. Burke
Published by: ESA Scientific and Technical
Publications Branch, ESTEC, Noordwijk (NL)
Printed in The Netherlands
ISSN 0379 - 4067
Price code: C2

ABSTRACT

The main structural material chosen for the Spacelab project is the aluminium alloy 2219. It is used extensively throughout the Modular Pressure Shell and the Igloo structure. As 2219 has a poor resistance to atmospheric corrosion it is always anodised or chemically oxidised.

The corrosion protection systems and various forms of wrought alloy selected for the Spacelab 2219 applications have been subjected to surface-corrosion and stress-corrosion test programmes involving salt spray or alternate immersion in 3.5 % sodium chloride solution.

2219-T851 derives its high strength from the precipitation of $CuAl_2$ along slip planes and grain boundaries. Large $CuAl_2$ intermetallic particles are surrounded by a region depleated in copper and can give rise to localised galvanic corrosion. With the exception of weldments, which will be re-inspected during service life and possibly refurbished, the test results demonstrate that all chemically oxidised (e.g. Alodined) surfaces must be finished with space approved paints in order to avoid corrosion. Anodised finishes are expected to survive the Spacelab 10-year life requirement.

2219-T851 in the form of forged rings, rolled plate and welded plate (TIG, electron beam and repaired) has successfully passed standard stress-corrosion tests. Samples were stressed in the short transverse direction, at 75 per cent of the 0.2 per cent proof stress, for a period of at least 30 days. For comparative purposes the alloy BS L 93 (equivalent to AA 2024) was simultaneously tested and observed to fail the ESA stress-corrosion requirements.

(BLANK PAGE)

CONTENTS

1 GENERAL INTRODUCTION

The aluminium-copper-magnesium (silicon) wrought alloys belonging to the AA 2000 series were initially developed in the 1920's and have been used extensively for aerospace structures. In the last decade the alloys 2618 and 2219 have been chosen for advanced aircraft and spacecraft projects when good creep strength was required together with high strength/elongation properties.

The 2219 alloy is a heat-treatable wrought alloy developed by Alcoa in 1954. It provided industry with a material having elevated-temperature (260°C-300°C) properties exceeding those of all other aluminium alloys. Its weldability is excellent. The mechanical properties of both wrought and welded 2219 are also excellent at temperatures down to -250°C.

As with all AA 2000 series alloys, 2219 has somewhat less resistance to atmospheric corrosion than the lower strength Al-Si-Mg (AA 6000 series) and Al-Mg (AA 5000 series) wrought alloys. Inhomogeneities frequently initiate localised surface corrosion attack and for maximum resistance to corrosion the composition of each aluminium alloy must be kept as homogeneous possible. This principle applies to all the AA 2000 series of alloys, of which 2219 is typical. The high copper content (5.8 - 6.8 percent by weight) of 2219 generally depresses the electrode potential of aluminium in the cathodic (more noble) direction, as shown in Table I.

From both a mechanical-strength and an optimum corrosion-resistance standpoint it is essential that, during alloy fabrication, copper should be fully dissolved into the aluminium. It is the solid-solution, or homogenising, treatment that dissolves the copper, and this is performed in the temperature range 535°C±5°C. Cooling from this temperature must be rapid to prevent the formation of the intermetallic compound $CuAl_2$ at the grain boundaries. If excessive numbers of $CuAl_2$ intermetallics do form at grain boundaries they are surrounded by adjoining volumes of alloy depleted in copper, and this will facilitate corrosion attack.

The selection of a main structural alloy for the European Space Agency (ESA) Spacelab project was made in the mid-70's. A decision to select the alloy 2219 was based on the need for a material having an optimum combination of properties including those of mechanical strength, fracture toughness and resistance to general corrosion and stress-corrosion cracking. This material was commercially available as sheet and plate, extruded rod and bar, it could be forged and made available as Alclad sheet and plate. A wealth of 2219 property information was in

TABLE I - COMPATIBLE COUPLES FOR BIMETALLIC CONTACTS

Group No.	Metallurgical category The metals having the greater negative EMF will tend to corrode and form oxides	EMF between a calomel electrode and sea water
1.	Gold, solid or plated; gold-platinum alloys; wrought platinum	+0·15
2.	Rhodium plated on silver-plated copper	+0·05
3.	Silver, solid or plated on copper; high silver alloys	0
4.	Nickel, solid or plated; monel metal and high-nickel-copper alloys; titanium	−0·15
5.	Copper, solid or plated; low brasses or bronzes; silver solder; German silver; high copper-nickel alloys; nickel-chromium alloys; austenitic high corrosion-resistant steels	−0·20
6.	Commercial yellow brasses and bronzes	−0·25
7.	High brasses and bronzes; naval brass; Muntz metal	−0·30
8.	18% chromium type corrosion-resistant steels	−0·35
9.	Chromium or tin plated (non-porous) metals, 12% chromium type corrosion-resistant steels	−0·45
10.	Tin-lead solder, solid or plated; Terne plate	−0·50
11.	Lead, solid or plated; high lead alloys	−0·55
12.	Duralumin type aluminium wrought alloys $\boxed{2219}$ →	−0·60
13.	Iron, wrought, grey or malleable; Armco iron; plain carbon and low alloy steels	−0·70
14.	Aluminium, wrought alloys other than Duralumin type; aluminium case alloys of the silicon type	−0·75
15.	Aluminium, cast alloys other than silicon type; cadmium platings (generally not approved for space-use) →	−0·80
16.	Hot dipped zinc plate (generally not approved for space-use)	−1·05
17.	Zinc, wrought; zinc-base die casting alloys; zinc plate (generally not approved for space-use)	−1·10
18.	Magnesium and magnesium-base alloys, cast or wrought	−1·60

Compatible couples
Maximum potential difference for
A) 0·25 V Non-cleanroom environment
B) 0·5 V Clean-room or hermetically sealed environment

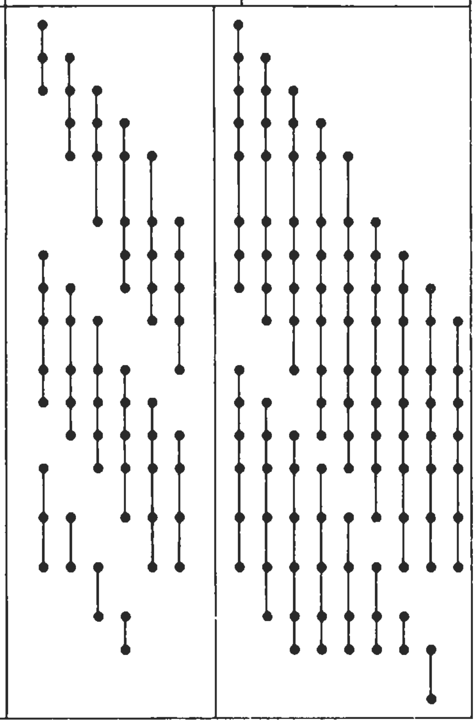

NOTE : Many of the less noble metals shown in this tabulation require additional protection from general surface corrosion in the form of platings, conversion coatings, anodic films, paints, etc.

existance and although the majority emanated from the United States it was also made available by European users who had only recently begun to utilise this alloy.

Several types of corrosion characteristics had been established for the 2219 alloy. General surface attack and pitting corrosion were not considered difficult to control, so by far the greatest importance was attributed to the control of stress-corrosion cracking. Despite the fact that this alloy has been designated as having a high resistance to stress-corrosion cracking when in the T6 or T8 condition, it can, if incorrectly worked or heat treated, have an increased susceptibility to all types of corrosion (see NASA MSFC Spec 522A and ESA PSS-01-736).

A general prequalification programme was undertaken to assess the suitability of 2219 alloy cast, wrought and fabricated in Europe for the Spacelab Project. This paper summarises a part of that programme which evaluated the surface and stress-corrosion resistance of samples of 2219 processed into Spacelab hardware configuration. Some of the Spacelab weldments are highlighted in Figures 1 to 7. NASA has also utilised aluminium alloy 2219 extensively in the Space Shuttle vehicle (Figures 8 to 10).

2 SURFACE PROTECTION TREATMENTS

The corrosion protection of 2219 can be greatly improved by a wide variety of surface treatments.

Those chosen for use by ESA projects are summarised in Table II. The Alclad forms of 2219 have a very high inherent resistance to corrosion and may be used without the application of further protective coatings. The most effective protection against stress-corrosion cracking of machined structural parts is obtained by the application of an epoxy-polyamide paint to shot-peened or electroplated surfaces of the alloy.

TABLE II - SURFACE TREATMENTS FOR THE ALLOY 2219

ALCLAD PRODUCTS	A core of 2219 sheet material is sandwiched between thin sheets of either pure aluminium or 7072 alloy, then hot rolled to effect bonding. Surface has a high resistance to corrosion and is sufficiently anodic to the 2219 core to afford electro-chemical protection.
MECHANICAL FINISHES	Sand blasting or shot peening gives a rough matt finish which causes surface of 2219 to be under slight compression. This may slightly reduce susceptibility to general and stress corrosion but must be covered with an organic coating.
ANODISING	Anodic coatings formed by electrolysis in sulphuric acid or chromic acid baths. Sulphuric acid provides thickest and most corrosion protective finish (2 to 25 µm depending on anodising time) for 2219.
CHEMICAL CONVERSION COATINGS	Processes such as Alodine and Irridite provide only temporary corrosion protection on 2219. They are an excellent base for paints.
ELECTROPLATING	2219 can be immersed in sodium zincate of controlled composition. This is a satisfactory base for depositing finishes of copper then nickel, chromium, gold, silver, etc.
PAINTING	Oil and oxides on 2219 must be removed by dipping 2219 in solvents then phosphoric acid (room temperature). Surface can be mechanically treated, primed with a conversion coating or special primer, then painted with epoxy - polyamide or polyurethane resins.

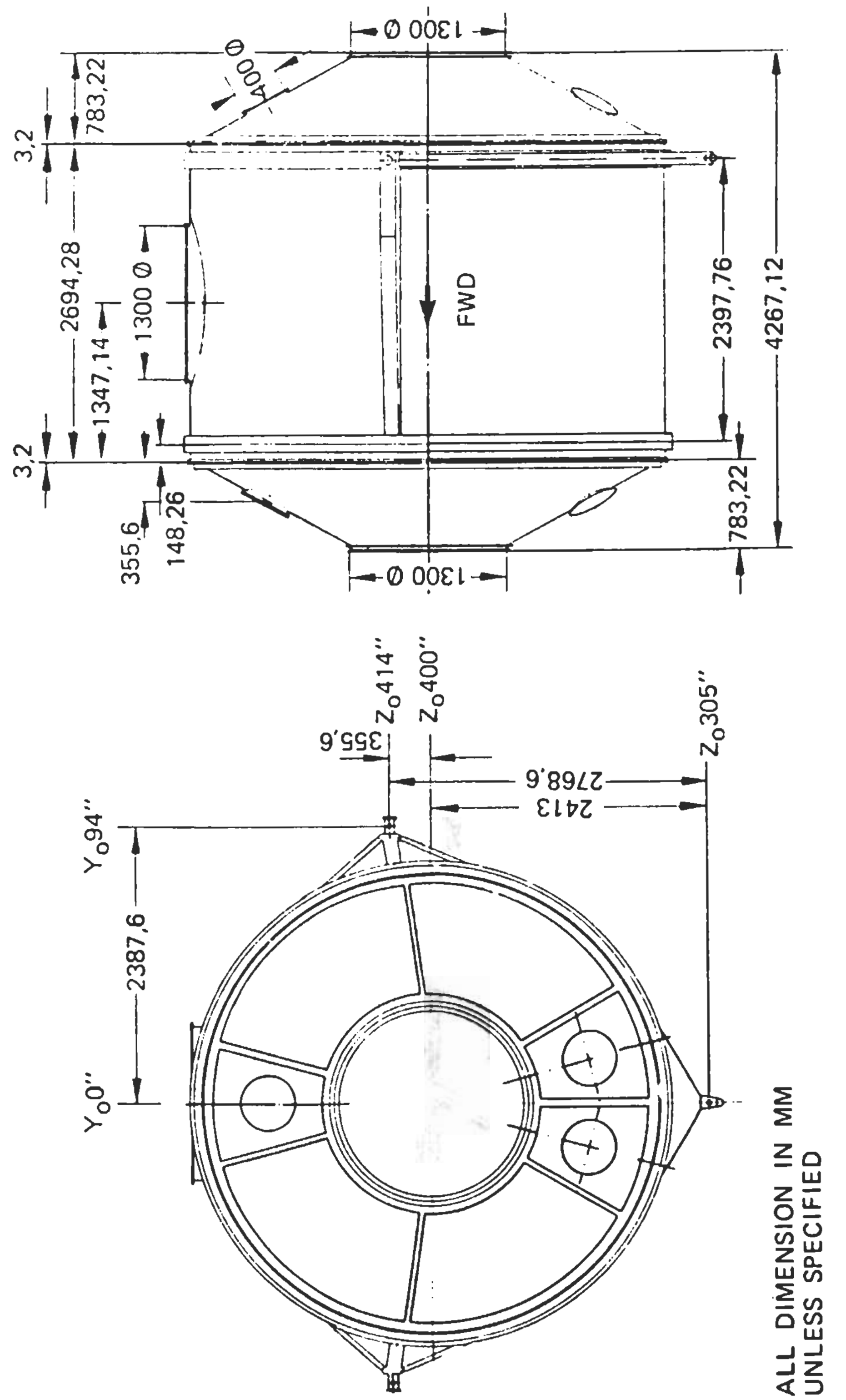

Figure 1 - Spacelab Short Module, physical dimensions. TIG welding processes were used to weld panels and rings for Modular Pressure Shell. Base material is 2219 T851 (plates and rings), filler metal is 2319 (to QQ-R-566).
Thicknesses of weld configurations are :

Cylinder - Longitudinal weld 4 mm
Circumferential weld 4 mm

Cone - Longitudinal weld 7 mm
Circumferential weld 7 mm

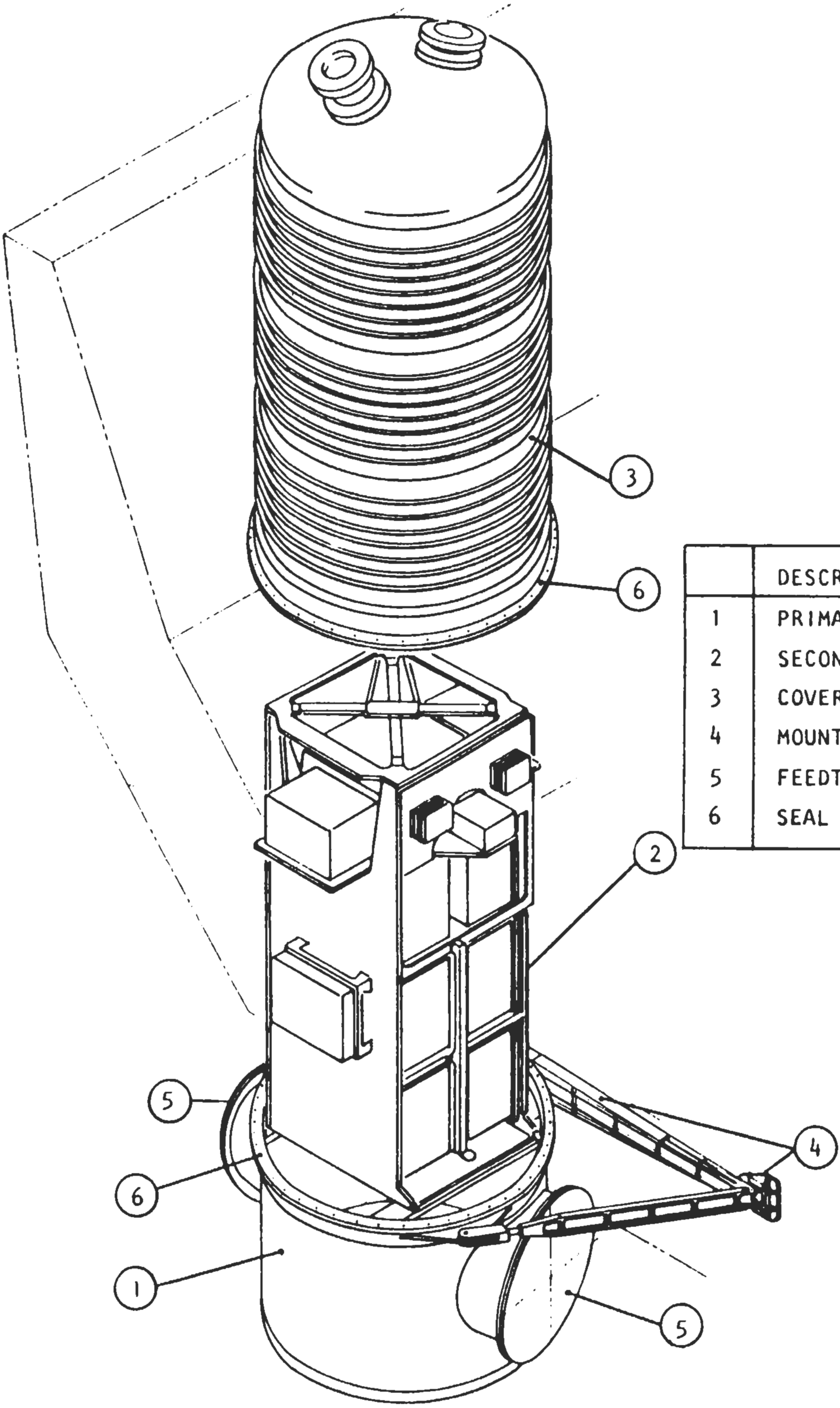

	DESCRIPTION
1	PRIMARY STRUCTURE
2	SECOND. STRUCTURE
3	COVER
4	MOUNTING STRUCTURE
5	FEEDTHROUGH PLATES
6	SEAL ASSEMBLY

Figure 2 - Igloo Structure Lay-Out and Equipment List, fabricated from 2219-T851. Both primary structure and cover welded by Electron Beam Process.

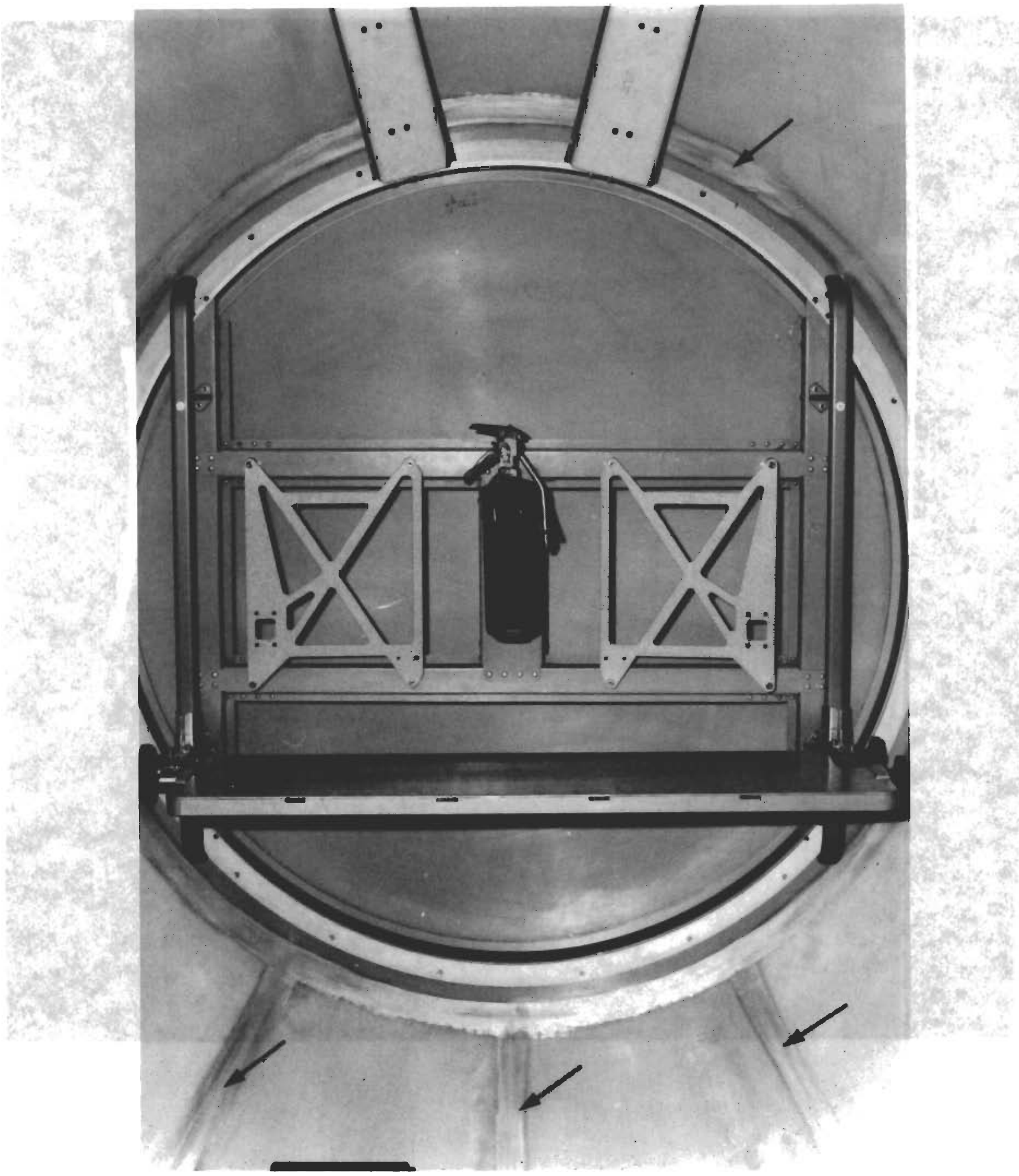

Figure 3 - Aft end cone showing the fire extinguisher, hand rails and foot support. Circumferential and longitudinal TIG welds are arrowed. All panels are chromic acid anodised; ground, polished and brush Alodined.

Figure 4 - Cone shell panel showing the numerically controlled machined waffle pattern and location of longitudinal seam TIG welds.

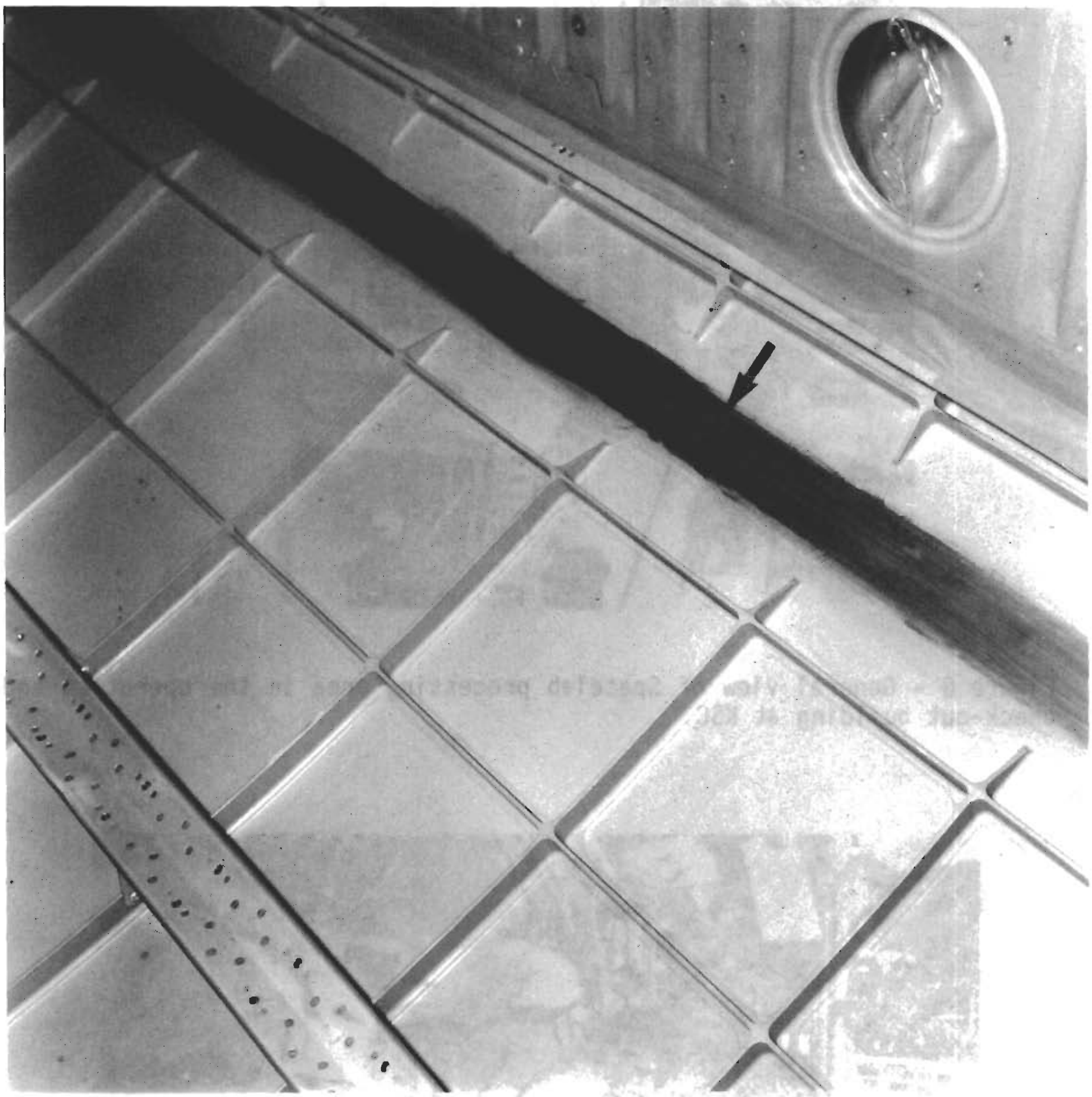

Figure 5 - Detail of waffle structure and interpanel weld zone. Surfaces were chromic acid anodised and the area to be welded was masked approximately 20 mm with special tape. This post-welded surface was later brush Alodined.

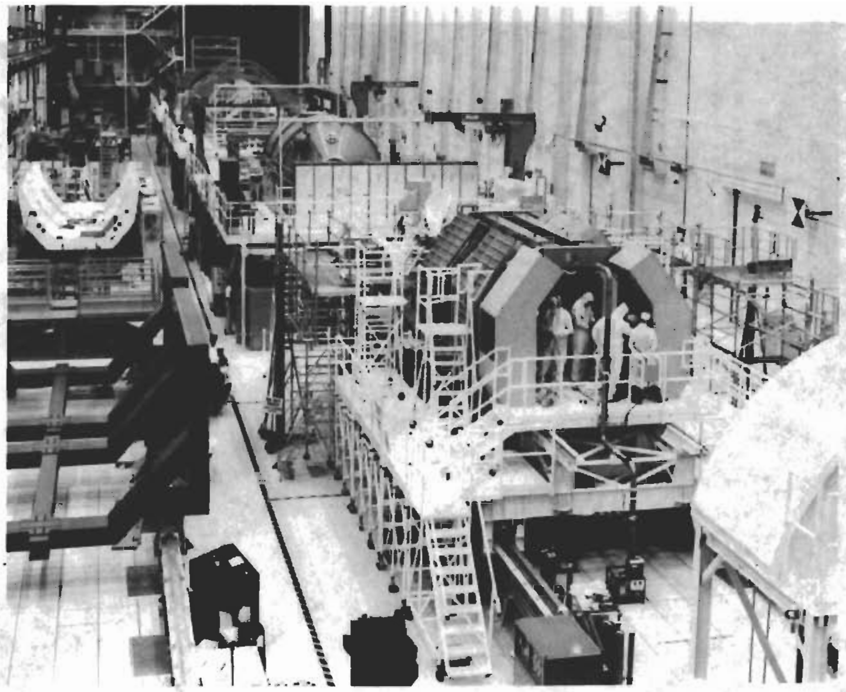

Figure 6 - General view of Spacelab processing area in the operation and check-out building at KSC.

Figure 7 - Early on-board activities during the Spacelab 1 - mission. Crew members Robert Parker and Ulf Merbold carrying out a "ballistocardiography" investigation (November 1983). The brush Alodined weld zones on the aft end cone are arrowed. Post-flight inspections of these accessible surfaces showed no evidence of degradation by corrosion.

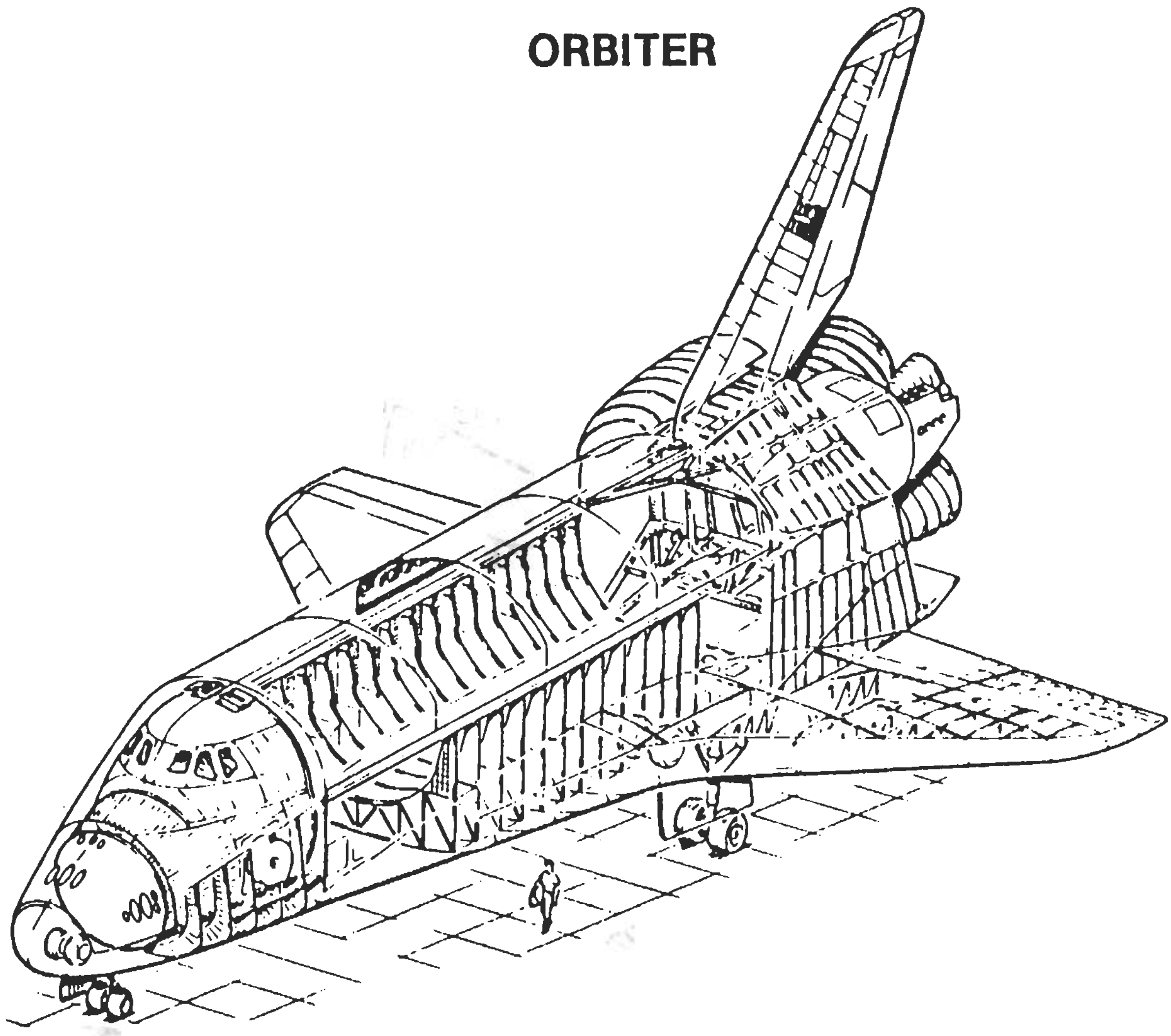

Figure 8 - 2219 is a major structural material for the NASA Orbitor.

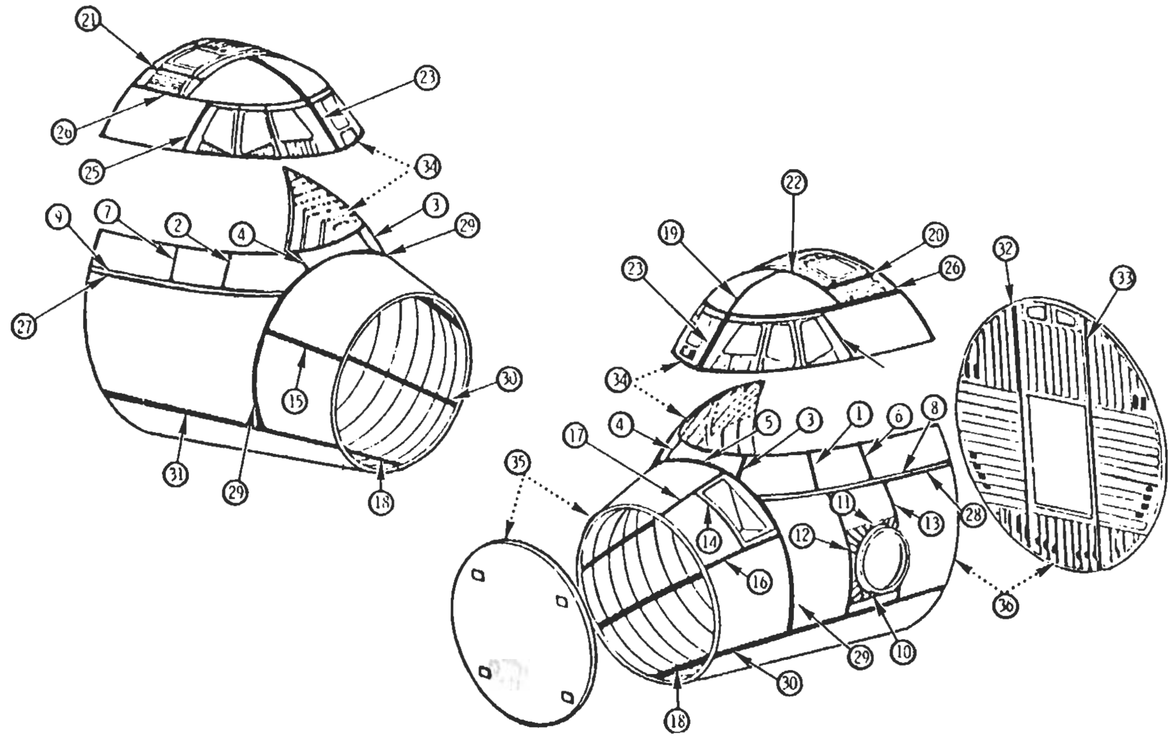

Figure 9 - Crew module weld locations on Orbitor. Material is 2219 in the following tempers : parts requiring little or no metal forming - T87; severe double contour - T62; and single contour - T851. Tempers are described in Appendix II.

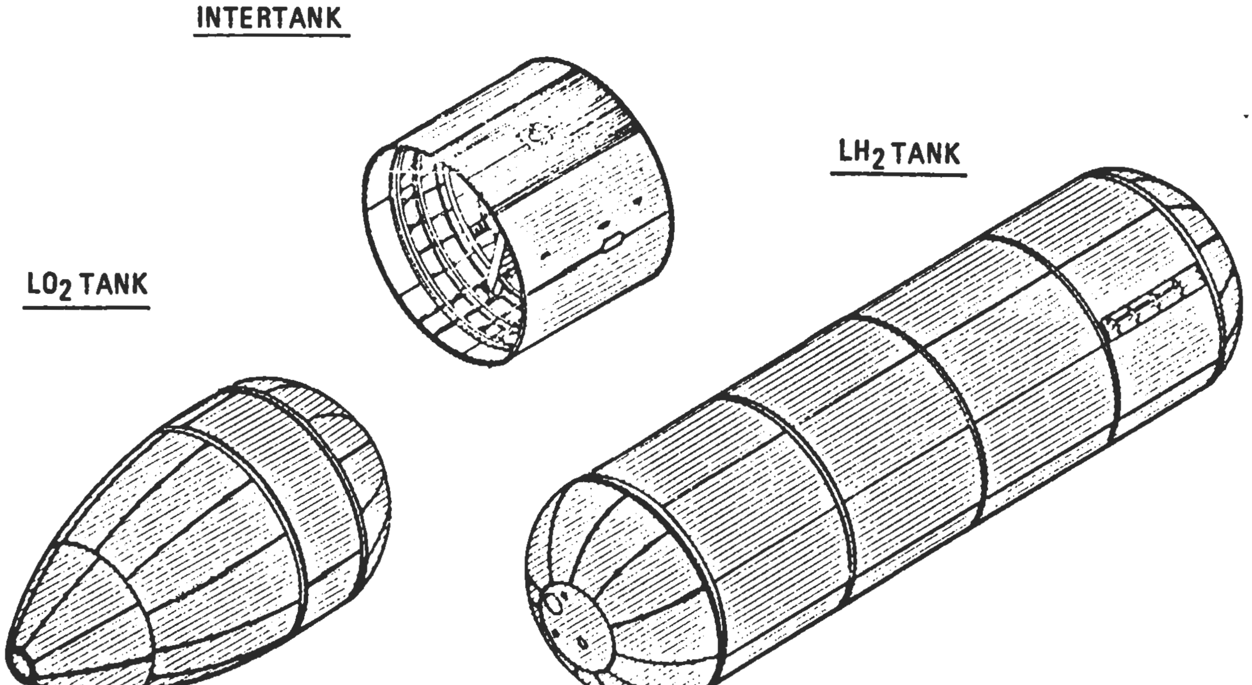

Figure 10 - The external Tank shown above, and the two Solid Rocket Boosters (recoverable after parachuting into the ocean) utilise 2219 aluminium alloy in the - T87 condition.

3 STRESS-CORROSION-CRACKING DATA FOR 2219 AS REPORTED IN THE LITERATURE.

Several of the most important graphs and Tables related to the alloy 2219 have been reproduced from the literature. They are presented in Appendix I. For a further explanation of this data, reference must be made to the original papers.

4 EVALUATION OF THE CORROSION RESISTANCE OF ANODIC AND CHEMICAL CONVERSION COATINGS ON NON-STRESSED ALUMINIUM 2219 SAMPLES

4.1 Introduction

Panel samples and a weld sample of Al 2219 were received from Air Italia (AIT) for corrosion testing. The panel samples had been chromic acid anodised and the weld sample Alodined. These surface finishes were proposed as a means of protecting the structure of Spacelab against general corrosion from the sheltered environment afforded by the mechanical ground support equipment (MGSE).

The current Natural and Induced Environment Specification states that Spacelab shall be capable of tolerating the following conditions during non-operational storage phases on the ground:-

Temperature	:	4°C to 55°C;
Humidity	:	10% to 90% RH;
Pressure	:	Ambient.

Except under emergency conditions, Spacelab equipment will not be exposed to uncontrolled terrestrial environments.

This chapter concerns an experimental programme which was undertaken to investigate the corrosion susceptibility of the proposed surface protection finishes for the high strength structural alloy Al 2219.

4.2 Description of Test Samples

4.2.1 Anodised Samples

Four anodised samples were submitted. Each had been cut from the same large test panel of 2219 in the T851 condition. Pretreatments and chromic acid anodic oxidation were according to the contractors' specifications. The test panel was a preproduction of the core shell having the waffle pattern shown in Figures 4 and 5.

As one dimension of this panel exceeded the depth of the anodising tank, it was impossible to oxidise completely in one step. The vertical panel was therefore partly submerged into the chromic acid electrolyte and anodised, then lifted out and rotated in order to anodise the untreated surfaces. The mid-plane of the panel was consequently exposed to two anodisation treatments, the last of which produced a dark immersion-line stain over the panel width. The submitted samples had been identified according to the following sketch :

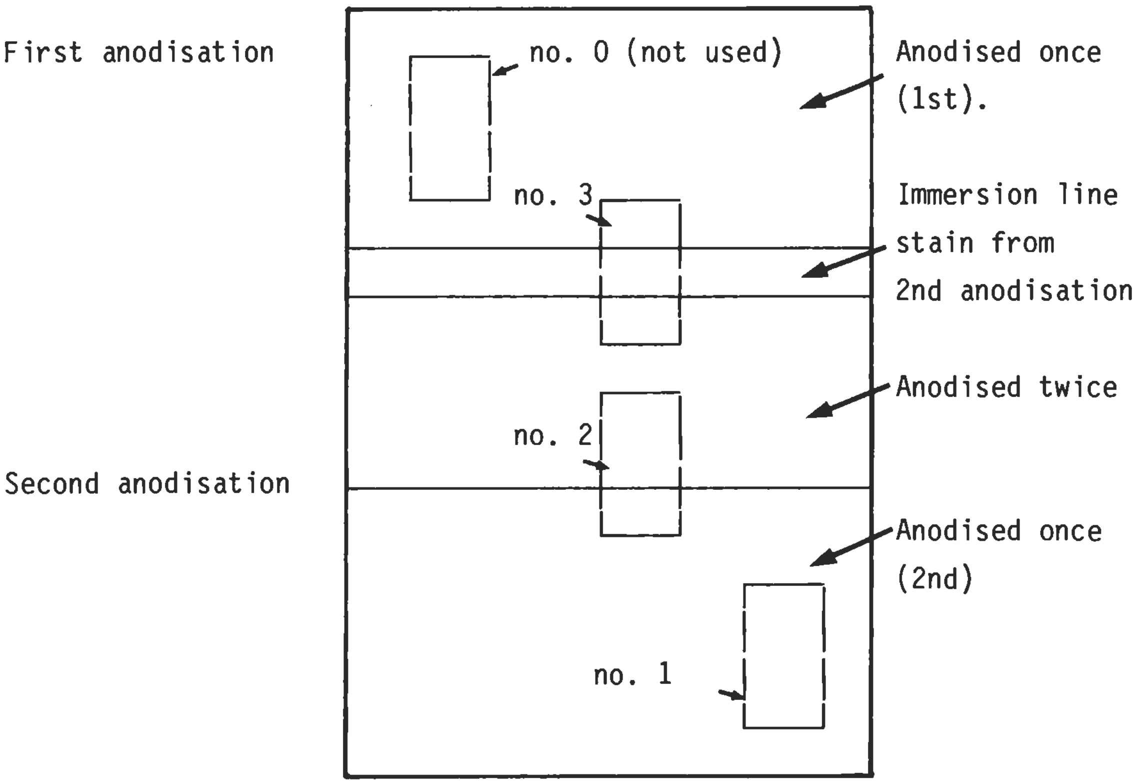

4.2.2 Welded and Alodined (Treatment 1200) Sample

As-received 7 mm plates were cleaned with Freon TF. 20 mm wide surface bands adjacent to the plate edges to be welded were prepared by buffing and re-cleaning in Freon TF. The plates were then TIG welded, using a filler rod of Al 2319. These welds were later shaved, etched, dye penetrant-tested recleaned and chemical conversion-finished with Alodine 1200. They are representative of the cone welds shown in Figures 1 and 3.

4.3 Experimental Procedure

4.3.1 Visual Inspection

All surfaces were examined under a binocular microscope. Certain aspects of the anodised and Alodined finishes were viewed in detail with a Reichert projection microscope.

4.3.2 Thermal Cycling of Anodised Finish

One small (16 cm^2) specimen was carefully sawn from an area of the panel which had received a double anodisation. This piece was attached to the copper heater plate of a thermal cycling equipment by means of a low outgassing high thermal conductivity silicone paste. Following 100 thermal cycles between -150°C and +100°C, under a vacuum of 10^{-6} torr, the sample was re-examined at x600 magnification for signs of surface crazing.

4.3.3 Surface Roughness of Anodised Samples

Surface roughness measurements were made with Talysurf equipment.

4.3.4 Corrosion Resistance

a) All submitted samples were scribed with a "standard" scratch by means of a constant load applied via a diamond pyramid indentor. The depth of the scratch was such that it would just break through the anodised finish and reveal the underlying 2219 alloy.

b) All panels and plates were carefully cut transversely to the scratch to provide five rectangular test pieces. Self-adhesive numbers were attached to each surface for traceability purposes. The bare cut edges of the test pieces were completely masked with impervious shellac.
Once the masking varnish had dried, the test pieces were washed in distilled water and dried with a soft cloth. Four test pieces from each sample were then subjected to a 5% salt spray test in accordance with ASTM B 117 except that the exposed surface was inclined approximately 6 degrees from the vertical.
The remaining "as-received" test pieces were kept in a desiccator (containing silica gel) for control purposes. Test pieces were withdrawn from the salt spray chamber at intervals of 7, 14, 21 and 30 days. After exposure, they were thoroughly cleaned with distilled water, dried and stored in a desiccator.

c) At the end of the 30-day exposure test, all test pieces were photographed. Every surface was closely examined and compared against standards (visual aids) which identified certain accept/reject criteria (i.e. the specimen panels shall show no more than a total of 5 isolated spots or pits, none larger than 1/32 inch in diameter, in a total of 30 square inches from one or more test pieces). The surfaces adjacent to the "standard scratch" lines were examined separately.

d) The peel or pull-off strength of coatings after the 30-day exposure was assessed by a method utilising adhesive tapes.

e) Sections were carefully sawn from several test pieces which had been marked for further metallographic examination. They were mounted in bakelite, ground and polished to 1/4 µm finish and viewed with a Reichert projection microscope. Photographs of the as-polished microsections were taken at various magnifications up to x1000. Occasionally, polarised light was used to highlight certain intermetallic phases.

4.4 Results and Discussion

4.4.1 Surface Inspection of Protective Films

The as-received test panels were noted to have rough, grey-coloured surface finishes. The anodic film is seen to be covered in a fine network of crevices and pit marks. It is noted that no additional surface crazing or micro-cracking became visible after temperature cycling.

4.4.2 Pits on Surface of "As-received" Anodised Sample

The rough surface appearance of the as-received anodised sample is highlighted in Figure 11 which shows details from a microsectioned non-exposed test piece. Several pits were measured to have depths of betweeen 30 and 40 µm. These values are far in excess of those measured by the Talysurf technique, as it is noted that many pits extend into the aluminium alloy by following narrow, tunnel-like paths such as that arrowed in Figure 11. The contractor explained that the submitted sheet had been deoxidised prior to the anodic treatment by a chemical etching process and that this pretreatment will account for the deep surface pits by the following reasoning.

The material is noted to contain a distribution of intermetallic particles having lengths of 5 - 8 µm which are strung out parallel to the sheet-rolling direction. These particles have a composition of $CuAl_2$ which has been shown by experiments to exhibit corrosion potentials of between -0.84V and -0.53V when coupled to pure aluminium (i.e. the alloy matrix). The etch-cleaning procedure undoubtedly enhances etch-pitting in an uncontrollable manner by the formation of microscopic local electro-chemical cells between exposed $CuAl_2$ particles and their surrounding surfaces. Intermetallic particles are seen for instance in Figure 12.

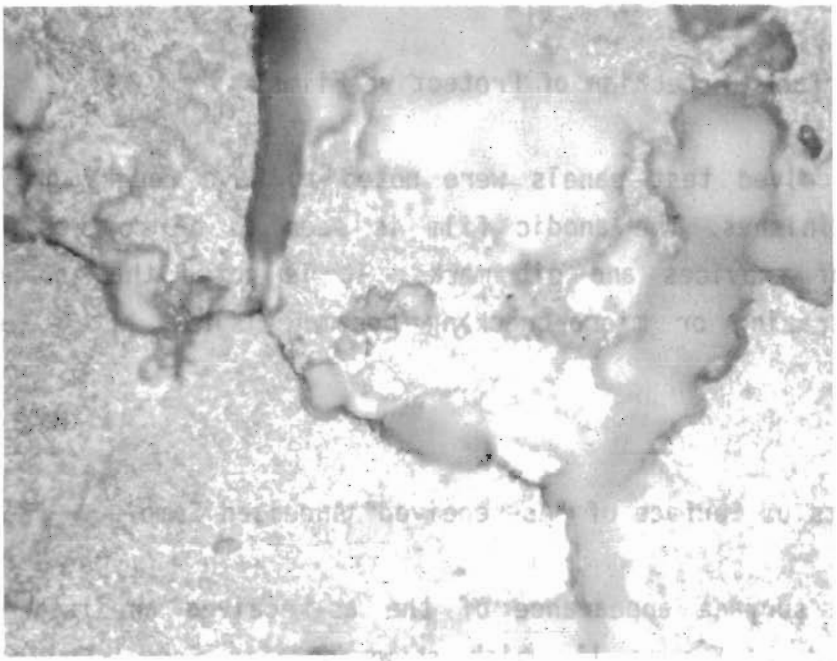

Figure 11 - Topography of anodised surface of as received material. Pit depths may reach 40 microns.

Figure 12 - Microsection made through region shown in figure 11. Photographed with polarised light to reveal opaque anodic film and copper-rich inclusions. (x1000)

4.4.3 Thickness of Protective Layers.

The appearance of the anodic film in cross-section was difficult to distinguish by normal metallographic techniques using white incident light. The most suitable method for observing the semi-opaque Al_2O_3 layer was found to be photographing the slightly tilted microsection under polarised light (Figure 12). The anodic layer is noted to have a consistent thickness of 2 μm and is present as a continuous protective film around the profile of each pit.

The thickness of the Alodine film could not be determined by microsectioning because it was too thin. Actual values for the surface roughness of each test panel (see sketch in Paragraph 4.2.1) were assessed from Talysurf traces. Average results are shown in Table III.

TABLE III - SURFACE ROUGHNESS OF FINISHES ON 2219

Specimen Panel no.	Max. Depth of Open Pit (μm)	Centre Line Average (μm)
1. Anodised once	7.5	100
2. Anodised twice	5.0	50
3. Alodined	2.5	7

4.4.4 Visual Inspection Following Exposure to Salt Spray.

Results of the visual inspections following exposure of test pieces to the salt spray corrosion-resistance tests are shown in Table IV. The overall view of these test pieces is shown in Figure 13.

a) The anodised pieces are noted to possess an excellent resistance to corrosion. The anodic films maintain their original yellow-grey appearance, even after completion of the 30-day exposure to salt

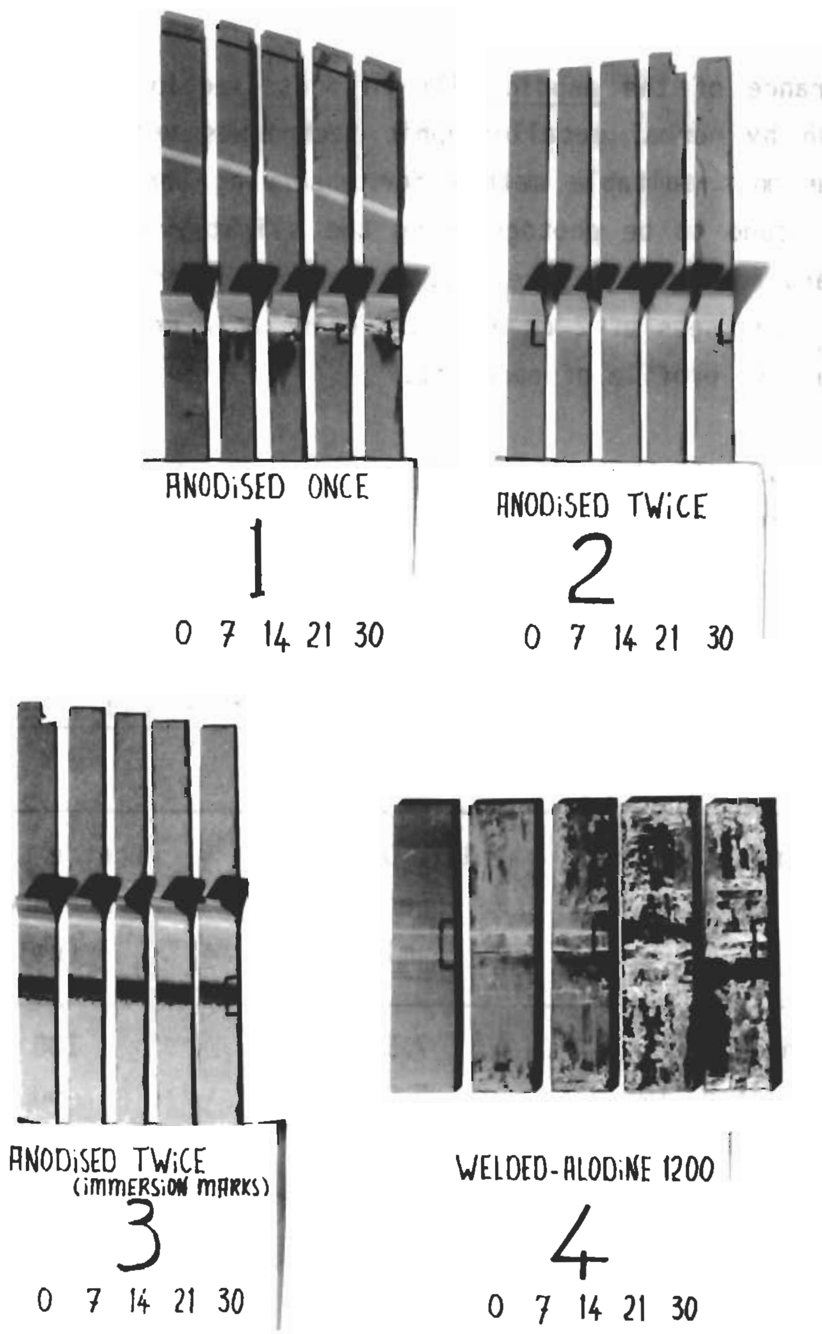

Figure 13 - Overall view of test pieces following salt spray (ASTM B 117) exposures of up to 30 days.

spray. Discoloration is confined to an area directly beneath the structural rib of specimen no. 1. These ribs form part of the waffle pattern shown in Figure 5. Microsectioning confirmed the absence of corrosive attack in this area.

b) The welded and conversion coated (Alodine 1200) test pieces are seen to be partially attacked on the exposed side following the first 7-day period of the salt spray test. Corrosion products seen in Figure 13 have run from several large corrosion sites and slightly discoloured the remaining surface. It is interesting to note that after 7 days, there is no marked preferential corrosion of the weld metal surface or

TABLE IV - VISUAL INSPECTION RESULTS FROM TEST PIECES FOLLOWING EXPOSURE TO SALT SPRAY

SPECIMEN PANEL	EXPOSURE DAYS	NUMBER OF CORROSION SITES EXPOSED SIDE	UNDERSIDE	ALONG SCRATCH
1. Anodised once (2nd treatment)	0	0	0	0
	7	10 *	0	0
	14	20 *	0	0
	21	>50 *	0	0
	30	>50 *	0	1
2. Anodised twice	0	0	0	0
	7	0	0	0
	14	0	0	0
	21	0	0	1
	30	0	0	1
3. Top part anodised twice; bottom part anodised once (first treatment) with immersion line	0	0	0	0
	7	0	0	0
	14	0	0	0
	21	0	0	2
	30	0	0	2
4. Welded plate finished with Alodine 1200	0	0	0	0
	7	10	0	5
	14	>100	20	complete
	21	complete	>100	complete
	30	complete	complete	complete

* Only in position B, under rib (gas bubbles released during anodising had become trapped under this protrusion and prevented adequate build-up of anodic layer). These ribs are part of the core shell panel which has a waffle structure as shown in Figures 4 and 5.

its heat-affected zone. General surface corrosion is evident after two weeks and this becomes a complete surface network after three weeks. The remaining test pieces which received a 4-week exposure to salt spray were seen to be totally covered in white and dark-grey powder-like corrosion products.

c) The score lines which were made to expose a thin line of unprotected aluminium alloy on each of the test pieces were examined after the test under a microscope. As listed in Table IV minute pits only were observed within the scratches of the anodised test pieces after three weeks of exposure to salt spray. However, scores on the Alodined sample were readily attacked.

4.4.5 Adhesion Test Results

Each of the pieces that had been exposed to 30 days of salt spray testing was submitted to the adhesion test. The results showed all anodic films to have passed this test, being fully adherent to their substrates. The adhesive tape was noted to readily remove the surface corrosion products and remaining film on the Alodined sample.

4.4.6 Metallographic Results

The surfaces of test pieces which contained features to be examined in cross-section are identified by the box markings shown in Figure 13. The cross-sections of each mounted sample are made in a plane which is parallel to the rolling direction of the plate and normal to the surface which was exposed to the salt spray. Figures 11 and 12 clearly highlight the very rough appearance of the surface. An account of the mode of pitting was given in Paragraph 4.4.2.

The chromic acid anodising produced an adherent oxide film with excellent protection even after 30 days of exposure to the salt spray. The results listed in Table IV show the poor corrosion resistance of the Alodine 1200 sample. Although general surface corrosion was apparent on this plate, no deep pitting of the parent metal could be observed from any of the microsections. Corrosion cavities were seen on the surface of the weld metal and its heat-affected zone (Figures 14 and 15). These corrosion fronts are noted to follow an intergranular path to a maximum depth of 162 µm after 30 days of exposure to the salt spray.

It is likely that the poor corrosion resistance of chemical conversion films is due to the presence of copper dispersed in the thin complex-oxide layer and that this will prevent complete passivation of the 2219 Al surface.

4.5 Conclusions

4.5.1 In the absence of any requirement defining the corrosion resistivity of high strength structural alloys, in particular Type 2219, it is suggested that an accelerated test method, involving the submission of test samples to a standard salt spray (i.e. ASTM-B-117) for a period of two weeks (336 hours) without resultant corrosion, will suitably screen materials and their protective finishes for the 10-year Spacelab life.

This proposal is based on the existing Spacelab environmental requirements, as outlined in Paragraph 4.1, and the findings of this evaluation.

4.5.2 The results of this evaluation are in agreement with those previously reported in the literature.
The salt spray tests showed :

a) All of the anodised samples exhibited good resistance to surface corrosion following a 4-week (672 hours) exposure to salt spray.

b) The Alodine 1200 samples did not satisfy the MIL-C-5541 requirements for chemical conversion coatings (i.e. 7 days salt spray). General surface corrosion and crevice corrosion in the weld heat affected zone renders this finish unsuitable for unrestricted Spacelab use. It would be a suitable base for a paint or resin coating.

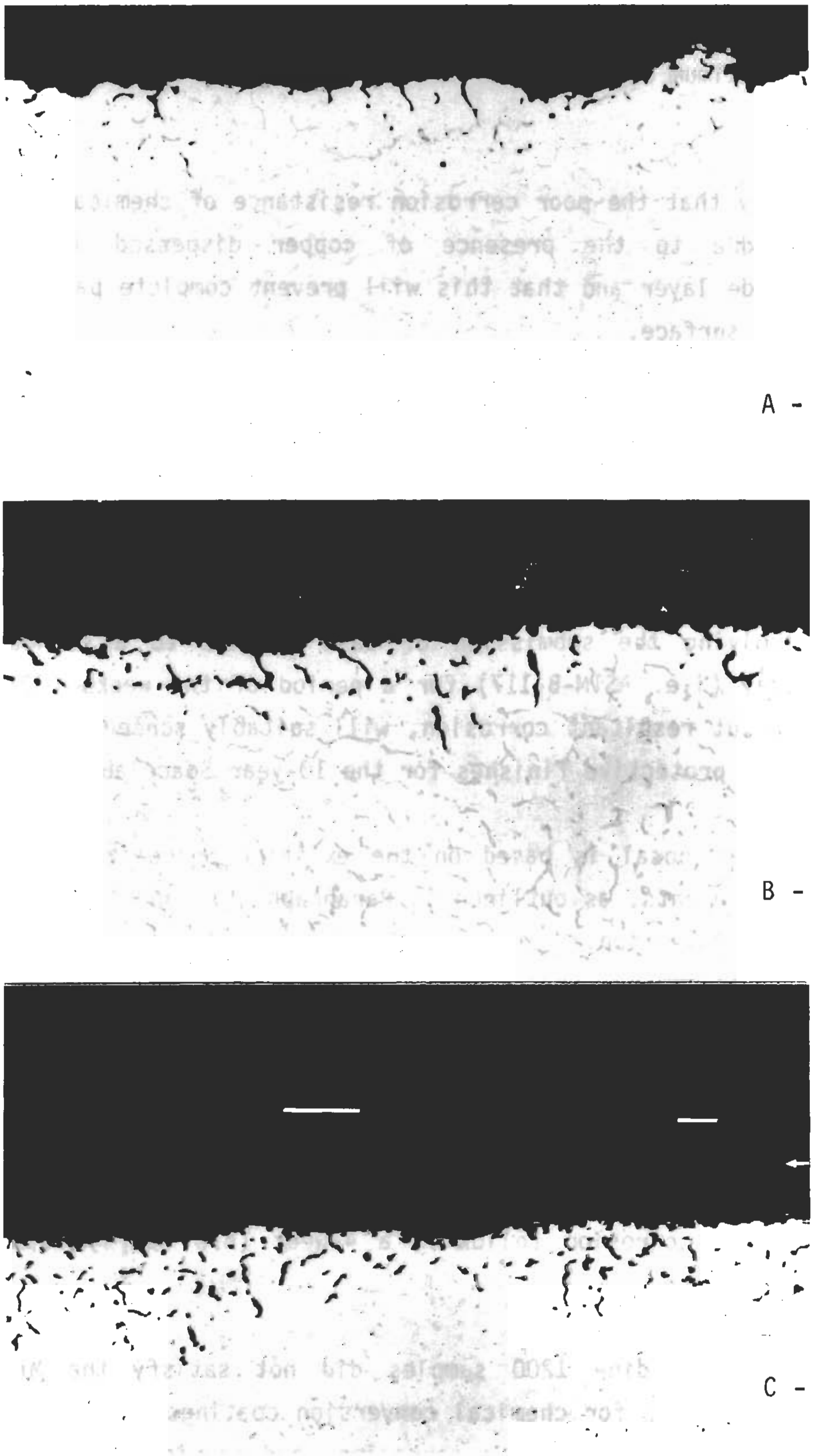

A - As received
(0 hours)

B - 14 days exposure
(336 hours)

adhering corrosion product

C - 30 days exposure
(720 hours)

Figure 14 - Photomicrographs made in the weld metal of the plate sample which had received an Alodine 1200 surface treatment. Depth of corrosion after 30 days exposure to salt spray is 45 µm. Micro-structure is as-cast divorced Al-$CuAl_2$ eutectic (x430).

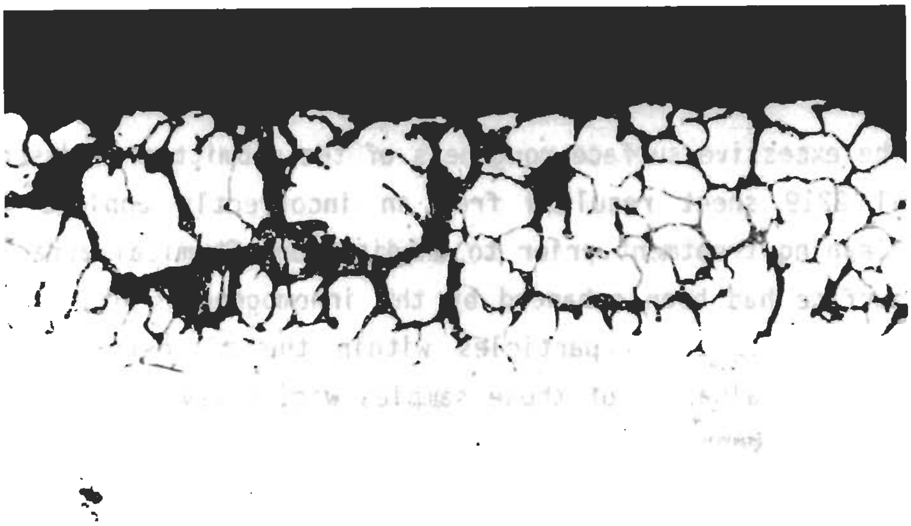

A - as received (0 hours)

B - 30 days exposure (720 hours)

Figure 15 - Alodined surface above the weld heat-affected zone. Depth of corrosion after 39 days is 162 μm (x430).

4.5.3 The anodic finish was unaffected by 100 thermal cycles between -150°C and 100°C at a pressure of 10^{-6} Torr.

4.5.4 The excessive surface roughness of the submitted anodised Al 2219 sheet resulted from an incorrectly applied chemical cleaning treatment prior to anodisation. Chemical attack of the surface had been enhanced by the inhomogeneous distribution of undissolved $CuAl_2$ particles within the microstructure of the alloy. Evaluation of those samples was, however, interesting as they are considered to represent a worst case condition.

5. EVALUATION OF THE CORROSION RESISTANCE OF PAINTED AND CHEMICAL CONVERSION COATED SAMPLES OF NON-STRESSED AL 2219 WELDMENTS

5.1 Introduction

Following the corrosion tests on Al 2219 described in Chapter 4, it was proposed that the standard salt spray test method, as prescribed by ASTM-B-117, would suitably screen Spacelab structural materials and their protective finishes. Exposure of test samples to the salt spray for a period of two weeks (336 hours) should represent a Spacelab life of at least 10 years. Whereas anodised Al 2219 samples were seen to pass this test readily, the Alodine 1200 samples were noted to suffer from general surface corrosion and crevice corrosion, particularly in weld heat affected zones. It should be noted that these tests were designed to assess this material's susceptibility to general surface corrosion and not the effect of stress corrosion, which will be reported in Chapters 7-9.

The present investigation aimed at studying two protective finish systems which were proposed for the non-anodised surfaces present in the vicinity of Al 2219 plate weldments. Ideally, protective finishes should be reasonably transparent in order that in-service visual inspection may be conducted for flaws, including fatigue cracks. The proposed finishes are : -

- Alodine 1200, brush-applied to the weld area every two years as a maintenance routine;

- Application of a room temperature curing protective layer to the Alodined weld.

Bearing in mind the requirements for space materials, a computer search found that Cuvertin 001* would be the most suitable candidate for a transparent paint.

*Cuvertin 001 is manufactured under licence in West Germany by Henkel of Dusseldorf.

5.2 Description of test samples

One Al 2219 welded plate (330 x 200 x 7 mm) in the T 851 condition was forwarded for testing. This plate had been TIG welded across its centre line, using a filler rod of Al 2319. The weld bead had been shaved, etched, dye penetrant-tested, recleaned and chemical conversion-finished with Alodine 1200.

5.3 Preparation of samples

5.3.1 The welded plate was cut into 9 strips running perpendicular to the weld. The machined edges of these samples were carefully painted with a liberal coating of Cuvertin 001 to prevent unwanted corrosion of these surfaces during subsequent exposure to the salt spray environment.

5.3.2 The nine samples were divided into three groups according to Table V.

TABLE V - DESCRIPTION OF SAMPLES

SAMPLE NO.	DESCRIPTION OF FINISH
1, 2 and 3 *	Control samples finished with the original coating of Alodine 1200, degreased.
4, 5 and 6 *	As samples 1-3, but restored with fresh Alodine 1200 at 3-days intervals during the salt spray exposure.
7, 8 and 9 *	As samples 1-3, but painted with Cuvertin 001

* Note : Samples 3, 6 and 9 were later thermally cycled under vacuum.

Refurbishment of samples 4, 5 and 6 was carried out after the first, second and third inspection periods by abrading the chemically converted surfaces with 240 grit carborundum paper until a "waterbreak free" surface was obtained and until all corrosion and Alodine was removed. Each sample was then re-alodined by brush application and returned to the salt spray cabinet.

Painting of samples 7, 8 and 9 was achieved by diluting the Cuvertin 001 clear polyurethane paint 20% with toluene and applying by spray gun to a nominal thickness of 50 µm. The paint was then cured for 7 days at room temperature. This is a treatment which provides for acceptable outgassing values within the limits defined in PSS-01-702.

Thermal Cycling under vacuum to ESA Specification PSS-01-704 was performed on samples 3, 6 and 9 for 100 cycles between the temperature extremes +60°C and -10°C. These temperatures were chosen to simulate the extreme thermal environments to be encountered by Spacelab hardware. The tests were also performed to assess the effect of space vacuum on the corrosion-resistance properties of the applied finishes.

5.4 Test Programme

The samples were numbered for traceability purposes and photographed before any salt spray exposure (Figure 16). They were then subjected to the 5% salt spray test in accordance with ASTM-B-117 except that the exposed surfaces were inclined approximately 6 degrees from the

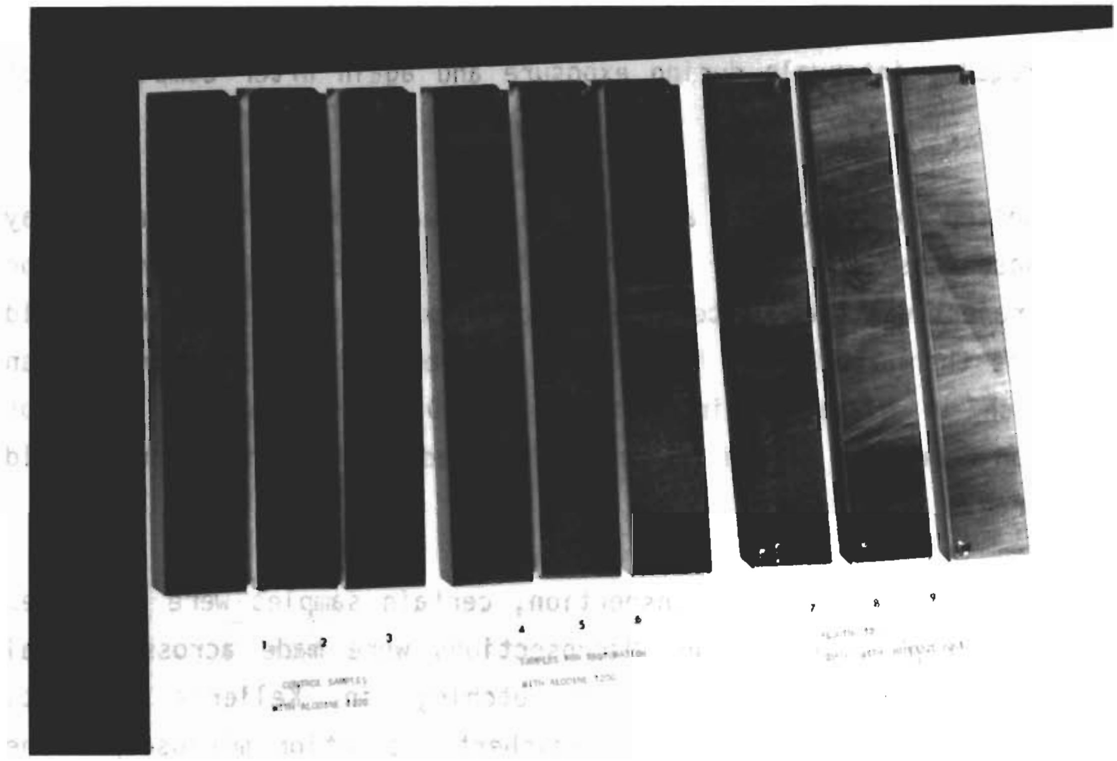

Figure 16 - Samples in the as-prepared state, prior to salt-spray tests.

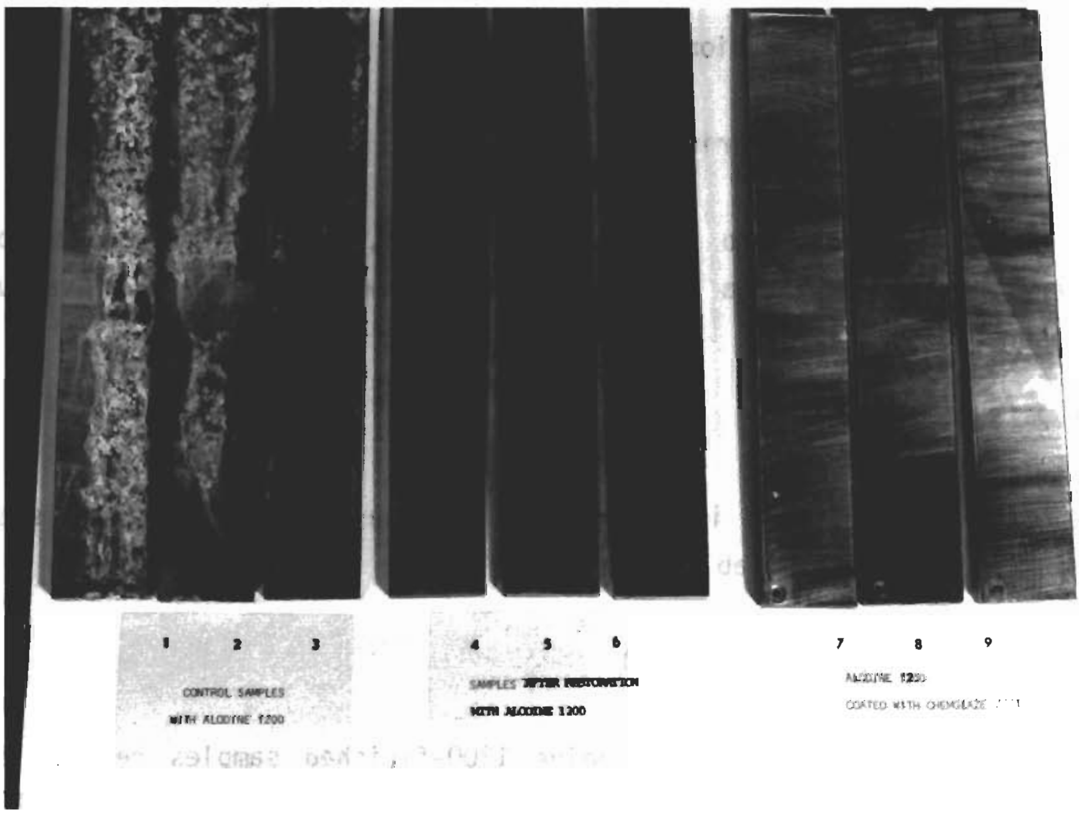

Figure 17 - Samples after 14 days exposure to 5% salt spray test. (Note that thermally cycled sample no. 3 has retained its golden brown appearance whereas samples nos. 1 and 2 have faded and are more corroded).

vertical. The panels were inspected before the salt spray exposure, at three regular intervals during exposure and again after completion of the test.

As suggested in Chapter 4, a 2-week (336 hours) exposure to salt spray was chosen as the test duration. The inspection criterion for accept/reject was that, after the 336-hour exposure, no specimen should show more than a total of 5 isolated pits or spots, none larger than 1/32 inch in diameter, in a total of 30 square inches. Areas of corrosion occurring within $^1/_4$ inch of the edges of each specimen would be ignored.

On completion of the final inspection, certain samples were submitted to metallographic inspection. Microsections were made across typical pits and, after polishing and etching in Keller's reagent, photomicrographs were taken on a Reichert projection microscope. The full test programme is detailed in Table VI.

5.5 Results and Discussion

5.5.1 Thermal Cycling Prior to Salt Spray

No samples were seen to have become cracked, crazed, delaminated or otherwise degraded as a result of the thermal cycling under vacuum exposure.

5.5.2 Salt Spray Test

The samples are shown in Figure 17 and the results of the visual inspections listed in Table VII.

a) Control samples (nos. 1 - 3)

Rapid degradation of the Alodine 1200-finished samples results in severely discoloured surfaces after the 14-day exposure. The excessive number of corrosion sites is cause for this finish to be unsuitable for the proposed total Spacelab life of 10 years. These results confirm the findings of Chapter 4.

It is interesting to note that sample no. 3, which underwent thermal cycling under vacuum, supports considerably less corrosion sites than the non-cycled (heat treated) samples. This sample also remained deep brown in colour after the final exposure to salt spray; samples nos. 1 and 2 changed from deep brown to a pale straw colour after only 3 days' exposure to the spray. The reason for this is not known, but it is assumed that the chromate conversion finish is modified and has become denser and more tenacious. Dissolution or breakdown of this modified film by the presence of chloride ions is

TABLE VI - PLANNING OF TEST PROGRAMME

CONTROL SAMPLES (Alodine 1200)			RESTORATION SAMPLES (Alodine 1200)			PAINTED SAMPLES (Cuvertin 001)			STEPS
1	2	3	4	5	6	7	8	9	1) Preparation
						x	x	x	2) Painting
		x			x			x	3) Thermal Cycling
x	x	x	x	x	x	x	x	x	4) Inspection
x	x	x	x	x	x	x	x	x	5) Salt spray exposure
x	x	x	x	x	x	x	x	x	6) Inspection on day 3
			x	x	x				7) Restoration
x	x	x	x	x	x	x	x	x	8) Salt spray exposure
x	x	x	x	x	x	x	x	x	9) Inspection on day 7
			x	x	x				10) Restoration
x	x	x	x	x	x	x	x	x	11) Salt spray exposure
x	x	x	x	x	x	x	x	x	12) Inspection on day 10
			x	x	x				13) Restoration
x	x	x	x	x	x	x	x	x	14) Salt spray exposure
x	x	x	x	x	x	x	x	x	15) Inspection on day 1
	x	x		x			x		16) Metallographic inspection

TABLE VII - VISUAL INSPECTION RESULTS FROM SAMPLES AFTER EXPOSURE TO SALT SPRAY

SAMPLE NO.		EXPOSURE DAYS	NUMBER OF CORROSION SITES EXPOSED SIDE	UNDERSIDE
ALODINE 1200	1	3	2	0
		7	4	3
		10	50	7
		14	> 100 (*)	7
	2	3	3	0
		7	5	3
		10	50	7
		14	> 100 (*)	28
	3	3	0	0
		7	7	0
		10	10	2
		14	50	2
RESTORATION SAMPLES	4	3	4	0
		7	6	0
		10	20	0
		14	53	3
	5	3	3	1
		7	2	1
		10	20	1
		14	58	1
	6	3	4	0
		7	10	0
		10	20	1
		14	52	3
PAINTED SAMPLES	7	3	0	0
		7	0	0
		10	0	0
		14	0	0
	8	3	0	0
		7	0	0
		10	0	0
		14	0	0
	9	3	0	0
		7	0	0
		10	0	0
		14	0	0

* 70% of surface area covered in corrosion products

markedly reduced, whereas dissolution and corrosion of the unmodified film progresses rapidly with the formation of a blend of $AlCl_3$ (normally soluble in water) and $Al(OH)_3$. These are the corrosion products seen in Figure 17 (Samples nos. 1 and 2).

b) Refurbished samples (nos. 4 - 6)

These samples were noted to fail the test having more than the permitted number of corrosion sites (see Table VII). However, refurbishing has held the corrosion at bay quite well, presumably because corrosion products are cleaned away so as to leave a visually more acceptable finish, and any pitting which does commence is retarded by the periodical application and surface conversion produced by the Alodine 1200. The corrosion is confined to the areas away from the weld.

c) Painted Samples (no.s 7-9).

All samples in this group passed the test and remained unaffected by the salt spray environment except for slight seepage under the edge coating due to exposure of the sharp aluminium alloy corners through the paint. It should be noted that all corners and changes in section need to be radiused as, otherwise, they will not be covered by a sufficiently thick layer of paint. The paint remained transparent throughout the test, thus facilitating visual inspection of the underlying chromated aluminium.

5.5.3 Metallography

The surfaces of test pieces which contained features to be examined in cross-section are identified in Table VI. The microsections are made in a plane which is parallel to the rolling direction of the plate and normal to the surface which was exposed to the salt spray. The non-exposed sides of specimens are noted in Table VII to have suffered very little corrosion. Sample no. 2 was observed to support very shallow pitting on its underside (Figure 18) and the thin, intact chromate conversion finish was not detected by optical microscopy. The exposed side of this sample was noted to exhibit deeper pits (Figures 19, 20 and 21) in both the parent metal and weld pool. Only isolated pits were observed on Sample no. 3 which had been thermally cycled, they were similar to those shown in Figures 19-21. The refurbished Sample no. 5 was also noted to support a cleaner surface and, although pits were observed in cross-section, they were wide-mouthed, presumably due to the intermediate abrasive treatments described in Paragraph 5.3.2. The Cuvertin 001 paint system afforded good protection, being an effective barrier layer of 45-50 µm. The principal disadvantage, characteristic of paint systems, is that they will not remain effective once mechanically damaged. Their use is therefore only recommended for applications where considerable traffic or abrasions are not expected. This paint can be seen to have adhered well to the Alodined plate finish. Thermal cycling and salt spray were not observed to cause micro-crazing of the cured paint.

5.6 Conclusions

5.6.1 The results indicate that non-stressed Al 2219 weldments are best protected from general surface corrosion by a paint system applied to a chromated aluminium finish. The recommended paint, Cuvertin 001, is acceptable from an outgassing point of view and remains optically transparent after exposure to the test environments. This will facilitate periodic visual inspection of the welds.

5.6.2 As reported in Chapter 4, the Alodine 1200 again failed to pass the 14-day exposure to salt spray. It also failed to satisfy the MIL-C-5541 7-day exposure to salt spray.

5.6.3 Although the "restoration" treatment failed the test programme, this system may be suitable for <u>easily accessible</u> non-stressed weldments on Spacelab. Possibly, after careful visual inspection, a decision to refurbish flight hardware might be approved, thus permitting removal of corrosion products, Alodine and pits by abrasion, followed by the re-application of fresh Alodine 1200. Figure 7 illustrates the location of some easily accessible weld zones.

Figure 18 - As-polished section showing the underside surface of Alodined sample no. 2 At this magnification the exceedingly thin (< 0.2 μm) chemical conversion finish cannot be detected in cross-section (x400).

Figure 19 - As-polished section of the exposed face of Alodined sample no. 2. Pits are noted to be 15 μm deep (x400).

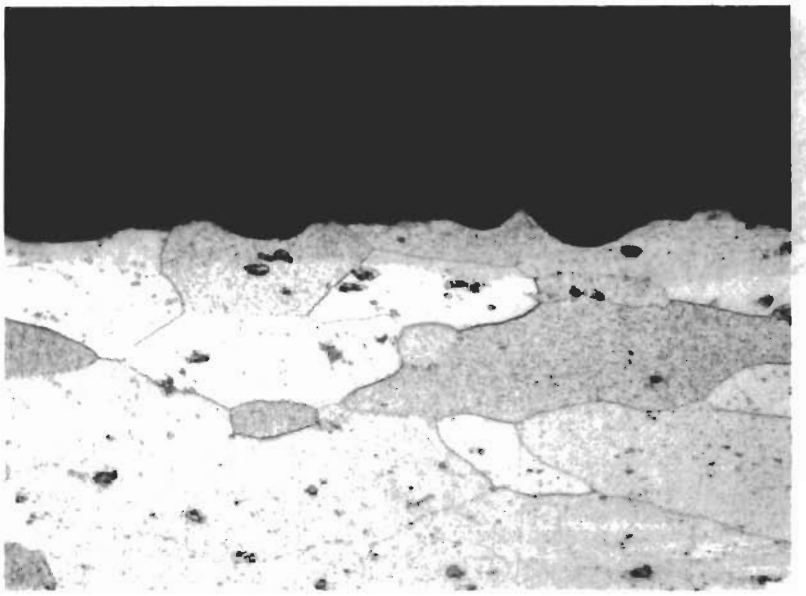

Figure 20 - As in Fig. 19, but etched with Keller's reagent to reveal grain structure in a region of the parent metal. Pits have a depth of 12 µm (x400).

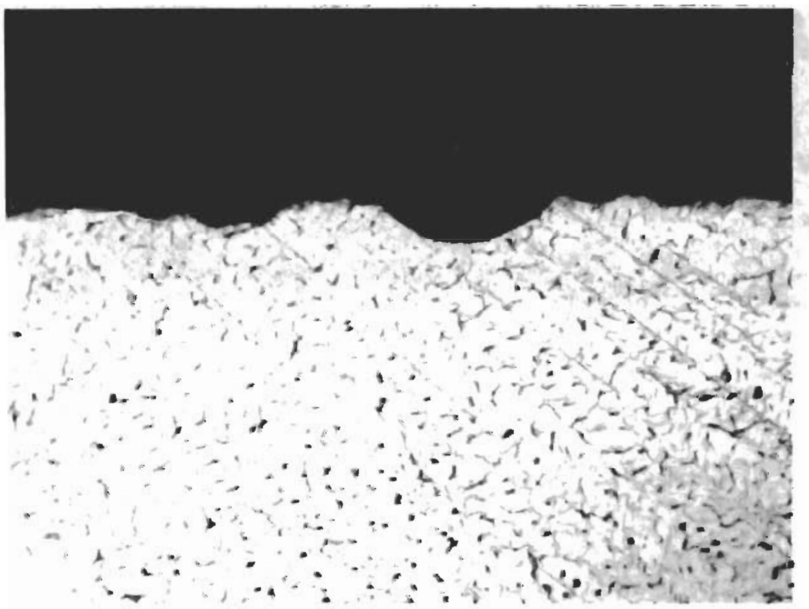

Figure 21 - As Fig. 20 but in weld pool. Pits have a depth of 10 µm (x400).

6. INTERGRANULAR CORROSION TESTING OF WELDED PLATE

6.1 Introduction

A rapid test to assess the susceptibility of welded 2219 alloy to intergranular corrosion in the absence of stress is detailed in Federal Test Method Std. no. 1516 (method 822.1) and in U.S. Military Specification MIL-H-6088E. The test will provide a control as to the homogeneiety of the copper content within the grain structure of 2219. Incorrect solution treatments and undesirable welding schedules that promote the formation of large $CuAl_2$ intermetallic particles along grain boundaries can be identified if exfoliation of the surface is observed after the test exposure.

6.2 Test Procedure.

The samples consisted of 4 mm thick 2219-T851 plate TIG welded to standard procedures with an Al 2319 filler alloy. Each sample was pre-etched in a solution of sodium hydroxide to produce a uniform surface condition. Samples were then immersed in a corrosive medium made up of :

57 g	Sodium chloride
10 ml	Hydrogen peroxide, dissolved in
1 l	Distilled water.

The temperature of the corrosive medium was 30 °C ± 5 °C and immersion time was 6 hours.

After exposure the samples were visually examined and then prepared metallographically to ascertain whether or not intergranular corrosion had occurred.

6.3 Results

No intergranular corrosion was found to have taken place in any region of these samples. Very slight pitting corrosion appeared in the parent metal well away from the weld pool and its heat-affected zone.

6.4 Conclusion

From these findings it was assumed that the welding process had been performed correctly.

7. METALLURGICAL EXAMINATION OF 2219-T851 'C' RING SAMPLES (THICK PLATE) AFTER STRESS-CORROSION TESTING

7.1 Introduction

Stress-corrosion tests were carried out on the 2219 aluminium alloy by Alcan Booth Sheet Ltd. The tests were carried out on samples which had been machined from three plates of different thicknesses, i.e. 35, 80 and 105 mm. The test samples consisted of fifteen 'C' rings and three constant-strain tension specimens, each of which was stress corrosion tested in accordance with ASTM Method G38-73. The stress levels were set up at 75% of the 0.2% proof stress as determined in the transverse direction for these plate thicknesses.

Although only a 30-day exposure to testing was the requirement, the 'C' rings remained under test for 48 days without developing stress-corrosion cracks. The constant strain tension specimens were all unbroken after the required 30 days. Eventually one specimen broke after 69 days, the other two were still intact after 86 days. Three of the 'C' ring samples, one from each plate size, have been submitted to ESA for examination.

7.2 Materials Details

7.2.1 Cast Analyses (weight per cent)

PLATE SIZE (mm)	Cu	Mn	Mg	Fe	Si	Zn	Ti	Zr	V
80 & 105	6.3	0.28	<0.1	0.12	0.07	0.03	0.07	0.14	0.09
35	6.5	0.28	<0.1	0.12	0.07	0.03	0.07	0.14	0.09

7.2.2 Heat Treatment

Pre-heat for rolling : 24 hours at 500-520°C.
Solution heat treatment : <63 mm 4 hours >63 mm 8 hours at 530-540°C.
Control Stretch : 1 - 2 %
Precipitation treatment : 18 hours at 172-177°C

7.2.3 Tensile Properties

Plate Size (mm)	Test Direction	0.2% Proof Stress (N/mm^2)	UTS (N/mm^2)	Elongation %
105	Transverse	362	454	8.5
80	"	348	462	9.0
35	"	374	474	10.0

7.3 Method of Examination

Samples were cut from each of the three 'C' rings, and then mounted in a clear, cold-setting epoxy resin.

The mount was ground and polished to a 0.25 μm finish then examined under a Reichert projection microscope in both the polished and etched conditions. The etching was carried out with Kellar's reagent, i.e.

HF	1.0 ml
HNO_3	2.5 ml
HCl	1.5 ml
H_2O	95.0 ml

The resulting 'smutting', common with alloys containing large amounts of copper, was removed in a 50% solution of nitric acid.

7.4 Results

7.4.1 Metallography revealed that no stress-corrosion cracks were present on any of the samples and that there was no obvious difference in the extent of the corrosive attack from one plate size to another. Figure 22 shows a typical example.

7.4.2 Figures 23-25 detail various aspects of the corrosion. On the faces that were under tensional stressing the corrosive attack was generally that of wide-based pitting. Compression faces exhibited pitting that was predominantly laminar with only occasional instances of wide-based pits.

On all samples, both on tension and compression faces, the attack was mainly transcrystalline, with only occasional instances of intercrystalline attack (See Fig. 24).

7.5 Conclusions

From this evidence it is quite clear that the 2219-T851 alloy possesses the required resistance to stress-corrosion cracking. Also, since the corrosion takes the form of predominantly transcrystalline pitting, it is probable that the ultimate failure condition would be due to a reduction in section rather than an intergranular weakening.

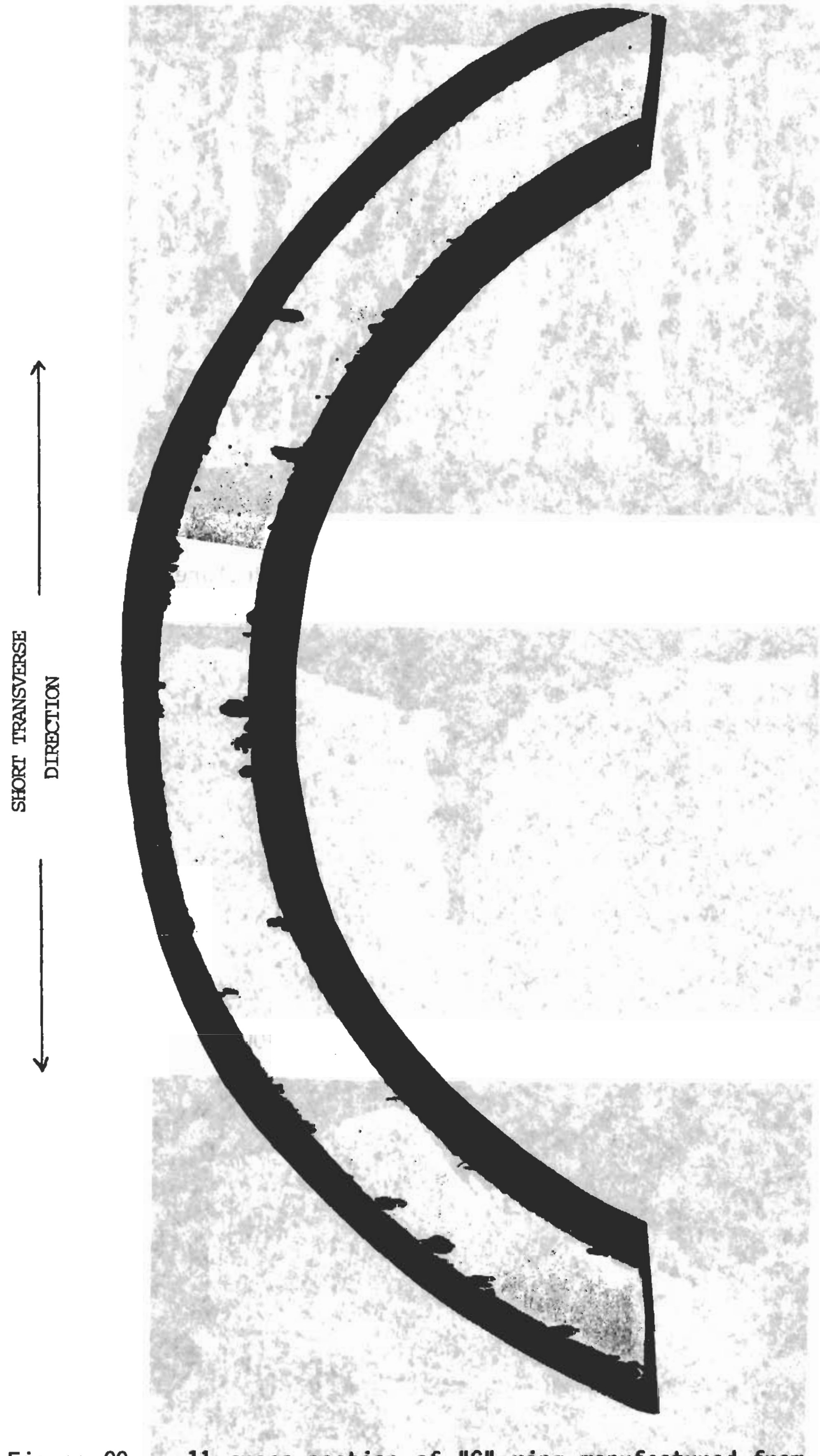

Figure 22 -x 11 cross-section of "C" ring manufactured from 35 mm thick plate.

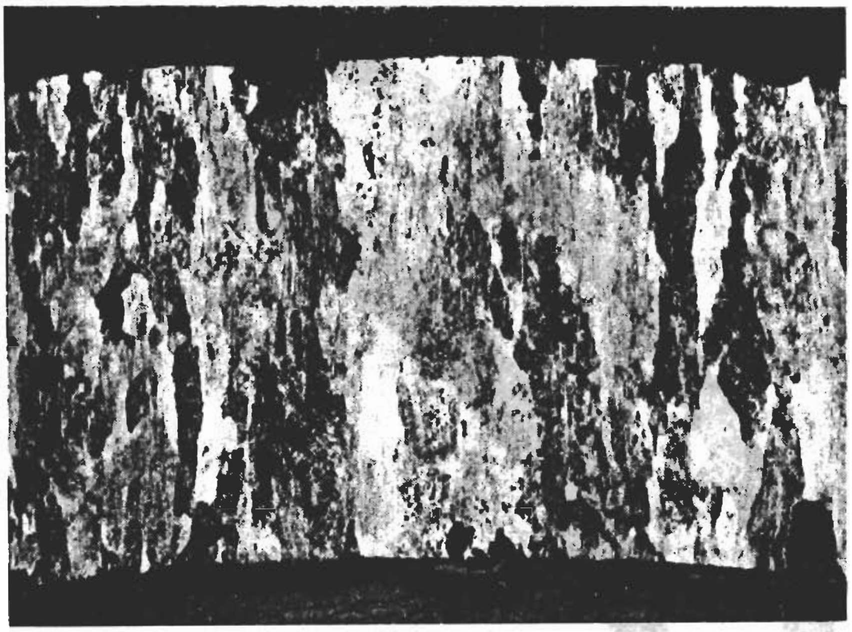

Figure 23 - As Fig. 22 but etched to reveal microstructure (x45).

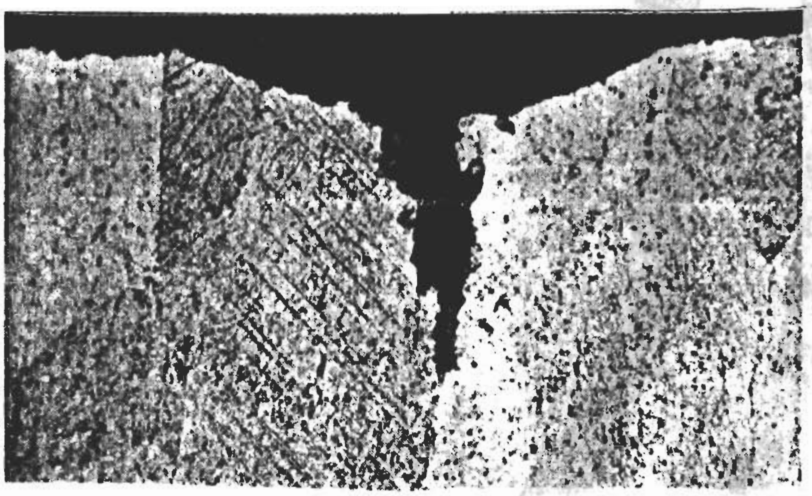

Figure 24 - Example of intergranular corrosion. (x4000).

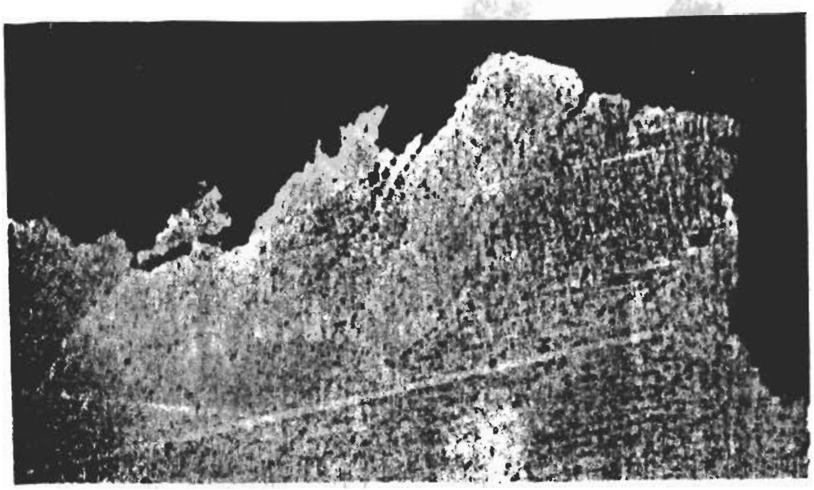

Figure 25 - Example of transgranular corrosion. (x400).

8. METALLURGICAL EXAMINATION OF 2419-T 851 ROUND TENSION BAR SAMPLES (LARGE FORGED RINGS) AFTER STRESS-CORROSION TESTING

8.1 Introduction

Stress-corrosion-cracking (SCC) tests have been performed on samples of 2419 aluminium forged rings in the T 851 condition. This material was produced and tested by Thyssen Henrichshütte. The test method followed ASTM specification G38-73 (for C-rings), stress consideration, stressing methods, machining, surface preparation and inspection being as specified although round tension bars were employed instead of C-rings.These tests were performed on six samples from the remainders of the three Thyssen pre-production rings. These 4 m diameter rings were the largest to have been made in Europe from a high-strength aluminium alloy.

The stressed test samples were subjected to alternate immersion in a salt solution according to Fed. Test Method Std. no. 151b for an agreed duration of 30 days. No sample failures were noted after 30 days and after an extended period the exposed pieces were taken from the environmental chamber and submitted to ESA for metallurgical analysis.

8.2 Materials Data

8.2.1 Chemical Composition

RING No.	COMPOSITION PER CENT								
	Cu	Si	Fe	Mn	Mg	Zn	Ti	V	Zr
3580	6.4	0.07	0.13	0.29	0.01	0.03	0.08	0.10	0.14
256	6.8	0.08	0.16	0.31	0.01	0.04	0.07	0.09	0.13
2814	6.8	0.08	0.16	0.31	0.01	0.04	0.07	0.08	0.13
Spec. Limits 2219	5.8 - 6.8	0.20	0.30	0.20-0.40	0.02	0.10	0.02-0.10	0.05-0.15	0.10-0.25
are 2419	5.8 - 6.8	0.15	0.18	0.20-0.40	0.02	0.10	0.02-0.10	0.05-0.15	0.10-0.25

CHEMICAL COMPOSITION OF RINGS AND SPECIFIED VALUES

8.2.2 Heat Treatment

- Forging temperature : 430-390°C (roll forging).
- Heat treatment : Solution heat treat, 533 °C ± 5 °C (10 hours).
  Quench time, 90 seconds.
  Quench medium, water.
  Cold stretch, 2-3%.
  Precipitation harden 175 °C ±5 °C (30 hours).

8.3 Experimental Procedure

8.3.1 Stress Corrosion Cracking (SCC) Test.

Round tension bars were machined from the six samples (two samples from three different locations) taken from the three pre-production rings. The machined specimens, having a 6 mm diameter, were stressed perpendicular to the grain flow of the forged rings, and held at a constant strain. The specimens were stressed to a level as defined in ASTM-Method G38-73, which is 75% of the material yield strength in the tangential direction for the applicable thickness of each ring; this was determined to be 75% of 262 N mm^{-2} (i.e. 196 N mm^{-2} perpendicular to grain flow).

The stressed specimens had been exposed to a solution of 3.5 percent NaCl for a duration of 30 days by alternate immersions of 10 minutes in the solution and 50 minutes out of the solution (according to Fed. Test Method 151b). No failures occurred after 30 days, so the test was extended providing for a total exposure of 80 days. One sample failed after 39 days, another after 75 days.

8.3.2 Metallographic Examination

The as-tested specimens were removed from the corrosion rig and photographed. Two samples were submitted for metallographic examination, they were :

a) Sample fractured after 39 days.

b) No fracture after 80 days' exposure under load, but this sample broke on removal from clamping device.

8.4 Results

8.4.1 The environmental test results performed by the Thyssen laboratories showed that the AA 2419 Alloy, in the T 851 condition successfully completed the SCC test (i.e. no failures after 30 days). The first failure occurred after 39 days' total alternate immersion in the NaCl solution (Thyssen believed this to be due to electrolytic or bimetallic corrosion caused by the lack of insulation between test sample and the test fixture). The following fracture occurred after 75 days' exposure. The test was stopped after 80 days.

8.4.2 The fracture surfaces of all the failed samples were visually identical. Figures 26 and 27 show these surfaces to be masked by the corrosion debris, a light grey film which is expected to be a mixture of Al_2O_3 and $AlCl_3.H_2O$.

8.4.3 The cross sections shown in Figures 28-31 show the 39-day failed sample to have a microstructure identical to that of the 80-day sample. No cracks which could be attributed to SCC were identified. The corrosive attack was confined to localised pitting and laminar pitting.
The corrosion paths were unrelated to the grain structure of the material. Figure 32 clearly highlights the fact that pitting corrosion follows adjacent to the coarse network of particles within both samples. Most of the large inclusions are shown up by polarised light as predominately $CuAl_2$ which, owing to the high copper content of this alloy, was unable to dissolve completely into the saturated solid during the solution treatment. These $CuAl_2$ particles have no doubt been broken up and redistributed during the forging treatment but they exist in a displaced network that had originally formed during solidification of the cast metal. The present fine elongated grains result from subsequent forging and heat treatments; their boundaries have little relationship to the massive $CuAl_2$ particles.

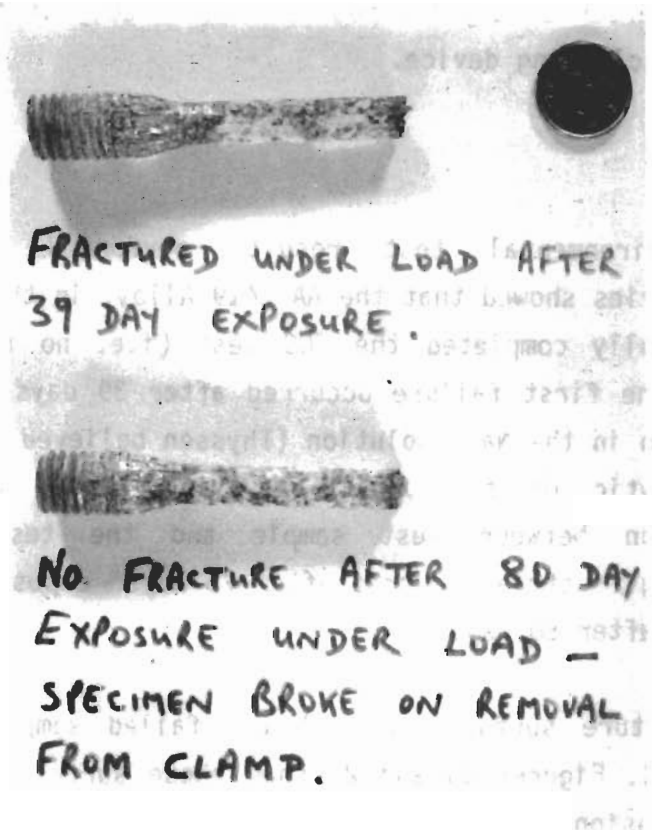

Figure 26 - Exposed specimens, as received from Thyssen.

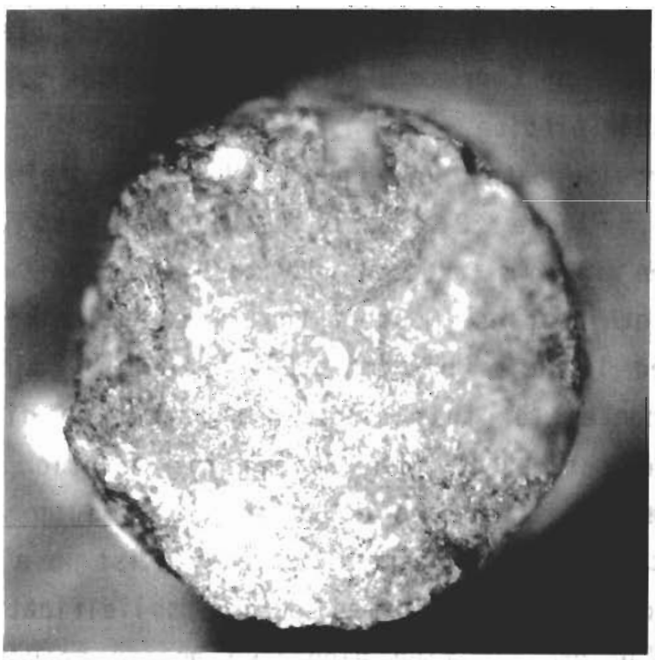

Figure 27 - Fracture surface of sample which failed after 39 days (x12).

Figure 28 - As polished.

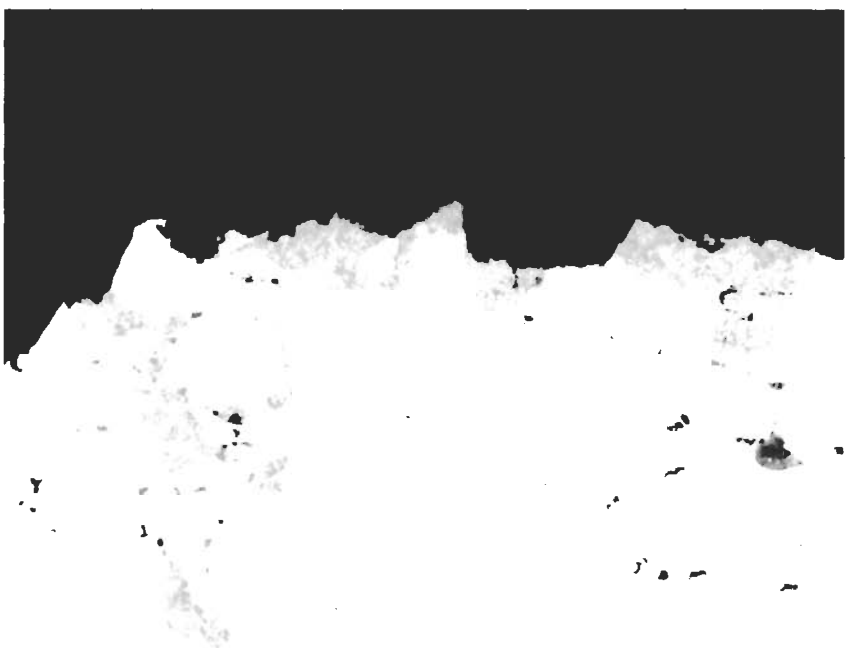

Figure 29 - Detail from Fig. 28 adjacent to fracture surface (x125).

MICROSTRUCTURE OF 39 DAY SAMPLE

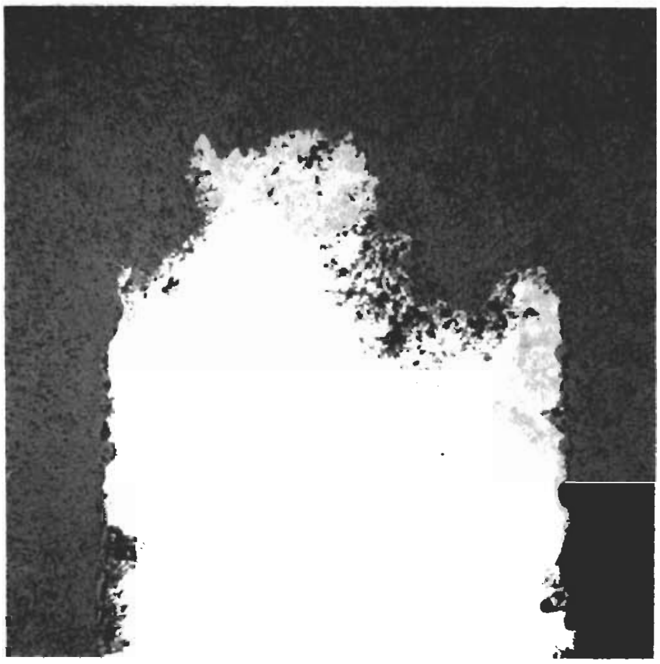

Figure 30 - As polished 80 days sample. (x12).

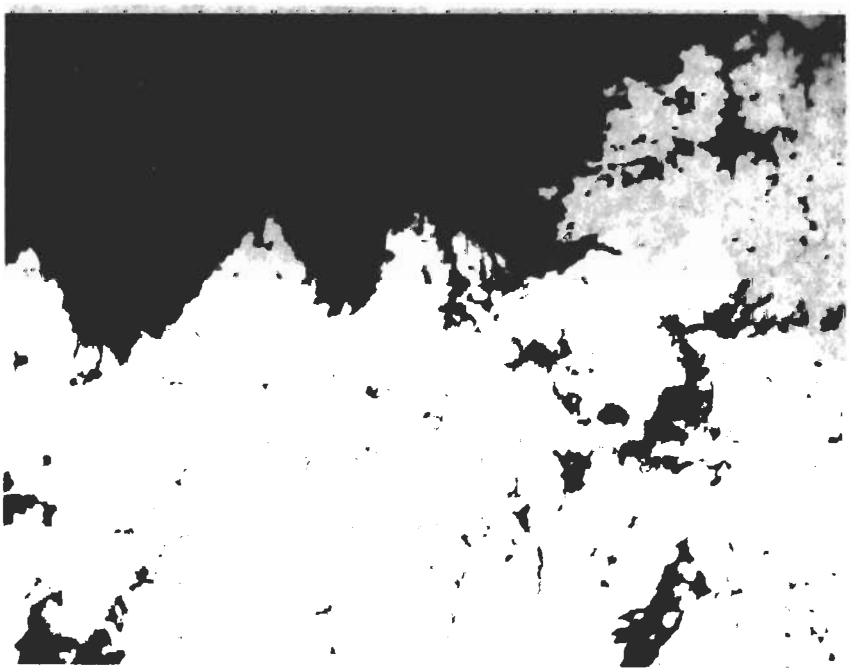

Figure 31 - As Fig. 30, but etched; showing general pitting corrosion. (x125).

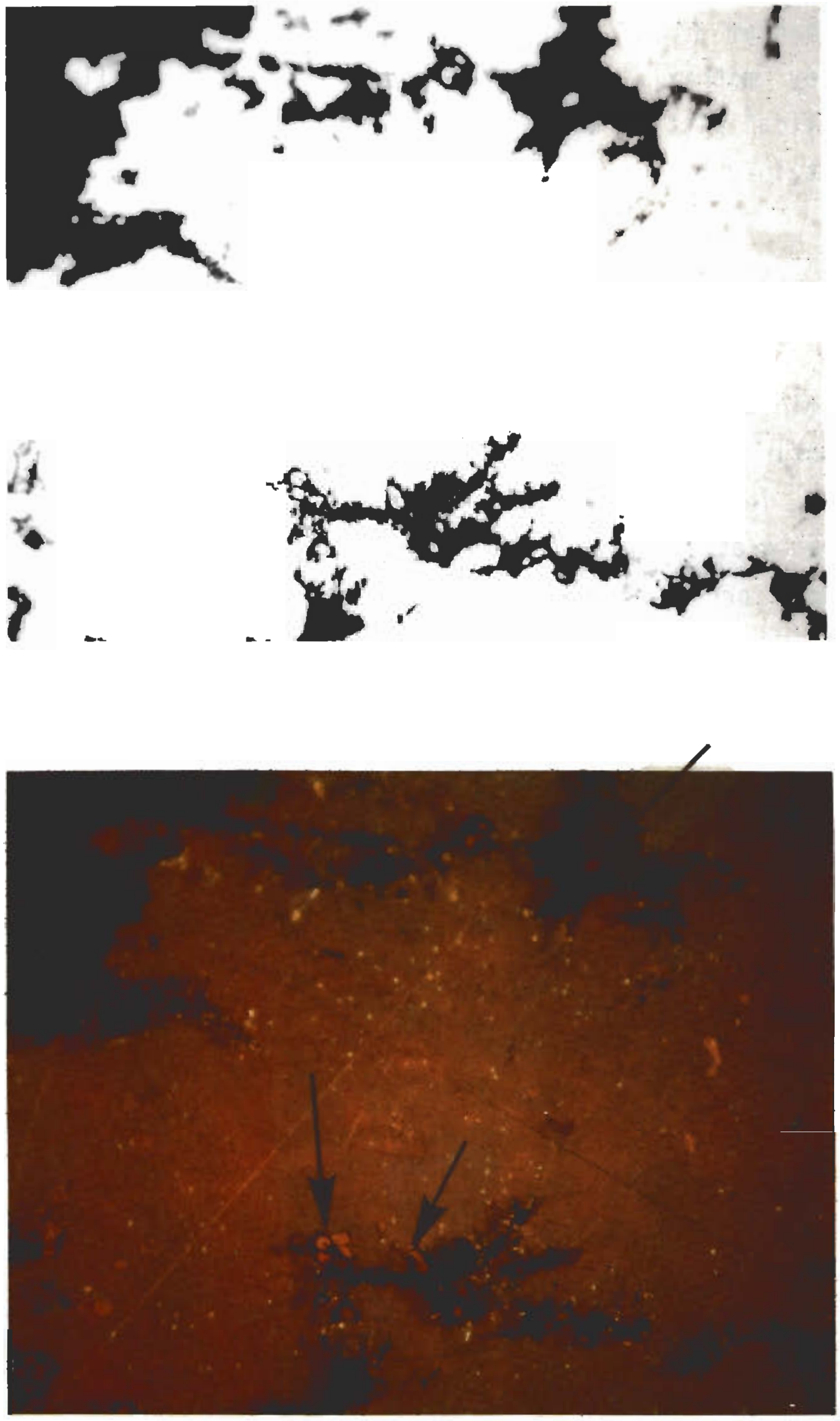

A

B

Figure 32 - Detail from 39-day sample near fracture surface using polarised light. The colour photograph (B) reveals the arrowed $CuAl_2$ inclusions as bright orange.

In salt solutions these particles will behave as minute cathodes causing the surrounding material to corrode by a galvanic mechanism (i.e. $CuAl_2$ is electro positive with respect to the alloy matrix). The test samples will naturally fail once a critical pitting depth is reached and the applied stress cannot be sustained by the remaining cross-sectional area.

8.5 Conclusion

8.5.1 Aluminium wrought alloys are most susceptible to stress-corrosion cracking when stressed at right angles to the direction of working (i.e. in the short transverse direction). This is probably because more grain-boundary area of the elongated grains along which cracks propagate come into play. The present samples had been machined so as to expose this most susceptible grain direction.

8.5.2 The results of this test show that AA 2419 in the T851 condition is essentially immune to stress-corrosion cracking. Similar conclusions were drawn in Chapter 7 for plate material.

8.5.3 The long-term mode of failure of these samples is assessed to result from microscopic galvanic corrosion between copper-containing intermetallic particles and the alloy matrix.

9. STRESS CORROSION TESTING OF 2219-T851 WELDMENTS

9.1 Introduction

Welded samples were made in-line with the first Spacelab production weldments. Identical materials and process parameters were used to ensure that all destructive tests made on those samples would yield results representative of flight hardware material. The work reported in this Chapter concerns constant-load stress-corrosion testing carried out on various forms of welded 2219-T851 alloy made to standard company practices.

Unwelded short transverse specimens from BS L93 (equivalent to slightly overaged AA 2014) were performed in parallel as this was thought to be an alloy susceptible to stress corrosion and one that could be used as a control. The samples were assigned the following codes :

A 2219-T851	Single pass TIG welded 7 mm plate with a matching filler AA 2319, with no post-weld heat treatment applied. The weld bead had been machined off. Processes were those for the modular pressure shell shown in Fig. 1.
B 2219-T851	As A, but Double Pass TIG welded before removal of weld bead.
C 2219-T851	As A, but repaired according to a standard practice. Metal was removed from initial weld pool by machining, followed by further TIG passes with a matching filler.
J 2219-T851	Single pass electron beam (EB) welded 5 mm thick plate. The process procedure was that employed for the Igloo structure shown in Fig. 2.

E BS L93 — 90 mm thick plate. Samples taken in short transverse direction having a 60 mm^2 cross-sectional area.

ST. BS L 93 — As E, but samples having a 36 mm^2 area.

The welded samples were to be tested at a stress level of 75% of the 0.2% proof stress of the weldment as supplied.

The BS L 93 unwelded specimens were to be stress-corrosion tested at 15%, 25% and 75% of the 0.2% proof stress of this material tested in the short transverse direction.

9.2 Test Procedure

The general test procedure follows that detailed in ESA specification PSS-01-737 "Determination of the Susceptibility of Metals to Stress Corrosion Cracking". The tests were carried out under alternate immersion conditions in 3.5% sodium chloride over a thirty-day (720 hours) exposure period. Unstressed control specimens were exposed to the same environment to provide a basis for comparison in assessing stress-corrosion susceptibility of alloys that survive thirty days in the test. The susceptibility is assessed by tensile tests to compare the residual strengths of the specimens exposed stressed and unstressed, and by metallographic examination of microsections from stressed and unstressed specimens to distinguish between stress corrosion and intergranular corrosion or pitting occurring independantly of stress. The test rig is shown in Figures 33 and 34.

The dimensions of the as-received plate samples determined the overall sizes of the flat stress corrosion specimens which were :

SAMPLES	GAUGE LENGTH (mm)	WIDTH (mm)	THICKNESS (mm)	END SECTION (mm)
A, B, C	50	10	7	50 x 30
J	50	5	5	50 x 25
E	28	10	6	30 x 25
ST	28	6	6	30 x 25

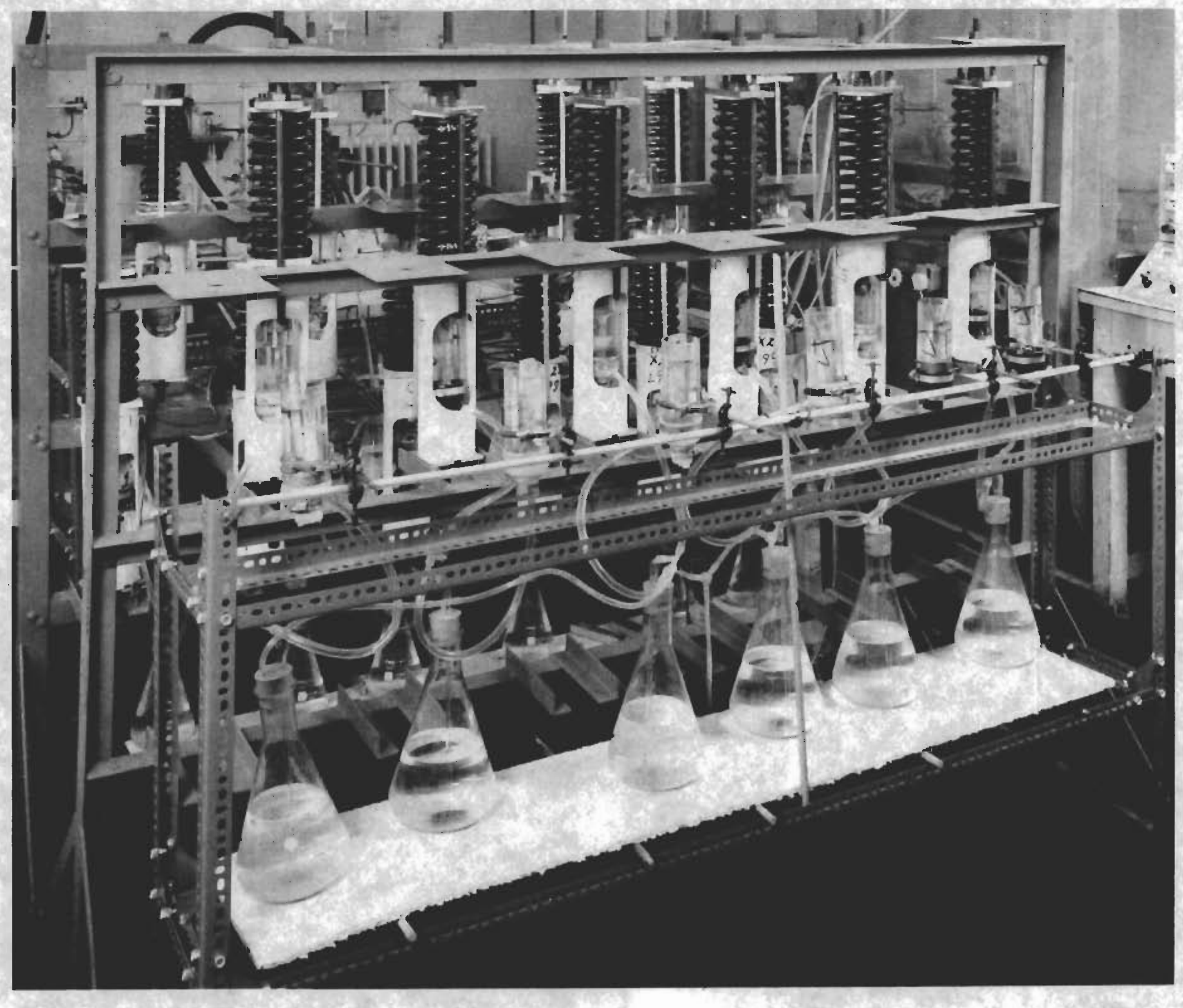

Figure 33 - General view of stress-corrosion tests and unstressed control. Test facility is at the BNF Metals Technology Centre.

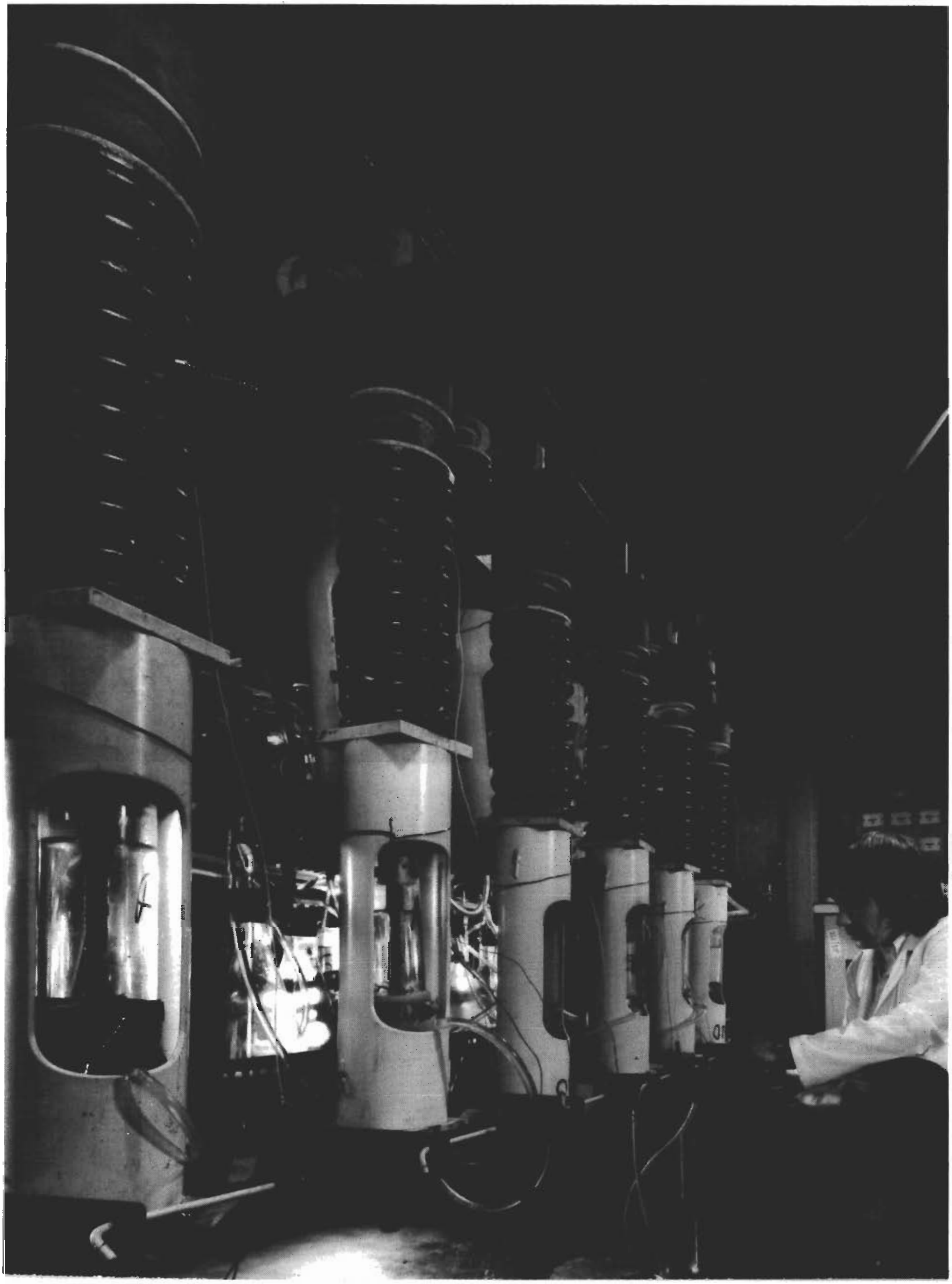

Figure 34 - General photograph showing laboratory set-up for constant load stress-corrosion testing at the BNF Metals Technology Centre.

The 0.2% proof stress was established for each type of sample from an average of three tensile tests. These values would establish the stresses at which the stress-corrosion tests were to be conducted and provide reference values of tensile strength and elongation for comparison with specimens to be tensile tested after surviving thirty days in the stress-corrosion test.

The stress-corrosion tests were carried out in triplicate, the specimens being loaded in tension by calibrated springs according to the ESA PSS test procedure. The time to failure was recorded automatically for the stressed samples. They were then removed together with the corresponding unstressed sample. After removal from the salt environment, and at the end of the thirty day period, all specimens were washed in warm water with gentle scrubbing to remove most of the salt and corrosion products on them. They were dried in warm air and stored in a desiccator. The samples were then tensile tested and subjected to metallographic examination in accordance with the ESA PSS test procedure.

9.3 Results

9.3.1 Results for 'Type A' Single Pass TIG welded 2219 Specimens.

Specimens A8, 9 and 10 were fitted in the stress corrosion jigs and loaded to 75% of the average proof stress obtained in tensile tests on specimens A1, 2 and 3, i.e. 115 N mm^{-2} (11.7 kgf mm^{-2}). Specimens A4, 5 and 6 were set up as unstressed controls. No failures of the loaded specimens occurred during the 30-day test period. The stressed specimens A9 and 10 and the unstressed control specimens A5 and A6 were, therefore, tensile tested. The broken tensile test specimens together with specimens A4 and A8 which had not been tensile tested were then metallographically examined.

The full results are given in Table VIII and the samples and photomicrographs shown in Figures 35 and 36. No stress-corrosion cracks were observed in any of the specimens, either in the weld pool, the heat-affected zone (HAZ) or the parent plate material.

TABLE VIII - SINGLE PASS TIG WELDED 2219-T851 ALLOY SPECIMENS

RESULTS OF MECHANICAL AND STRESS-CORROSION TESTS

SPECIMEN NUMBER	DESCRIPTION	MECHANICAL TEST RESULTS			STRESS-CORROSION TEST RESULTS			
		0.2% PS N/mm^2	TS N/mm^2	ELONGATION % ON 50 mm	TIME TO FAIL (hours)	Max. Depth of Corrosion Visible in Microsection* (µm)		
						PARENT	HAZ	WELD
A 1	Tensile test specimen	153.4	281.7	6	Not exposed			
A 2	"	153.6	281.5	6	Not exposed			
A 3	"	153.4	276.2	5	Not exposed			
Average	"	153.4	279.8	6				
A 8	SC Specimen	- not pulled -			U	430	208	none
A 9	"	178.6	276.4	4	U	410	208	none
A 10	"	174.3	231.6	3	U	510	250	none
A 4	Unstressed control (720 h.)	- not pulled -				208	542	none
A 5	"	147.1	250.3	4		210	210	none
A 6		148.6	269.7	6		240	250	none

stress-corrosion specimens were stressed at 75% of 0.2% ps of weldment = 115 N/mm^2

U = not failed after 30-day test (720 hours)

* no stress-corrosion cracking was observed on these specimens

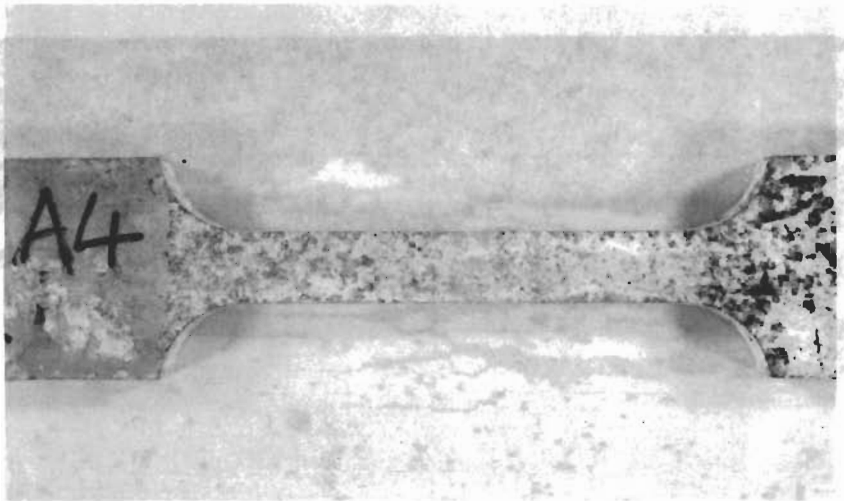

Figure 35a) - Sample A4 unstressed control showing general pitting over surfaces.

Figure 35b) - A4 as polished in HAZ, general exfoliation.

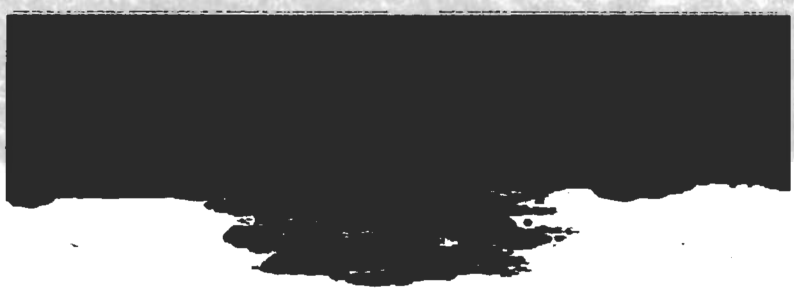

Figure 35c) - A4 as polished in parent metal, general pitting and some exfoliation. (x29).

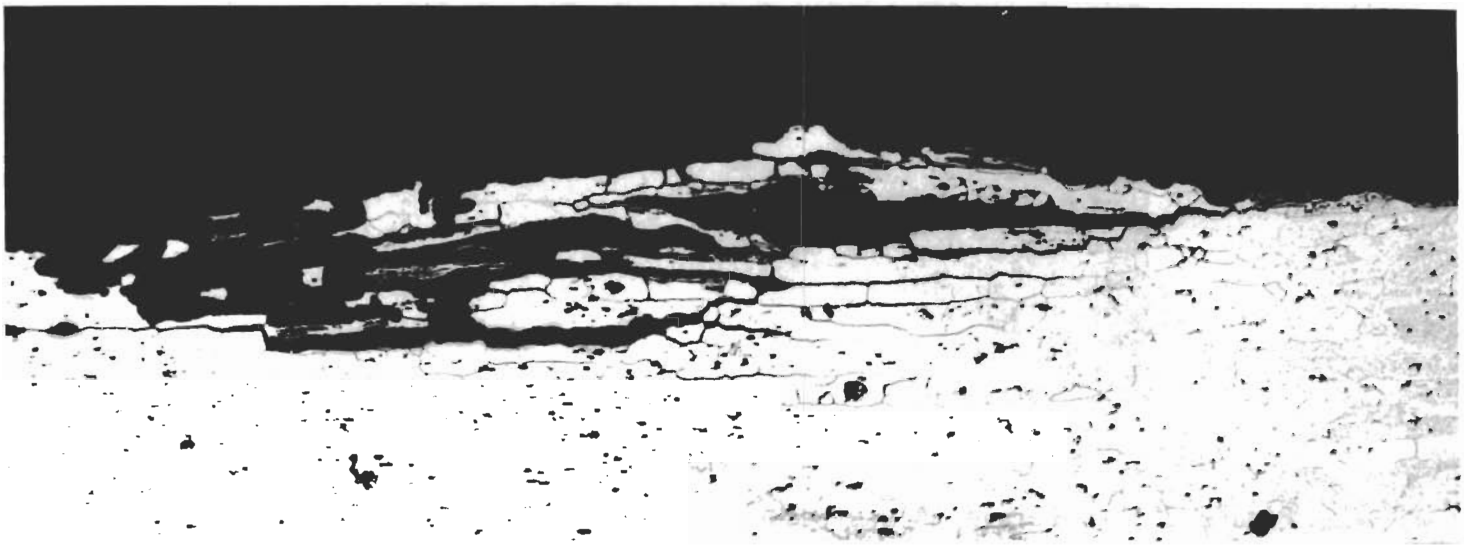

Figure 35d) - A4 worst intergranular corrosion and exfoliation adjacent to weld pool in HAZ, maximum depth is 208 µm. (x120).

Figure 35e) - A4 worst exfoliation in parent metal, maximum depth is 430 µm (x120).

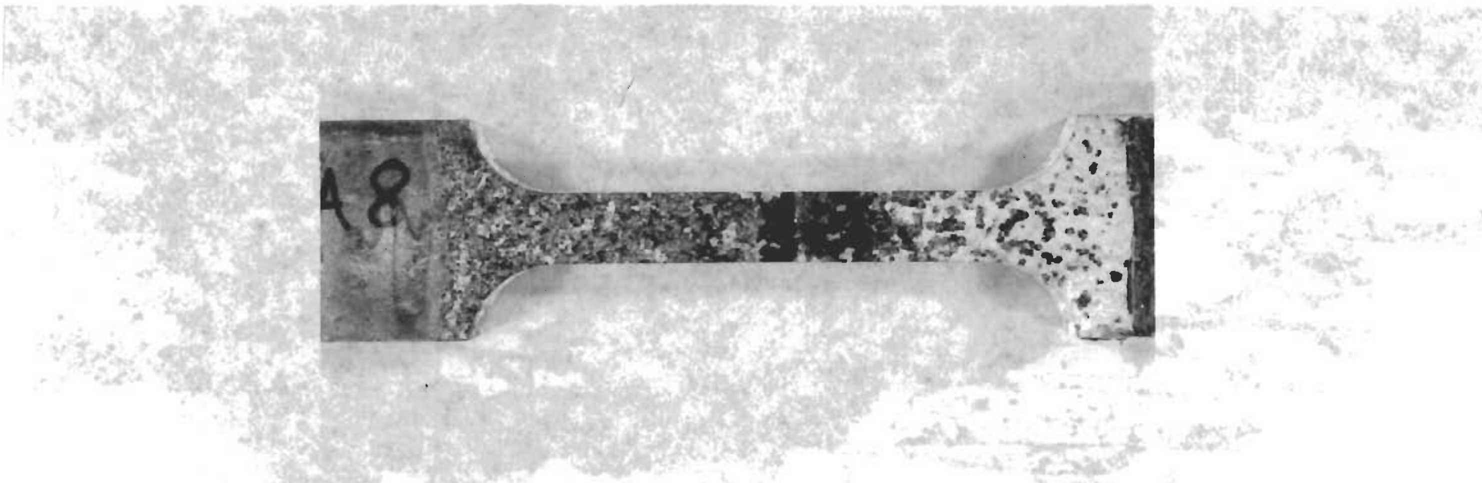

Figure 36a) - Sample A8. Stressed corrosion sample showing general pitting over surfaces.

Figure 36b) - A8. Pit and intergranular crack in HAZ. (x29).

Figure 36c) - A8. Pit and intergranular crack in HAZ. (x29).

Figure 36d) - A8. Deepest pit in HAZ adjacent to weld pool. Depth is 542 µm. (x120).

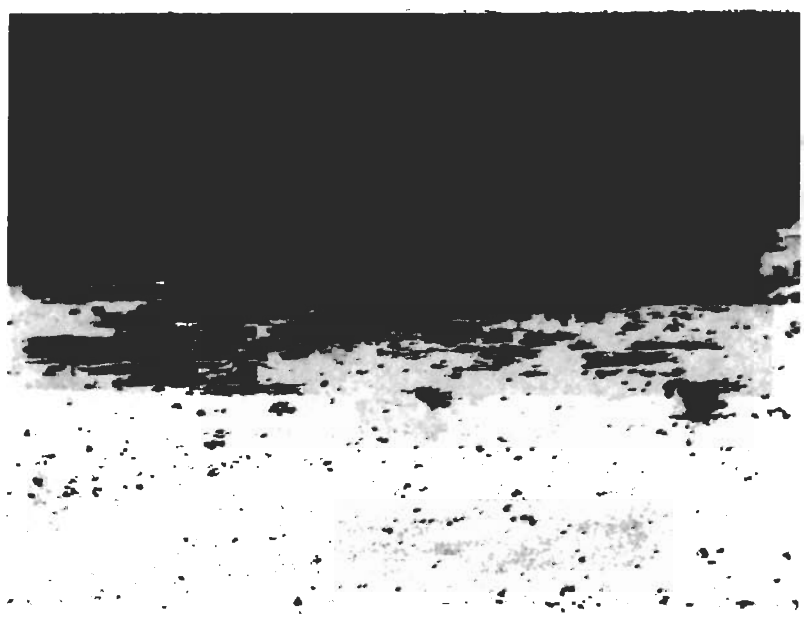

Figure 36e) - A8. Deepest pit in parent materials is 208 µm. (x120).

9.3.2 Results for 'Type B' Double Pass TIG welded 2219 Specimens.

The stress level was held at 112 N mm^{-2} (11.4 kgf mm^{-2}). No failures of the stress-corrosion specimens occurred during the 30-day test period. See Table IX and Figures 37 and 38.

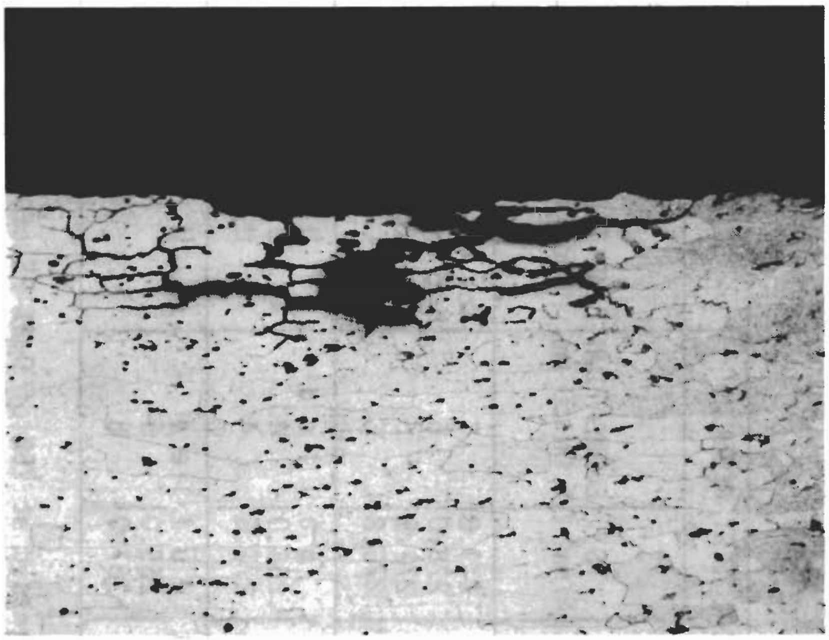

Figure 37a) - B4 worst intergranular corrosion seen in the HAZ, maximum depth is 192 μm. (x120).

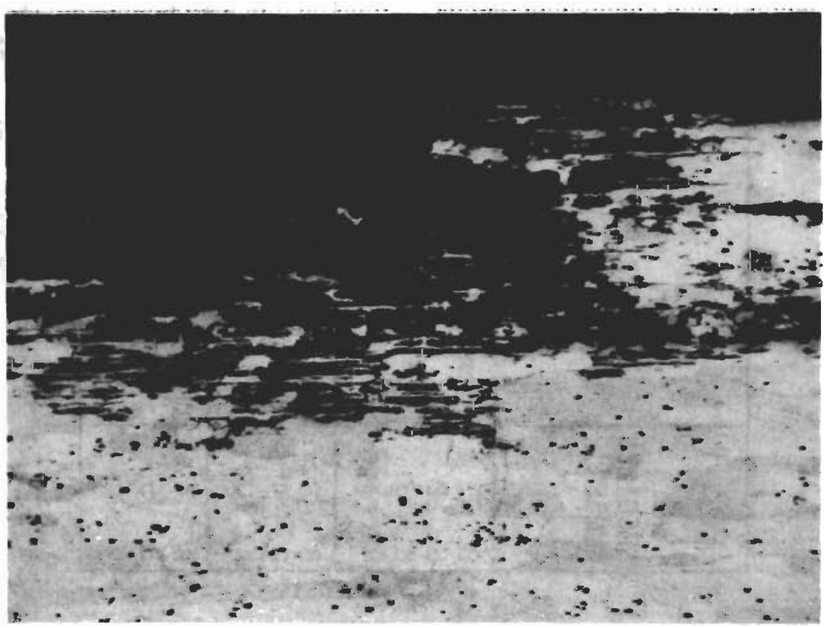

Figure 37b) - B4 worst exfoliation in parent metal, maximum depth is 364 μm. (x120).

TABLE IX - TWO-PASS TIG WELDED 2219-T851 ALLOY SPECIMENS

RESULTS OF MECHANICAL AND STRESS-CORROSION TESTS

SPECIMEN NUMBER	DESCRIPTION	MECHANICAL TEST RESULTS			STRESS-CORROSION TEST RESULTS			
		0.2% PS N/mm^2	TS N/mm^2	ELONGATION % ON 50 mm	TIME TO FAIL (hours)	Max. Depth of Corrosion Visible in Microsection* (µm)		
						PARENT	HAZ	WELD
B 1	Tensile test specimen	148.6	279.8	7	Not exposed			
B 2	"	149.2	278.0	6	Not exposed			
B 3	"	151.0	272.5	6	Not exposed			
Average	"	149.6	276.8	6				
B 8	SC Specimen	- not pulled -			U	364	192	none
B 9	"	166.4	264.0	4	U	245	175	none
B 10	"	164.3	271.6	4	U	380	400	none
B 4	Unstressed control (720 h.)	- not pulled -			U	280	375	none
B 5	"	141.4	265.0	5		170	200	none
B 6		144.3	267.0	5		308	500	none

stress-corrosion specimens were stressed at 75% of 0.2% PS of weldment = 112 N/mm^2
U = not failed after 30-day test (720 hours)
* no stress-corrosion cracking was observed on these specimens

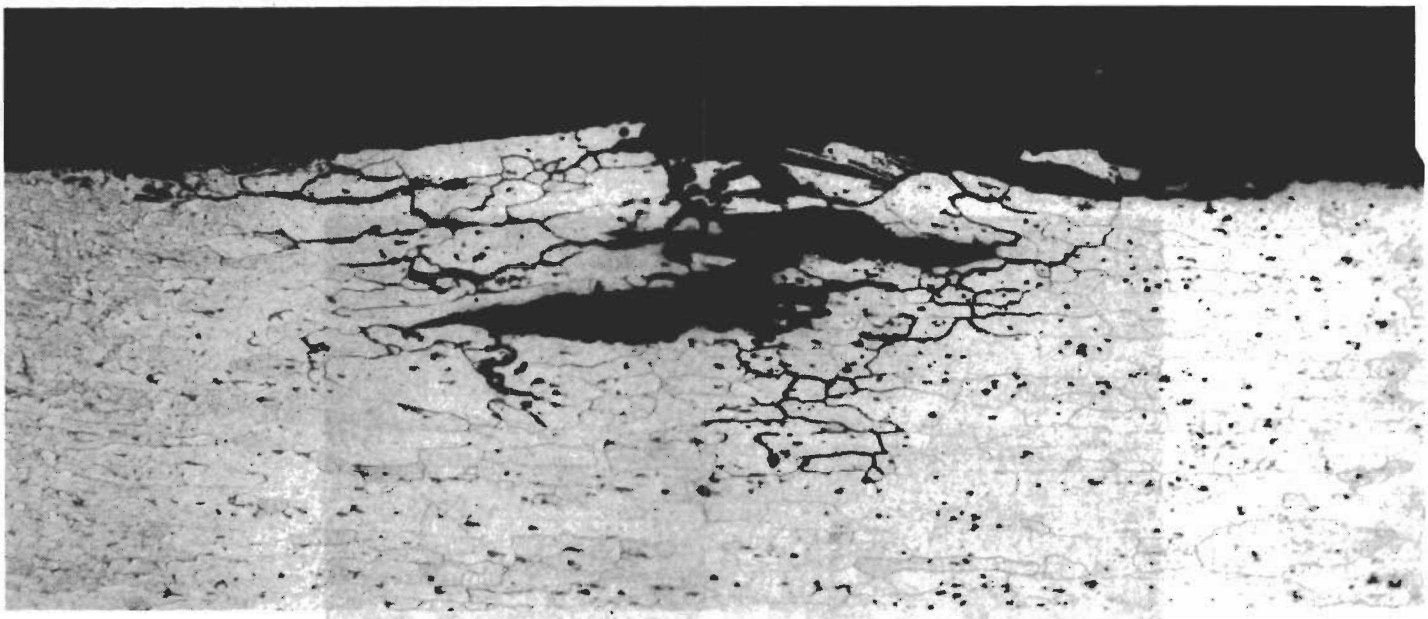

Figure 38a) - B8, Adjacent to weld pool the maximum depth of intergranular corrosion in HAZ is 375 μm. (x120).

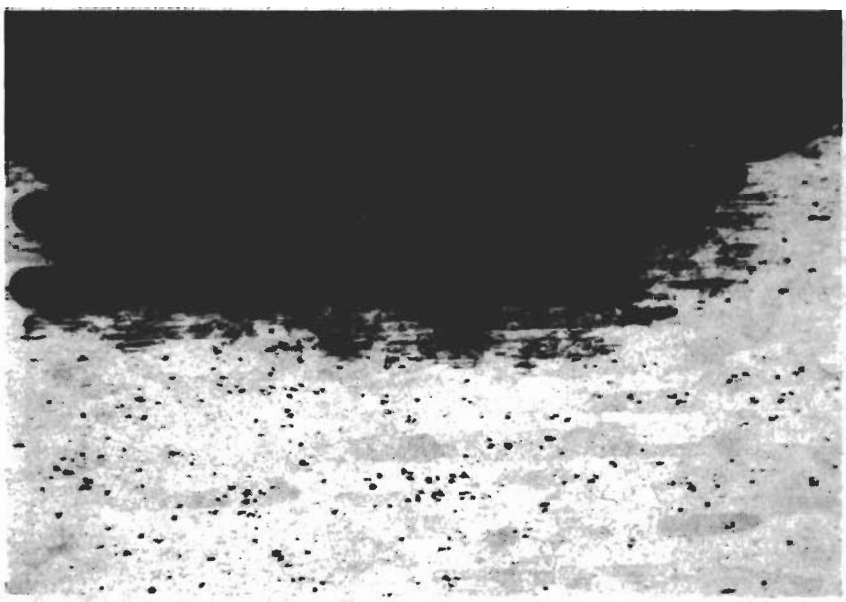

Figure 38b) - B8. Exfoliation in parent metal has depth of 280 μm. (x120).

9.3.3 Results for 'type C' Repair Welded 2219 Specimens.

The stress level was held at 123 N mm^{-2} (12.5 kg mm^{-2}). No failures of the stress-corrosion specimens occured during the 30-day test period. See Table X and Figures 39 and 40.

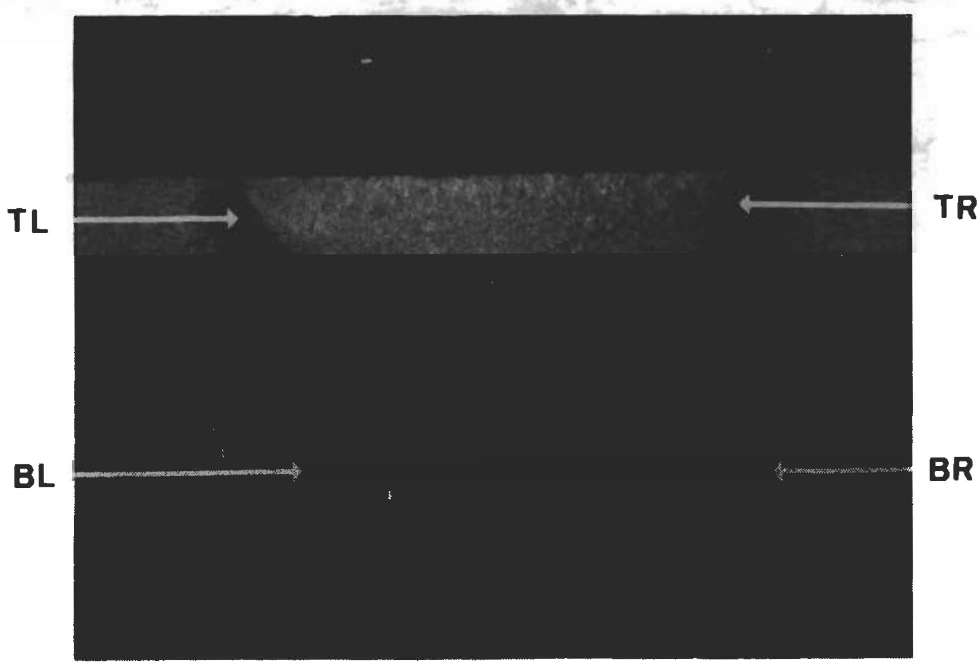

Figure 39a) - Sample C4 . Unstressed control sample sectioned (x6.5) to reveal positions of weld pool and HAZ.

TL = TOP LEFT TR = TOP RIGHT
BL = BOTTOM LEFT BR = BOTTOM RIGHT

Figure 39b) - Sample C4. Detail of corrosion pit present in weld pool. Depth is 250 μm. (x120).

TABLE X - REPAIR WELDED 2219-T851 ALLOY SPECIMENS

RESULTS OF MECHANICAL AND STRESS-CORROSION TESTS

SPECIMEN NUMBER	DESCRIPTION	MECHANICAL TEST RESULTS			STRESS-CORROSION TEST RESULTS			
		0.2% PS N/mm^2	TS N/mm^2	ELONGATION % on 50 mm	TIME TO FAIL (hours)	Max. Depth of Corrosion Visible in Microsection* (μm)		
						PARENT	HAZ	WELD
C 1	Tensile test specimen	173.3	287.2	6	Not exposed			
C 2	"	159.7	286.3	6	Not exposed			
C 3	"	156.2	285.2	7	Not exposed			
Average	"	163.7	286.2	6				
C 8	SC Specimen	- not pulled -			U	166	None	250**
C 9	"		239.6	3	U	-	-	-
C 10	"		229.7	3	U	-	-	-
C 4	Unstressed control (720 h.)	- not pulled -			U	466	330	233**
C 5	"		244.7	4		-	-	-
C 6			249.4	5		-	-	-

stress-corrosion specimens were stressed at 75% of 0.2% PS of weldment = 123 N/mm^2

U = not failed after 30-day test (720 hours)

* no stress-corrosion cracking was observed on these specimens
** pitting due to lack of weld fusion

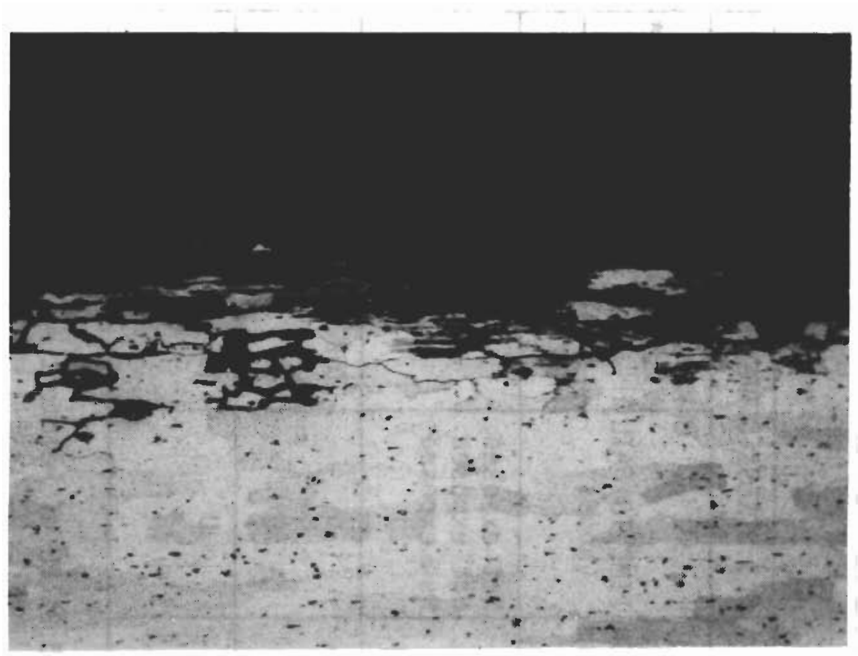

Figure 39c) - Sample C7. Detail from Fig. 39a) Position TL. Worst case of intergranular cracking in parent metal. Depth is 166 µm. (x120).

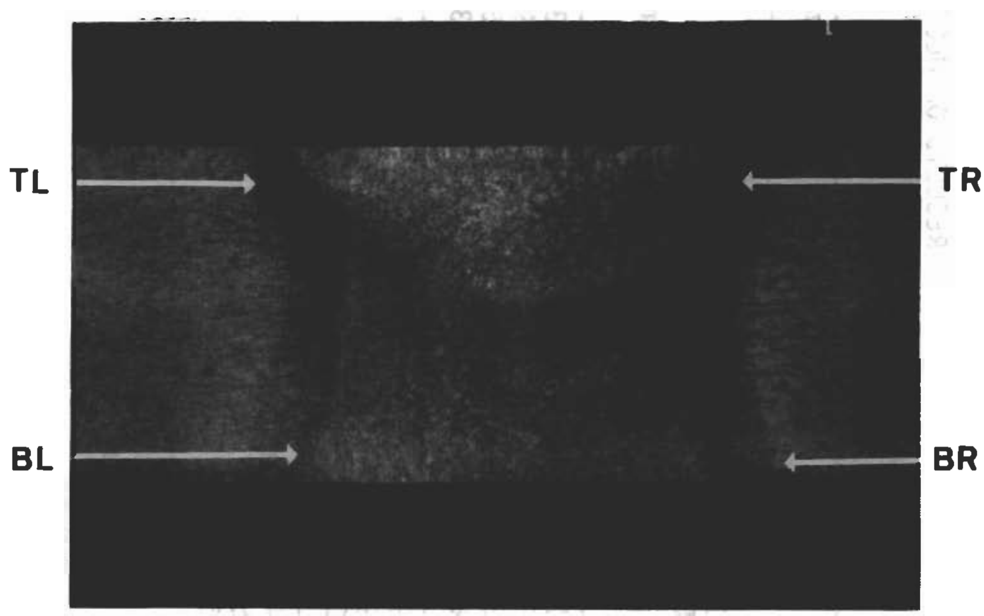

Figure 40 - Sample C-4, stress-corrosion test piece sectioned to reveal positions of weld pool and HAZ. (x6.5).

TL = TOP LEFT TR = TOP RIGHT

BL = BOTTOM LEFT BR = BOTTOM RIGHT

9.3.4 Results for 'Type J' Single Pass EB Welded 2219.

The stress level was held at 136 N mm^{-2} (13.9 Kgf mm^{-2}). No failures of the stress corrosion specimens occurred during the 30-day test period. See Table XI and Figures 41 and 42.

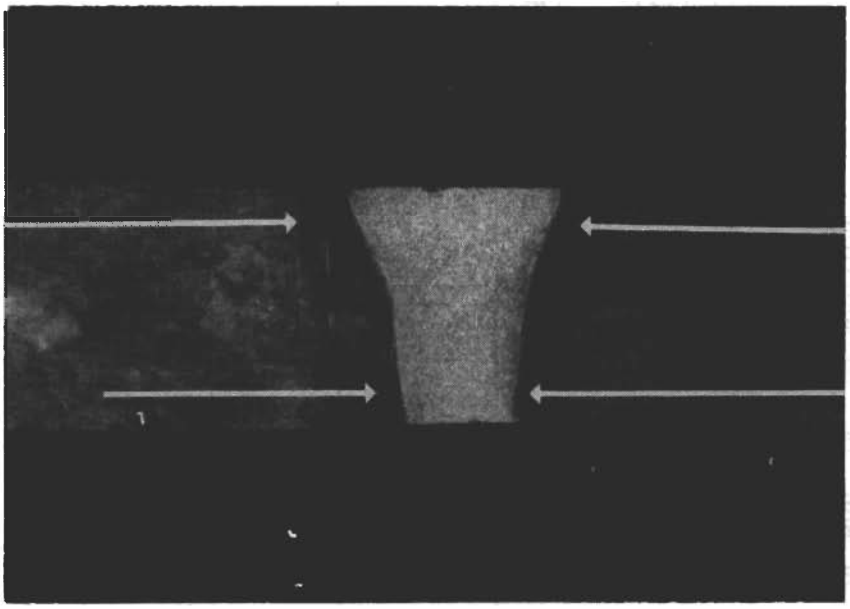

Figure 41 - Sample J7, unstressed control test piece, sectioned to reveal position of weld pool. (x6.5).

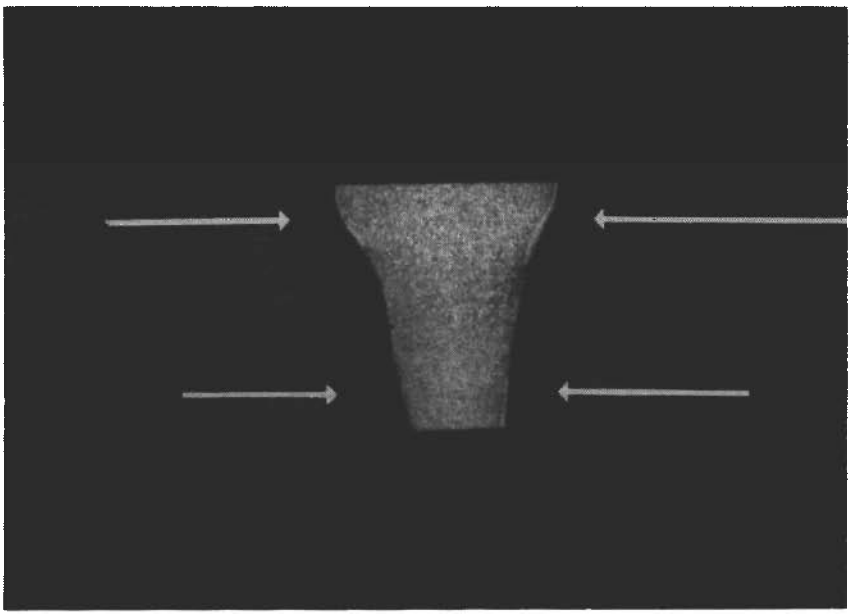

Figure 42 - Sample J7, stress-corrosion test piece (x6.5). Sectioned to reveal position of weld pool.

TABLE XI - SINGLE PASS EB WELDED 2219-T851 ALLOY SPECIMENS

RESULTS OF MECHANICAL AND STRESS-CORROSION TESTS

SPECIMEN NUMBER	DESCRIPTION	MECHANICAL TEST RESULTS			STRESS-CORROSION TEST RESULTS			
		0.2% PS N/mm^2	TS N/mm^2	ELONGATION % ON 50 mm	TIME TO FAIL (hours)	Max. Depth of Corrosion Visible in Microsection* (µm)		
						PARENT	HAZ	WELD
J 1	Tensile test specimen	179.3	287.0	4	Not exposed			
J 2	"	182.1	296.8	3	Not exposed			
J 3	"	180.9	300.1	3	Not exposed			
Average	"	180.8	298.0	3				
J 4	SC Specimen	- not pulled -			U	520	None	None
J 5	"		321.6	3	U	-	-	-
J 6	"		282.8	3	U	-	-	-
J 7	Unstressed control (720 h.)	- not pulled -				500	None	None
J 8	"		242.8	1		-	-	-
J 9			264.8	2		-	-	-

stress-corrosion specimens were stressed at 75% of 0.2% PS of weldment = 136 N/mm^2

U = not failed after 30-day test (720 hours)

* no stress-corrosion cracking was observed on these specimens

9.3.5 Results for 'Type E and ST' Short transverse BS L 93 alloy.

The 75% of 0.2 proof stress samples (ST 1 to 3) were held at 249.5 N mm^{-2} (25.4 Kgf mm^2). All failed within the 30-day period. The 25% and 15% of 0.2 proof stress samples survived the 30-day test exposure. The results are presented in Table XII.

Metallography revealed stress-corrosion cracks to exist in both the 75% and the 25% proof stress samples, as shown in Figures 43 and 44.

Figure 43a) - Pit at surface with SC crack below (sample ST1, 75% PS). (x50).

Figure 43b) - Detail of tip of crack from fig. 43a. (x500).

TABLE XII - BS L93 ALLOY PLATE SPECIMENS TAKEN IN SHORT TRANSVERSE DIRECTION
RESULTS OF MECHANICAL AND STRESS-CORROSION TESTS

SPECIMEN NUMBER	DESCRIPTION	MECHANICAL TEST RESULTS			STRESS CORROSION TEST RESULTS		
		0.2% PS N/mm^2	TS N/mm^2	ELONGATION % on 50 mm	TIME TO FAIL (hours)	Max. Depth of Corrosion Visible in Microsection* (µm)	
						PITTING	PITTING PLUS CRACKING
E 1	Tensile test specimen	334.1	373.9	4	Not exposed		
E 2	"	326.4	372.7	4	Not exposed		
E 3	"	337.4	375.3	4	Not exposed		
Average	"	332.6	374.0	4			
E 8	SC specimen (15% PS)	- n o t	p u l l	e d -	U	370	nc
E 9	"	> 360.0	360.0	> 1*	U	980	nc
E 10	"	361.7	372.0	1*	U	-	-
E 4	Unstressed control (720 h.)	- n o t	p u l	l e d -		1000	nc
E 5	"	341.7	342.0	2*		-	-
E 6	"	328.3	365.0	2		860	nc
ST 4	SC specimen (25% PS)	- n o t	p u l	l e d -	U	900	850
ST 5	"		326.9	1	U	650	800
ST 6	"		251.4	1	U	630	400
ST 7	Unstressed control (720 h.)	- n o t	p u l	l e d -		400	nc
ST 8	"		267.8	1		440	nc
ST 1	SC specimen (75% PS)	- failed	in SC	test -	625	800	1450
ST 2	"	"	"	"	504	650	670
ST 3	"	"	"	"	504	370	500
ST 9	Unstressed control (435 h.)		348.9	1		600	nc
ST 10	" (504 h.)		341.1	1		324	nc

Mark E specimens had 60 mm^2 cross-section area, Mark ST specimens had 36 mm^2 area.
*Specimen broke outside gauge length. U = not failed after 30-day test (720 hours).
nc = no cracking.

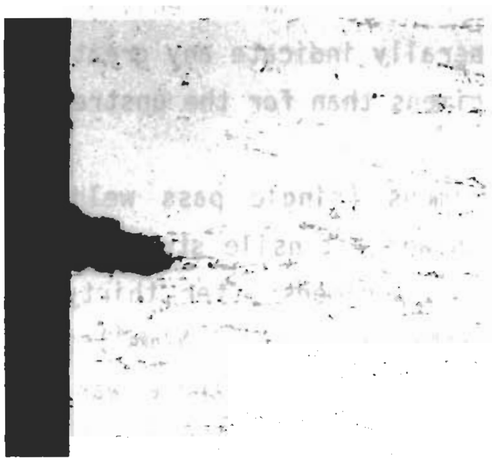

Figure 44a) - Pit at surface with SC crack below (Sample ST4, 25% PS). (x50).

Figure 44b) - Detail of tip of crack from Fig. 44a). (x500).

9.4 Discussion

9.4.1 Welded 2219 Alloy Specimens :

The results of the metallographic examination of the stress-corrosion and unstressed control specimens of welded 2219 alloy show that no stress-corrosion cracking of any of these groups of specimens took place. None failed during the 30-day test period and comparison of the residual strength of the two stress-corrosion specimens and two unstressed control specimens from each set which were tensile tested after thirty days' exposure does not generally indicate any greater loss of strength for the stress-corrosion specimens than for the unstressed controls.

For the Type A specimens (single pass weld) one of the two stress-corrosion specimens showed a tensile strength slightly below that of the two unstressed control specimens after thirty days, but the difference (232 N/mm^2 compared with 250 and 270 N/mm^2) is not significant. For the Type B specimens (two pass welds) there was no significant difference whatever between the tensile strengths of the two stress-corrosion specimens and the two unstressed controls tested after thirty days. The stress-corrosion specimens of the Type C set (repair welded) gave tensile strengths of 230 and 240 N/mm^2 compared with 245 and 249 N/mm^2 for the unstressed controls; this is again unlikely to be a significant difference. The tensile strength of the type J (EB welded) stress-corrosion specimens after thirty days was higher than that of the corresponding unstressed controls - a result which reflects the variability of tensile test results on welded specimens, but certainly does not indicate that any stress-corrosion cracking occurred.

All the welded specimens that were tensile tested failed in the weld bead itself. This is to be expected if no stress-corrosion cracking has taken place, since it will be the weakest part of the weldment. The weldment will in general comprise a central as-cast unheat-treated weld bead, next to which will be a zone of parent metal which has been re-solution treated by the heat of the welding and will subsequently naturally age but will not reach the strength of the original artificially aged material. Beyond the re-solution treated zone there will be a zone where the welding temperature has produced overageing of the parent metal but has not been sufficient to produce re-solution treatment. Beyond the band of overaged material will be the unaffected parent metal. Of these four zones the weld bead itself will have the lowest mechanical strength, but the greatest susceptibility to stress-corrosion cracking is usually found within the heat-affected zone usually in the re-solution treated material next to the weld bead itself. Consequently, if there had been any significant stress-corrosion cracking in the specimens tensile tested after thirty days' exposure, they would have been likely to fail in the heat-affected zone rather than in the weld bead. The variation in microstructure for each of the weld zones and parent plate was evaluated by transmission electron microscopy, as summarised in Appendix II.

Because of the composite nature of the weldments, the values of tensile strength which they give are the tensile strengths of the weakest part, i.e., the weld bead. Measurements of proof stress for welded specimens have little real meaning since they are calculated on a gauge length which consists principally of fully heat treated parent metal, whereas the actual yielding occurs almost entirely in the short length represented by the weld bead.

In interpreting the results of the stress-corrosion tests to the designers, however, it is important to make it clear that the freedom from stress-corrosion cracking shown in these tests does not refer to loads of 75% of the proof stress of the parent metal. According to the Alcoa Aluminium Handbook, 2219-T851 alloy gives a typical 0.2% PS of 50 ksi which is equivalent to 345 N/mm^2, the typical UTS being 66 ksi (455 N/mm^2). The stress at which the SCC tests on the Type A single pass welded specimens was carried out was 115 N/mm^2 which is 33% of the typical proof stress value quoted for the parent metal. The Type B two pass welded specimens were tested at 112 N/mm^2 equivalent to 32.5% of the typical parent metal proof stress. The Type C repair weld specimens were tested at 123 N/mm^2, equivalent to 35.6% of the typical parent metal proof stress, and the Type J electron beam welded specimens at 136 N/mm^2, equivalent to 39.4% of the typical parent metal proof stress.

9.4.2 Short transverse BS L93 Specimens:

There is no doubt about the susceptibility of this material to stress-corrosion cracking when tested at 75% of the 0.2% proof stress since all three of the type ST specimens tested at that stress level failed in less than thirty days; nor is there any doubt that the material was not susceptible when tested at 15% of the proof stress. In those tests the loss of strength shown by the two unstressed control specimens which were subsequently tensile tested was greater than that of the two stress-corrosion specimens.

Only two unstressed control specimens were exposed with the three SCC specimens tested at 25% of the proof stress. Consequently only one unstressed control specimen was tensile tested after thirty days' exposure. This gave a residual strength of 251 N/mm^2 compared with 327 N/mm^2 for the stress-corrosion specimens. Since the tensile strength of the specimens tested in the as-received condition was 374 N/mm^2, both the stressed and unstressed specimens showed a considerable reduction in strength, due in both cases principally to pitting corrosion and associated intergranular attack. The metallographic examination of the SCC specimens tested at 25% of the proof stress showed, however, the presence of intergranular stress-corrosion cracks in all three. The L93 plate material tested must, therefore, be regarded as susceptible to stress-corrosion cracking when loaded to 25% of the proof stress in the short transverse direction.

In comparing this conclusion with other published stress-corrosion test results for L93 material, it must be remembered that the degree of stress-corrosion susceptibility shown by this material in the short transverse direction depends on the rolling procedure used to produce the plate and on the heat treatment. Slightly underaged material shows the greatest susceptibility, while slightly overaged material is less susceptible than material aged to maximum strength.

9.5 Conclusions

All 2219-T851 Weldments :

> The mechanical-property results and photomicrograph results from all sets of specimens prove that no stress-corrosion cracking has initiated during the 30-day test period. These results direct these weldments into Table I of the ESA PSS-01-736 specification (i.e. having a high resistance to stress corrosion).

The BS L93 Plate :

> Stress-corrosion-cracking failures, observed by testing and metallography, existed for both sets of samples that were tested at 75% and 25% of the 0.2% proof stress for this alloy. The BS L93

plate must, therefore, be regarded as susceptible to stress-corrosion cracking. This material is equivalent to AA 2024 which, in all forms and tempers, is graded as a Table III alloy according to ESA PSS-01-736 (i.e. having a low resistance to stress corrosion).

A summary of the worst-case stress-corrosion test results derived from this work is given in Table XIII.

TABLE XIII - SUMMARY OF STRESS-CORROSION TEST MINIMUM RESULTS

Material is Al 2219 in T851 condition Test direction is short transverse Form of material : (Type of corrosion test sample)	Mechanical test results, 0.2% proof stress N/mm^2	Applied stress during corrosion test N/mm^2	Corrosion test 3.5% NaCl a.a. duration minimum (days)	SCC
Rolled sheet (C-rings) 35 mm thick	362	272	69	none
80 mm thick	348	261	86	none
105 mm thick	374	281	86	none
4 meter diameter forged rings: (tensile bars)	262	196	39	none
Weldments, 7 mm plate (tensile bars) TIG (single pass)	153	115	30	none
TIG (double pass)	149	112	30	none
TIG (repaired)	164	123	30	none
5mm plate, EB (single pass)	181	136	30	none
For comparison BS L 93 90 mm plate (equivalent to AA 2024) 15% P.S.	332	50	30	none
(tensile bars) 25% P.S.		83	30	failed
75% P.S.		249	21	failed

ACKNOWLEDGEMENT

This work was supported by the Spacelab Programme and the Product Assurance Division, ESTEC. Acknowledgement is given to Messrs D. Shaw and H.S. Campbell at the BNF Metals User's Consultancy Service who performed the stress-corrosion testing on the welded specimens and provided the results that have been compiled into Chapter 9. Thanks are also due to Messrs M. Froggatt, D.S. Collins and P.F. Fletcher for their assistance with the materials tests.

APPENDIX I

Tables and Graphs for 2219 as reproduced from the published literature.

TABLE 3.1.2.3.1. *Comparison of the Resistance to Stress Corrosion of Various Aluminum Alloys and Products*

Alloy and Temper	Test Direction	Estimate of Highest Sustained Tension Stress (ksi)[e] at Which Test Specimens of Different Orientations to the Grain Structure Would Not Fail in the 3½ % NaCl Alternate Immersion Test in 84 Days[f]				
		Plate	Rolled Rod and Bar	Extruded Shapes Section Thickness, Inch 0.25 - 1	Extruded Shapes Section Thickness, Inch > 1 - 2	Hand Forgings
2014 - T6	L	45	45	50	45	30
	LT	30	..	27	22	25
	ST	8[a]	15[b]	..	8[a]	8[a]
2219 - T8	L	40[c]	..	35[c]	35[c]	38[c]
	LT	38[c]	..	35[c]	35[c]	38[c]
	ST	38[c]	..	..	35[c]	38[c]
2024 - T3, T4	L	35	30	50[c]	50[c]	..
	LT	20	..	37	18	..
	ST	8[a]	10[b]	..	8[a]	..
2024 - T8	L	50[c]	47[c]	60[c]	60[c]	43[c]
	LT	50[c]	..	50	50	43
	ST	30	43[b]	..	45[c]	15
7075 - T6	L	50	50	60	60	35
	LT	45	..	50	32	25
	ST	8[a]	15[b]	..	8[a]	8[a]
7075 - T76	L	49[c]	..	52[c]	..	..
	LT	49[c]	..	49[c]	..	..
	ST	25	..	25	..	..
7075 - T73	L	50[c]	50	54	53[c]	50[c]
	LT	48[c]	48	48	48[c]	48[c]
	ST	43[c,d]	43[c,d]	46[c]	46[c,d]	43[c,d]
7079 -T6	L	55[c]	..	60	60[c]	50[c]
	LT	40	..	50	35	30
	ST	8[a]	..	..	8[a]	8[a]
7178 - T6	L	55	..	65	65	..
	LT	38	..	45	25	..
	ST	8[a]	..	..	8[a]	..
7178 - T76	L	52[c]	..	55[c]	..	..
	LT	52[c]	..	52[c]	..	..
	ST	25	..	25	..	..

[a]Lowest stress at which tests were conducted; failures were obtained.
[b]Ratings are for transverse specimens machined from round or square bar stock.
[c]Highest stress at which tests were conducted; on failure observed.
[d]These values will be lower for sections greater than 3" thick, but will be at least 75% of the guaranteed yield strength.
[e]See Section 9.5.2 for test method used to determine values.
[f]Tests performed at Alcoa Reasearch Laboratories.

Ref: Mil-Handbook 5c, 15 September 1976, page 3-19.

Table 2: Stress corrosion resistance of some 2000 and 7000 series aluminium alloys in 3.5% NaCl with stresses in the short transverse direction[42][43]

Alloy-temper designation	$K_{I_{SCC}}$ $MN/m^{3/2}$	Smooth specimen threshold stress MN/m^2
2024-T351	9	48
2024-T4		<55
2024-T62		300
2024-T851		275
2219-T37	< 9	< 69
2219-T62		>220
2219-T87	~28	>280
2014-T451	< 9	
2014-T651	< 8	55
7075-T651	8	48
7075-T7651	<22	170
7075-T7351	~23	>300
7178-T651	8	48
7178-T7651	~19	170
7050-T7651X	~10	
7050-T73651	25	
7475-T7351		>300

Ref: WANHILL, R.J. and VAN GESTEL, G.F., "Aluminium Alloys in the Aircraft Industries". Symposium organised by the Associazione Italiana Metallurgica and the Instituto Sperimentale dei Metalli Leggeri, Turin, 1-2 October 1976, pages 9-19.

Table III. Estimate of The Highest Sustained Tension Stress at Which Test Specimens of Different Orientations to The Grain Structure Would Not Fail by SCC in The 3,5 Pct NaCl Alternate Immersion Test (84 Days) or in Inland Industrial Atmosphere (1 Year), Whichever is Lower

Alloy and Temper	Direction of Applied Stress	Plates		Extrusions		Forgings	
		MN/m²	(ksi)	MN/m²	(ksi)	MN/m²	(ksi)
2014-T6	L	310	(45)	310	(45)	210	(30)
	LT	210	(30)	150	(22)	170	(25)
	ST	<55	(<8)	<55	(<8)	<55	(<8)
2219-T87	L	>270	(>40)	>240	(>35)	>260	(>38)
	LT	>260	(>38)	>240	(>35)	>260	(>38)
	ST	>260	(>38)	>240	(>35)	>260	(>38)
2024-T3, T4	L	170	(25)	>340	(>50)		
	LT	140	(20)	120	(18)		
	ST	<55	(<8)	<55	(<8)		
2024-T8	L	>340	(>50)	>410	(>60)	290	(43)
	LT	>340	(>50)	>340	(>50)	290	(43)
	ST	200	(30)	>310	(>45)	100	(15)
7039-T64	L	>290	(>42)				
	LT	240	(35)				
	ST	<35	(<5)				
7075-T6	L	340	(50)	410	(60)	240	(35)
	LT	310	(445)	220	(32)	170	(25)
	ST	<55	(<8)	<55	(<8)	<55	(<8)
7075-T76	L	>340	(>49)	>360	(>52)		
	LT	>340	(>49)	>340	(>49)		
	ST	170	(25)	170	(25)		
7075-T73	L	>340	(>50)	>360	(>53)	>340	(>50)
	LT	>330	(>48)	>330	(>48)	>330	(>48)
	ST	>300	(>43)	>300	(>43)	>300	(>43)
7178-T6	L	380	(55)	450	(65)		
	LT	260	(38)	170	(25)		
	ST	<55	(<8)	<55	(<8)		
7178-T76	L	>360	(>52)	>380	(>55)		
	LT	>360	(>52)	>360	(>52)		
	ST	170	(25)	170	(25)		
7079-T6	L	>380	(>55)	>410	(>60)	>340	(>50)
	LT	270	(40)	240	(35)	210	(30)
	ST	<55	(<8)	<55	(<8)	<55	(<8)
7049-T73	ST					≈170	(≈25)
7050-T736	ST					>170?	(>25?)
7175-T736	ST					≈170	(≈25)
RX 720	ST	>170	(>25)				
RR 58	L	>300	(>44)				
	ST	>270	(>40)				
DTD 3067	ST	140	(20)				
DTD 3066	ST	140	(20)				
AZ 74	ST					310	(45)

Ref: SPEIDEL, M.O., "Stress Corrosion Cracking of Aluminium Alloys", Met. Trans., 6A, 1975, pages 631-651.

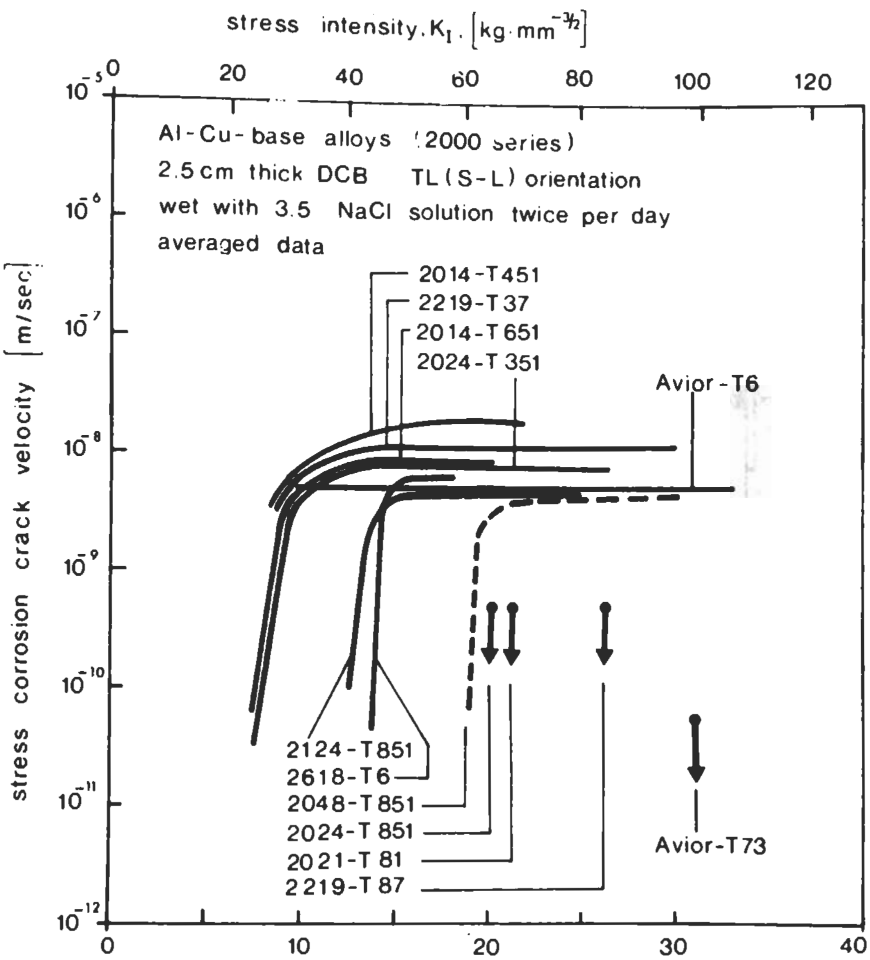

Fig. 21—Summary of stress corrosion crack growth rates in various alloys based on the aluminum-copper system.

Ref: SPEIDEL, M.O., "Stress Corrosion Cracking of Aluminium Alloys", Met. Trans., 6A, 1975, pages 631-651.

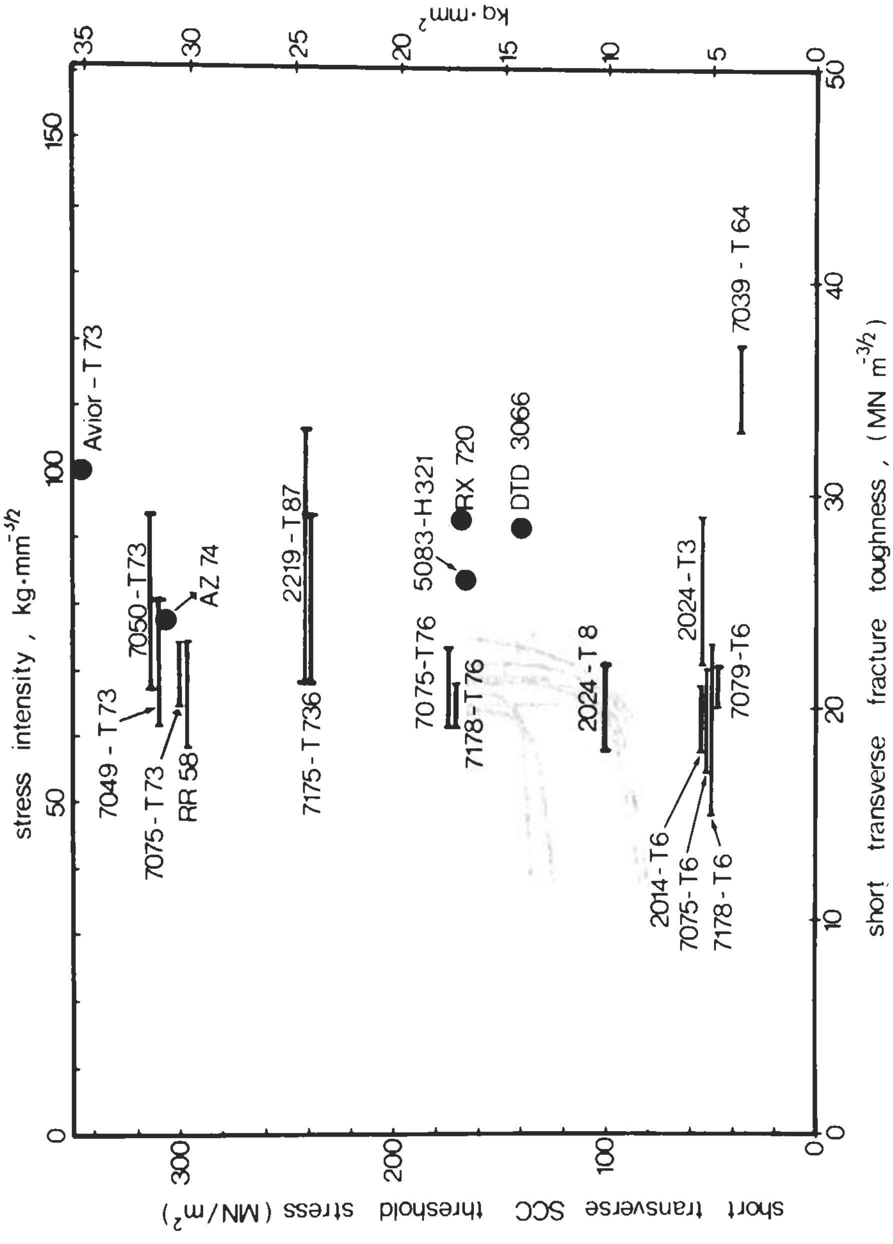

Ref: SPEIDEL, M.O., "Stress Corrosion Cracking of Aluminium Alloys", Met. Trans., 6A, 1975, pages 631-651.

TABLE 4. MDAC TEST DATA – 2219-T852 CONTOUR HAND FORGING – HOLDDOWN POST – DESTRUCT TEST

Forging P/N 14A30400(1)			Tensile Properties												Fracture Toughness		Stress Corrosion – 3.5% NaCl Alt. Imm.							
S/N 1			1/2" D Specimens												Compact Tension		Short Transverse (℄ t and w; 1/4" D X 1" GL)							
			Longitudinal				Long Transverse				Short Transverse				K_{Ic} – ksi $\sqrt{in.}$		Tensile Blanks				Unstressed		Stressed(2)	
Seg. No.	Location	t in.	UTS ksi	TYS ksi	EL %	RA %	UTS ksi	TYS ksi	EL %	RA %	UTS ksi	TYS ksi	EL %	RA %	(S-L)	(L-S)	UTS ksi	TYS ksi	EL %	RA %	UTS (% Change in 30 Days)	EL (% Change in 30 Days)	UTS (% Change in 30 Days)	EL (% Change in 30 Days)
2	℄	~7	-	-	-	-	-	-	-	-	*66.4	52.1	7.0	8.5	25.83(A)	-	65.7	51.5	7.0	9.3	-21.5	-71.4	-20.2	-71.4
											66.7	52.5	7.5	8.2	-	-	65.7	51.3	7.0	9.3	-20.2	-64.3	-21.1	-71.4
											-	-	-	-			65.8	51.3	7.0	9.4	-21.2	-71.4	-27.9	-85.7
											66.5	52.3	7.2	8.2			66.4	51.4	7.0	9.3	-20.9	-68.5	-23.0	-75.7
4		≈8 3/4	-	-	-	-	-	-	-	-	*63.7	49.1	7.0	9.0	28.09(B)	-	63.9	48.9	8.0	12.4	-22.0	-74.0	-18.8	-74.0
											64.5	49.6	7.0	7.4	-	-	63.8	48.9	8.0	13.1	-21.4	-74.0	-21.7	-74.0
											-	-	-	-			63.4	48.9	7.0	12.1	-20.1	-74.0	-19.5	-67.5
											64.1	49.3	7.0	8.2			63.7	48.9	7.7	11.9	-21.2	-74.0	-19.9	-71.4
																	(3) 62.7	49.3	5.7	8.1	-24.6	-72.7	–FH–	
6		~10 1/2	-	-	-	-	-	-	-	-	*61.2	47.2	8.0	13.6	28.45(B)	-	59.8	45.2	7.0	8.7	-21.5	-86.1	-18.4	-86.1
											61.6	47.2	8.5	10.9	-	-	60.7	45.6	7.5	11.0	-16.4	-79.2	-17.1	-93.1
											-	-	-	-			60.6	46.1	7.0	8.7	-13.7	-79.2	-17.1	-79.2
											61.4	47.2	8.2	12.2			60.4	45.6	7.2	9.5	-17.2	-81.9	-17.5	-86.1
8		~12 1/4	-	-	-	-	-	-	-	-	*59.5	45.5	8.5	13.2	28.99(B)	-	59.1	44.5	8.0	10.2	- 8.1	-63.4	-11.0	-69.5
											60.1	45.7	8.0	12.4	-	-	59.3	44.6	8.0	11.6	-10.7	-69.5	-10.2	-69.5
											-	-	-	-			59.0	44.7	8.5	15.4	-10.0	-69.5	-16.8	-81.7
											59.8	45.6	8.2	12.8			59.1	44.6	8.2	12.4	- 9.6	-67.1	-12.7	-73.2
10		~14	-	-	-	-	-	-	-	-	*57.7	45.0	8.5	13.2	29.23(B)	-	57.4	43.2	9.0	12.3	-13.1	-77.8	-13.5	-66.7
											58.0	44.0	8.5	13.2	-	-	57.8	43.8	9.0	11.6	-13.6	-72.2	-16.1	-77.8
											-	-	-	-			58.6	43.6	9.0	13.1	-20.0	-83.3	-11.1	-77.8
											57.8	44.5	8.5	13.2			57.9	43.5	9.0	12.3	-15.5	-77.8	-13.5	-74.4
																	(3) 63.9	49.7	6.5	9.4	-26.5	-91.2	-26.3	-82.4
																	62.5	49.3	5.5	8.6	-26.0	-91.2	-26.3	-100
																	61.7	48.9	5.0	6.4	-27.3	-100	-29.2	-100
																	62.7	49.3	5.7	8.1	-26.3	-94.7	-27.3	-94.7

See Page 43 for Notes

TABLE 4. (Continued)

Forging P/N 14A30400(1)			Tensile Properties												Fracture Toughness		Stress Corrosion — 3.5% NaCl Alt. Imm.							
			1/2" D Specimens												Compact Tension		Short Transverse (℄ t and w; 1/4" D X 1" GL)							
S/N 1			Longitudinal				Long Transverse				Short Transverse				K_{1c} — ksi $\sqrt{in.}$		Tensile Blanks				Unstressed		Stressed(2)	
Seg. No.	Location	t in.	UTS ksi	TYS ksi	EL %	RA %	UTS ksi	TYS ksi	EL %	RA %	UTS ksi	TYS ksi	EL %	RA %	(S-L)	(L-S)	UTS ksi	TYS ksi	EL %	RA %	UTS % Change in 30 Days	EL % Change in 30 Days	UTS % Change in 30 Days	EL % Change in 30 Days
12	℄; E(4)	~15 3/4	*57.7	45.0	11.5	22.3	*57.4	44.0	7.0	9.4	-	-	-	-	-	-	56.4	43.2	8.0	11.6	-19.7	-88.0	-13.7	-81.9
↓	℄	↓	56.6	45.3	10.0	23.7	57.9	43.8	6.5	10.5	*56.7	43.6	7.0	12.0	(27.43)(B) [0.791]	-	56.0	42.6	8.0	10.9	-13.7	-75.9	-15.4	-81.9
	↓		-	-	-	-	-	-	-	-	56.7	43.0	8.0	13.5	-	-	56.6	43.0	9.0	13.8	-12.4	-75.9	-16.3	-88.0
	℄; E(4)		58.1	44.8	11.5	26.0	57.2	43.1	6.3	10.9	-	-	-	-	-	-	56.3	43.0	8.3	12.1	-15.6	-79.5	-15.3	-83.9
			58.1	45.0	11.0	24.0	57.5	43.6	6.7	10.3	56.7	43.3	7.5	12.7			(3)							
																	62.7	49.3	5.7	8.1	-26.3	-94.7	-27.3	-94.7
14	℄	~16 1/4	57.6	44.7	11.0	21.9	-	-	-	-	57.7	44.9	8.5	12.1	26.71(B)	(35.38)(B) [1.170]	-	-	-	-	-	-	-	-
↓	↓	↓	58.5	45.5	11.0	21.9	-	-	-	-	56.5	43.6	8.5	12.8	26.65(B)	(35.46)(B) [1.183]								
			58.1	45.1	11.0	21.9					57.1	44.2	8.5	12.4										
2	Min. Gtd.	~7	62	50	6	-	61	49	4	-	60	46	3	-										
4	↓	~8 3/4	55	43	6	-	55	42	4	-	53	40	3	-										
6&8		10 1/2-12 3/4	52	39	6	-	52	38	4	-	50	30	3	-										
10,12&14		14-16 1/4	46	33	6	-	46	32	4	-	44	30	3	-										

Notes:
(1) Forged and HT dimensions ~7-16 1/4" t × ~22 1/2" w × ~100" l.
Alcoa cut into segments before aged.
(2) Stressed to 75% of TYS.
(3) Standard — specimens from 2219-T851 plate 6 1/8" t exposed simultaneously.
(4) Specimen 1 1/2" from outside edge of width, all others are ℄ width and thickness.
*Stress-strain curves available.
FH - Failed in handling during removal from stressing fixture.

Legend:
(A) — 1" wide specimens
(B) — 1.5" wide specimens
( ) — K_Q values in parentheses
[ ] — R_{sc} values in brackets

Ref: BRENNECKE, M.W., "Characterization of Large 2219 Aluminium Alloy Hand Forgings for the Space Shuttle Solid Rocket Booster", NASA Tech. Paper 1383, December 1978.

TABLE 9. 2219-T852 CONTOUR HAND FORGING
THRUST POST – DESTRUCT TEST

Forging P/N 14A20084(1) S/N 1 Seg. No.	Location	t in.	Tensile Properties, 1/2" D Specimens, Longitudinal UTS ksi	Longitudinal TYS ksi	Longitudinal EL %	Longitudinal RA %	Long Transverse UTS ksi	Long Transverse TYS ksi	Long Transverse EL %	Long Transverse RA %	Short Transverse UTS ksi	Short Transverse TYS ksi	Short Transverse EL %	Short Transverse RA %	Fracture Toughness, Compact Tension K_{1c} – ksi $\sqrt{in.}$ (S-L)	(L-S)	Stress Corrosion – 3 1/2% NaCl Alt. Imm., Short Transverse (℄ t and w; 1/4" D × 1" GL), Tensile Blanks UTS ksi	Tensile Blanks TYS ksi	Tensile Blanks EL %	Tensile Blanks RA %	Unstressed UTS (% Change in 30 Days)	Unstressed EL	Stressed(2) UTS	Stressed(2) EL
2	t/2; edge'	~5 3/4	64.1	53.4	9.0	21.6	63.4	51.6	7.5	10.9	63.6	51.2	7.5	9.8	-	-	63.5	50.3	6.5	7.1	-24.0	-76.9	— FH —	
↓	w/2	↓	*64.4	50.9	10.0	22.9	*64.2	50.4	7.5	9.7	*63.7	50.9	5.0	4.7			63.9	50.4	7.0	8.6	-26.5	-76.9	-25.4	-69.2
↓	edge'	↓	64.9	52.9	12.0	27.2	64.0	52.4	7.5	9.4	64.5	51.8	(5)	6.7			63.8	50.4	6.0	11.0	-22.3	-76.9	-27.2	-76.9
																	63.7	50.4	6.5	8.9	-24.5	-76.9	-26.4	-72.3
10	edge'	↓	63.6	52.9	11.0	24.7	63.4	50.6	6.5	6.7	63.8	51.4	5.0	5.0	-	-	65.4	51.9	7.0	10.3	-22.3	-70.6	-28.3	-85.3
↓	w/2	↓	*64.7	51.6	10.0	19.4	*64.4	50.2	5.0	10.1	65.0	51.3	5.5	8.5			64.6	50.1	7.0	7.1	-22.9	-70.6	-27.7	-85.3
↓	edge'	↓	67.4	54.7	11.0	22.2	64.3	51.6	5.0	7.3	67.7	55.6	5.5	7.4			65.1	51.8	6.5	7.2	-24.2	-70.6	-25.1	-70.6
																	65.0	51.3	6.8	8.2	-23.0	-70.6	-27.1	-80.8
																	(3) 63.9	49.7	6.5	9.4	-25.5	-91.2	-26.3	-82.4
																	62.5	49.3	5.5	8.6	-26.0	-91.2	-26.3	-100
																	61.7	48.9	5.0	6.4	-27.3	-100	-29.2	-100
																	62.7	49.3	5.7	8.1	-26.3	-94.7	-27.3	-94.7
5	t/4 bot.; edge†	~12	65.3	52.8	8.0	18.0	62.9	51.1	5.5	6.8	65.9	52.6	6.0	6.3	-	-	-	-	-	-	-	-	-	-
↓	w/2	↓	*61.5	47.2	8.0	16.8	*62.0	47.0	5.5	7.1	*59.4	46.3	4.5	7.0	(23.48)[0.590]	(4)								
↓		↓	-	-	-	-	-	-	-	-	-	-	-	-	(4)	(4)								
↓	edge†	↓	64.8	52.8	7.0	8.2	61.6	50.6	(5)	3.6	64.8	52.3	5.5	5.1	-	-								
6	w/4	~14	60.7	48.2	10.0	13.9	-	-	-	-	-	-	-	-	-	-	-	-	-	-	-	-	-	-
↓	w/3	↓	-	-	-	-	-	-	-	-	56.6	43.6	4.0	5.5	21.91									
↓	w/2	↓	60.3	47.6	10.5	21.9	-	-	-	-	-	-	-	-	-	-								
↓	w/3	↓	-	-	-	-	-	-	-	-	56.9	45.3	4.0	7.5	22.32									
↓	w/4	↓	60.7	48.4	10.5	16.5	-	-	-	-	-	-	-	-	-	-								
↓	t/4 top; w/4	↓	60.2	48.1	8.5	14.7	-	-	-	-	-	-	-	-	-	-	-	-	-	-	-	-	-	-
↓	w/3	↓	59.3	47.5	10.0	23.9	-	-	-	-	-	-	-	-	-	(39.64) [1.033]								
↓	w/2	↓	*60.4	48.1	10.0	22.2	-	-	-	-	-	-	-	-	-	-								
↓	w/3	↓	59.8	47.4	11.0	23.6	-	-	-	-	-	-	-	-	-	(38.31) [1.038]								
↓	w/4	↓	60.4	48.2	9.5	19.4	-	-	-	-	-	-	-	-	-	-								

TABLE 9. (Continued)

Forging P/N 14A20084(1)			Tensile Properties												Fracture Toughness		Stress Corrosion — 3.5% NaCl Alt. Imm.							
			1/2" D Specimens												Compact Tension K_{Ic} — ksi $\sqrt{in.}$		Short Transverse (℄ t and w; 1/4" D × 1" GL)							
S/N 1			Longitudinal				Long Transverse				Short Transverse						Tensile Blanks				Unstressed		Stressed(2)	
Seg. No.	Location	t in.	UTS ksi	TYS ksi	EL %	RA %	UTS ksi	TYS ksi	EL %	RA %	UTS ksi	TYS ksi	EL %	RA %	(S-L)	(L-S)	UTS ksi	TYS ksi	EL %	RA %	UTS (% Change in 30 Days)	EL (% Change in 30 Days)	UTS (% Change in 30 Days)	EL (% Change in 30 Days)
6 ↓	t/2; w/2 ↓	~14 ↓	-	-	-	-	-	-	-	-	56.3	44.8	5.0	7.0	20.84	-	-	-	-	-	-	-	-	-
											56.1	44.5	5.5	7.5	22.23	-								
8 ↓	↓	↓	-	-	-	-	-	-	-	-	56.6	43.9	7.0	8.6	22.96	-	57.2	44.0	7.0	12.5	-21.5	-85.7	-24.4	-92.8
											56.6	44.2	7.0	8.6	22.46	-	57.2	43.9	7.0	10.8	-25.5	-92.6	-23.7	-92.8
											-	-	-	-	22.67	-	57.4	43.9	7.0	10.3	-20.9	-85.7	-24.6	-100
																	57.3	43.9	7.0	11.2	-22.7	-88.6	-24.2	-95.7
																	(3)							
																	63.9	49.7	6.5	9.4	-25.5	-91.2	-26.3	-82.4
																	62.5	49.3	5.5	8.6	-26.0	-91.2	-26.3	-100
																	61.7	48.9	5.0	6.4	-27.3	-100	-29.2	-100
																	62.7	49.3	5.7	8.1	-26.3	-94.7	-27.3	-94.7
2 & 10	Min. Gtd.	~5 3/4	61	49	6	-	61	48	4	-	59	45	3	-	-		-	-	-	-	-	-	-	-
5 & 9	↓	~7 1/2-12	50	37	6	-	50	36	4	-	48	34	3	-	-									
6 & 8		14	50	37	6	-	50	36	3	-	48	34	3	-	-									

Notes:
(1) Forged and HT dimensions — ~5 3/4-14" t × ~29 1/2" w × ~115" l
Alcoa cut into segments before aged.
(2) Stressed to 75% TYS.
(3) Standard — specimens from 2219-T851 plate 6 1/8" t exposed simultaneously.
(4) Failed according to E399 sec. 8.2.4 — cracked at an angle >10°.
(5) Broke outside gauge marks.
FH — Failed in handling during removal from stressing fixture.
* — Stress-strain curves available.
†Surface for L and ST.

Legend:
( ) — K_Q values in parentheses
[ ] — R_{sc} values in brackets
1.5" wide specimens

Ref: BRENNECKE, M.W., "Characterization of Large 2219 Aluminium Alloy Hand Forgings for the Space Shuttle Solid Rocket Booster", NASA Tech. Paper 1383, December 1978.

APPENDIX II

Classification of tempers of Al 2219

FORM	CONDITIONS AVAILABLE
Sheet or plate	0, T31, T351, T37, T62, T81, T851, T87
Wire, rod and bar	T 851
Extruded rod, tubes	0, T31, T3510, T3511, T62, T81
Bar and shapes	T8510, T8511
Rolled ring	T6, T851

- 0 Annealed
- F As fabricated
- T31 Solution heat treated, cold worked by flattening or straightening.
- T351 Solution heat treated, stress relieved by stretching to produce a permanent set of 1 to 3% (no straightening after stretching).
- T37 Solution heat treated and cold worked by reduction of approx. 8%.
- T62 Solution heat treated and artificially aged by the user.
- T81 -T 31 precipitation heat treated in a manner to obtain certain* good mechanical properties.
- T851 Solution heat treated, stress relieved by stretching to produce a permanent set of 1 to 3%, and artificially aged. Plate shall receive no straightening after stretching.
- T87 -T 37 precipitation heat treated in a manner to obtain certain* good mechanical properties and to be capable of meeting stress-corrosion requirements.

*See Mil Spec.-A-8920A, 20 May 1963, Table II.

(BLANK PAGE)

APPENDIX III

TRANSMISSION ELECTRON MICROSCOPY OF Al 2219-T-851 WELD SAMPLE

1. One TIG welded plate sample has been submitted to transmission electron microscopy (TEM) examination and hardness testing. It was hoped to determine the extent of precipitation hardening in the parent plate, heat-affected zone (HAZ) and weld metal of a welded plate having similar composition, temper etc. to those of the specimen type A described in Chapter 9. A Siemens microscope was used with an acceleration voltage of 100 kV and the specimens consisted of foils machined and polished from appropriate regions of the weld sample.

   In the age hardening of aluminium alloy 2219, five structures can be recognised:-

   - Supersaturated solid solution
   - G.P. 1 zones,
   - G.P. 2 zones, also called Q",
   - Q' and
   - Q or $CuAl_2$.

   These structures generally form in the above-mentioned sequence, but -as in other ageing processes - there is disagreement as to whether they are successive steps of the transformation from supersaturated solid solution to $CuAl_2$ or independently nucleated, competing structures. Formation of G.P. 1 zones in bulk material is rapid and the zones tend to be nucleated on dislocations and other defects, most probably on the (100) planes of the matrix. G.P. 1 zones grow in size and are eventually replaced by platelets of G.P. 2 zones. With ageing time and temperatures in the order of 150 °C, the G.P. 2 zones grow slowly and precipitate as the intermetallic compound $CuAl_2$.

2. Parent Plate (Fig. A1).

From the morphology of the precipitates and their electron diffraction patterns, they were identified as predominantly Q' with some Q" (G.P. 2 zones). This is consistent with the plate heat treatment according to the T851 specification (18 hours at 175°C). No residual intermetallic particles were observed in this field of view.

3. Weld Metal

There was no evidence of Q' or $CuAl_2$ in the structure of the weld metal. This is also consistent with the weld temper (i.e. chill cast with no post-weld ageing).

4. Heat-affected Zone (Figures A3, A4 and A5)

Examination of the foils from the HAZ show less Q' precipitation and more evidence of $CuAl_2$ precipitation, particularly at the grain boundaries. Many of the large precipitates were lost during sample preparation - they are more noble than the matrix and cause rapid dissolution of their surrounding support material. The structures seen in Figures A3 - A5 are considered to show regions that are progressively more overaged.

A region of re-solution treated material in the HAZ immediately adjacent to the weld pool - and caused by the high welding temperature - was not found in this TEM examination.

5. Conclusions

The hardness variations across the welded plates show a change from approximately 140 DPN in the parent plate to 90 DPN in the weld. These values reflect the microstructure of the alloy :

- The parent plate material is strengthened by the presence of Q" (GP 2) and Q' precipitates.
- The HAZ shows Q' and $CuAl_2$ precipitates, the latter providing evidence of slight overageing and hence softening within the HAZ.
- The weld metal is single phase: no precipitates were found.
- Strengthening of the weld metal can be produced by artificially ageing the weld. This would, however, probably produce some softening of the parent plate and HAZ.

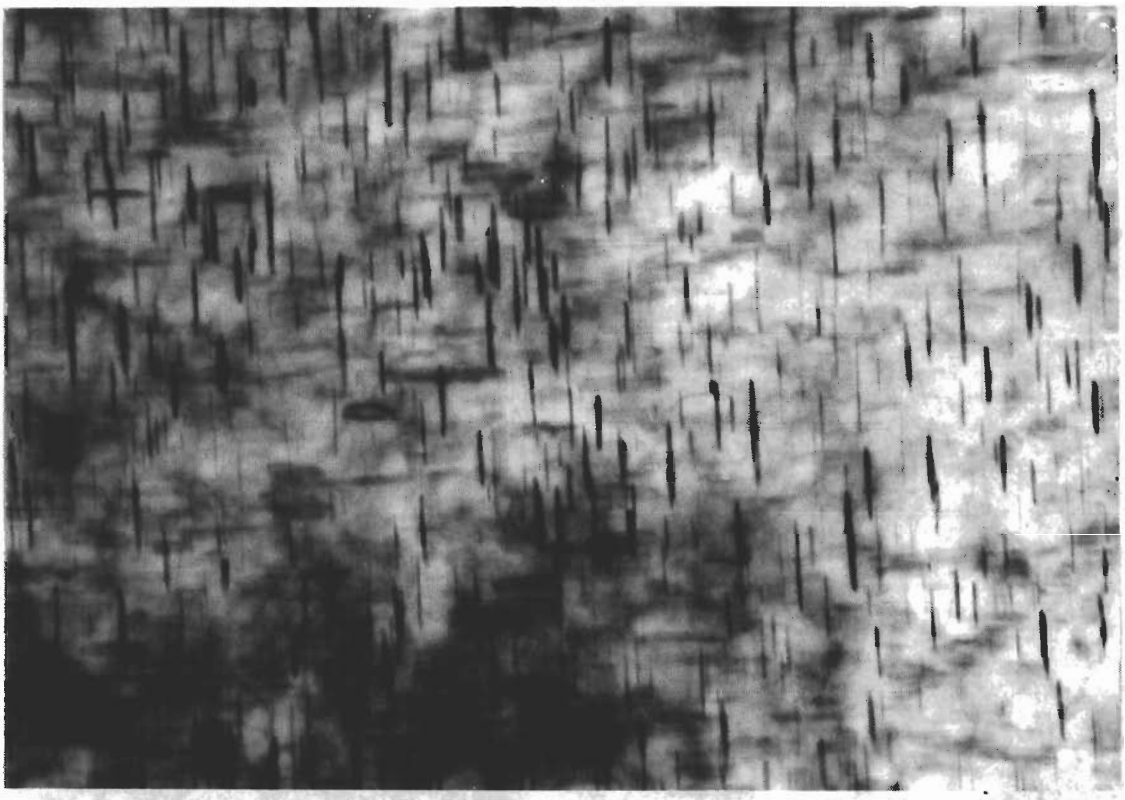

Figure A1 - Transmission electron micrograph of parent plate at x 80,000.

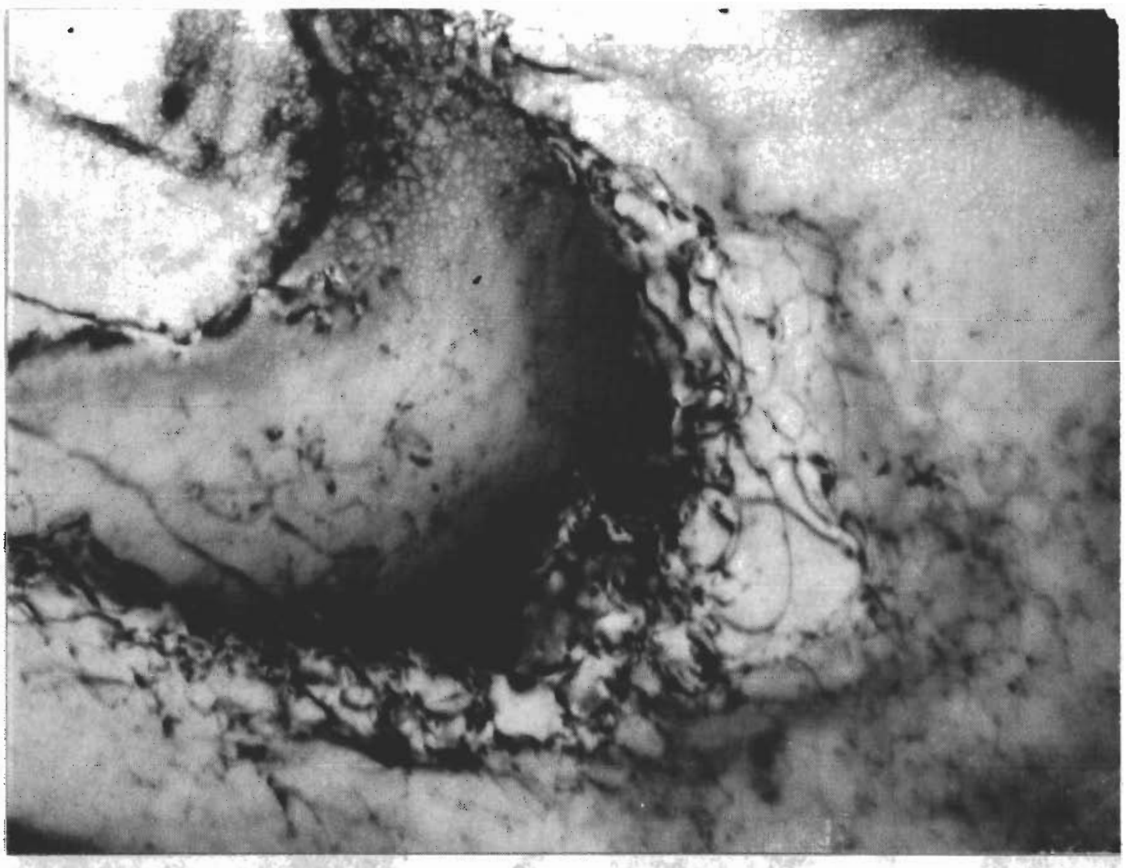

Figure A2 - T.E.M. of weld metal at x 70,000.

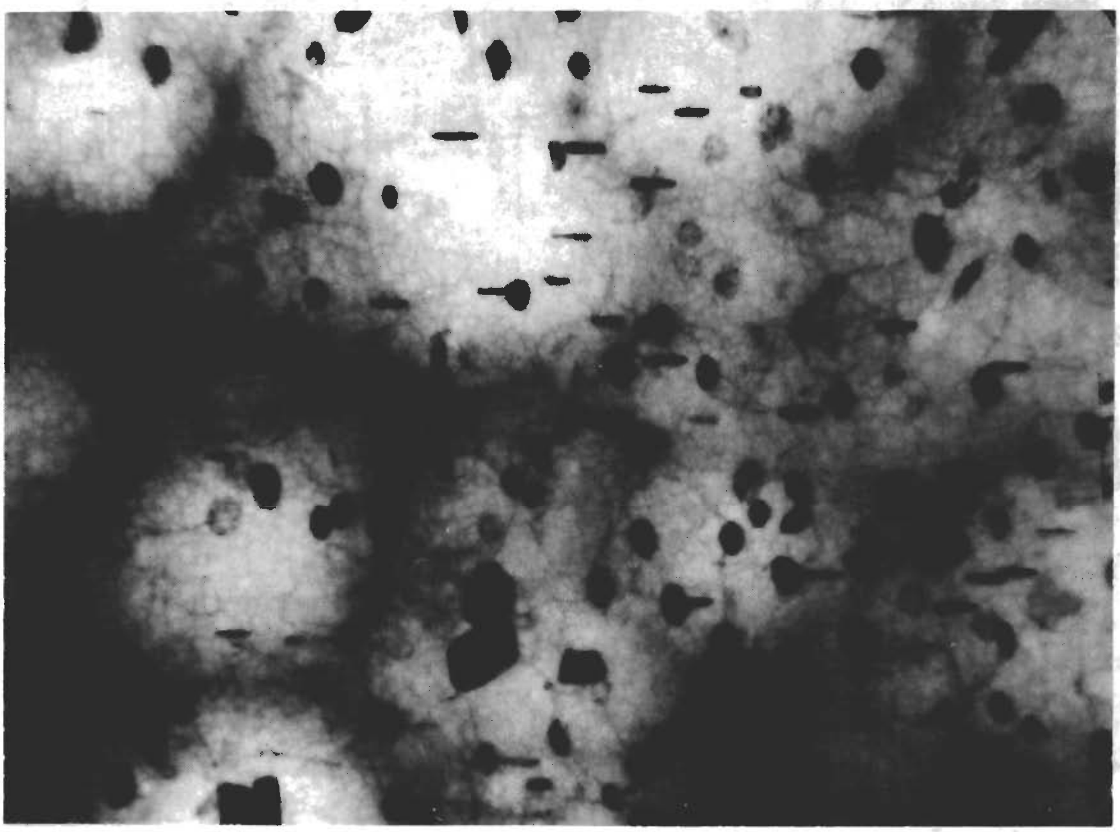

Figure A3 - T.E.M. of HAZ at x120,000.

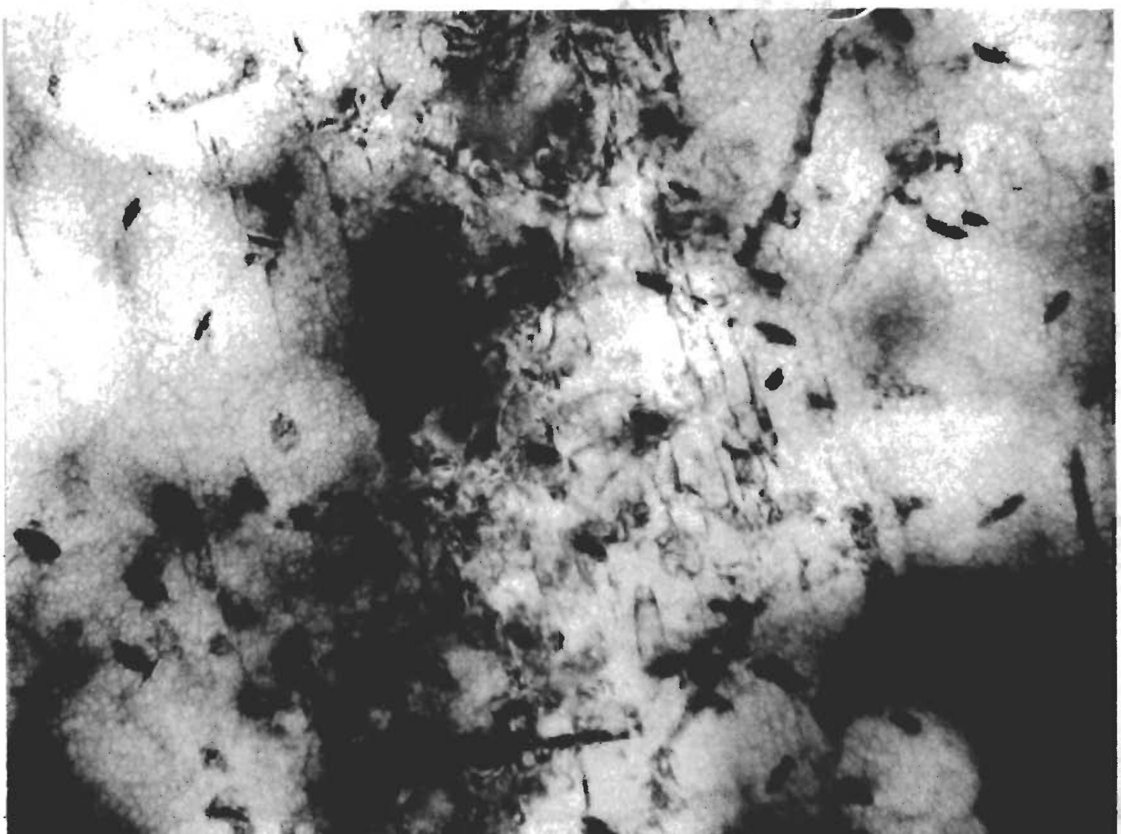

Figure A4 - T.E.M. of HAZ at x40,000.

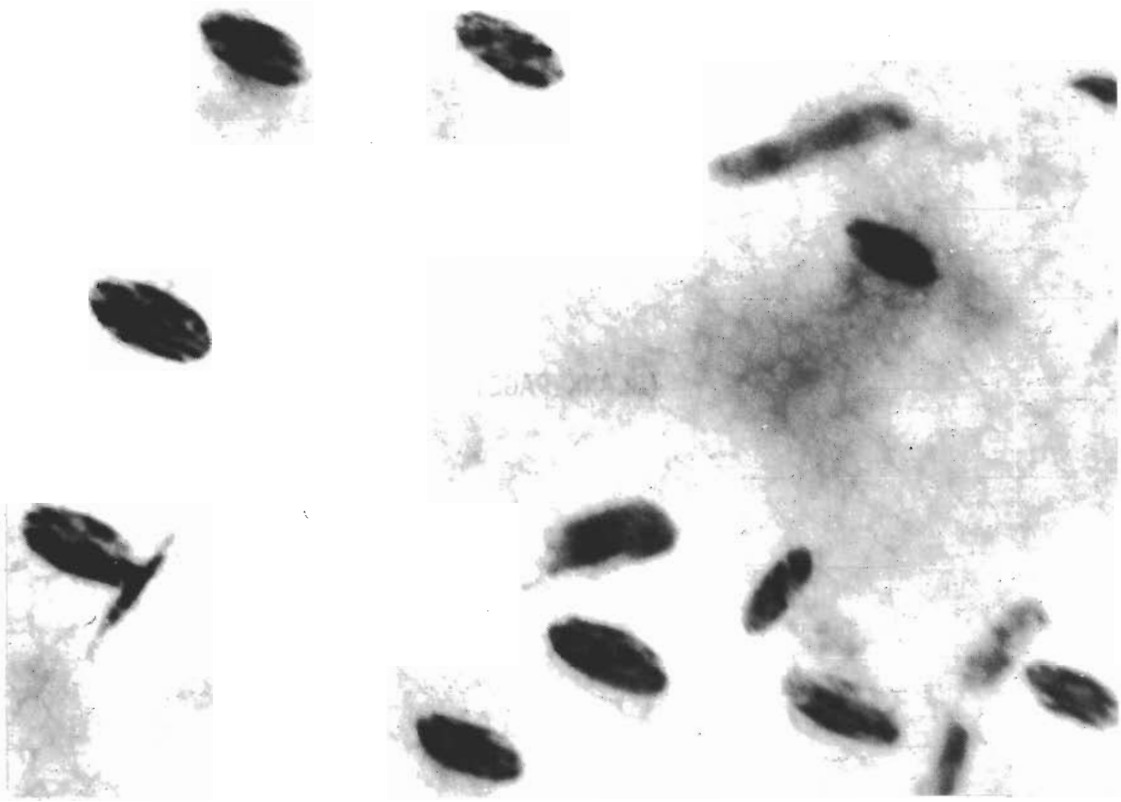

Figure A5 - T.E.M. of HAZ at x160,000.

(BLANK PAGE)